

The Role of IncV as a Tether of Endoplasmic Reticulum-
Chlamydia Inclusion Membrane Contact Sites

Rebecca Louise Stanhope
Tahoe City, California

Bachelor of Science in Microbiology, University of California San Diego, 2014

A Dissertation presented to the Graduate Faculty of the University of Virginia in
Candidacy for the Degree of Doctor of Philosophy

Department of Microbiology, Immunology, and Cancer Biology

University of Virginia
August 2020

Abstract

Chlamydia trachomatis is the leading cause of bacterial sexually transmitted infections and can lead to infertility if left untreated. *C. trachomatis* infects epithelial cells and replicate exclusively within a membrane-bound vacuole called the inclusion. *C. trachomatis* Inc proteins are translocated through a type III secretion system, then embedded into the inclusion membrane where they interact with host molecules to support the establishment of the *C. trachomatis* intracellular niche. The inclusion establishes direct contact with the endoplasmic reticulum (ER-Inclusion Membrane Contact Sites (MCS)), and these contacts have been proposed to be important for the *C. trachomatis* developmental cycle by facilitating lipid acquisition.

Our lab has demonstrated both bacterial and host factors that localize to ER-Inclusion MCS. The Inc protein IncD recruits the host ceramide transfer protein CERT to the inclusion membrane. This forms an IncD-CERT-VAP complex which has been proposed to function in facilitating the transfer of host lipids that become incorporated into inclusion and bacterial membranes. Additionally, the host ER calcium sensor protein STIM1 localizes to ER-Inclusion MCS, though its interacting partner and function there is still unknown. While we had learned about a possible function of ER-Inclusion MCS in lipid acquisition, how they are formed and maintained was unclear.

I showed that Inc protein IncV plays a structural role at ER-Inclusion MCS through its interaction with VAP via the molecular mimicry of two eukaryotic FFAT motifs. VAP interacts with proteins containing FFAT motifs, which contain a 7-residue core and

flanking acidic regions called the acidic tract. IncV contains two FFAT motif cores and mutating conserved core residues abolished the IncV-VAP interaction. IncV is sufficient, but not required, for the formation of ER-Inclusion MCS, suggesting IncV plays a supporting role in their formation and/or maintenance.

In eukaryotic cells, phosphorylation has been shown to regulate protein interactions with VAP and the cytosolic tail of IncV is highly enriched in phosphorylatable residues. I demonstrated that IncV is modified by a host factor and that IncV expressed by *C. trachomatis* in infected cells is phosphorylated. Phosphorylation of IncV is both necessary and sufficient for the IncV-VAP interaction *in vitro* and during infection. VAP recruitment to the inclusion is dependent on the host serine/threonine kinase Protein Kinase CK2 activity.

Altogether, my studies support a model in which CK2 phosphorylates IncV to promote the IncV-VAP interaction. I hypothesize that this phosphorylation event supports the maintenance of ER-Inclusion MCS. In this dissertation, I present the characterization of two novel components of ER-Inclusion MCS, the host CK2 and the *C. trachomatis* Inc protein IncV, and identify their roles in the formation of these contacts. I discuss how my findings add to our understanding of ER-Inclusion MCS formation and maintenance, as well as the MCS field, in general. Identifying molecules involved in the formation and maintenance of ER-Inclusion MCS could uncover potential targets for vaccine or therapeutic drug development.

Acknowledgements

The work presented in this dissertation was only possible with the support of the members of the Derré lab including Isabelle Derré, Rachel Ende, Clayton Bishop, Eugenia Cortina, Elli Flora, and Charlie Bayne. My thesis committee members, Alison Criss, Hervé Agaisse, Dave Kashatus, and Jim Casanova, provided input and advice that was essential for the development of this work. I would also like to acknowledge the many faculty and staff members of the Biomedical Sciences PhD program and the department of Microbiology, Immunology, and Cancer biology for their support. Lastly, I would like to acknowledge my friends and family for encouraging me throughout my graduate career.

Table of Contents

Section	Title	Page
1	Chapter 1: Introduction	1
1.1	<i>Chlamydia</i> , the disease	2
1.1.1	Epidemiology	2
1.1.1.1	The Incidence of Sexually Transmitted Infections Worldwide	2
1.1.1.2	The Incidence of Sexually Transmitted Infections in the United States	2
1.1.2	<i>C. trachomatis</i> Transmission	4
1.1.3	Risk Factors for <i>C. trachomatis</i> Infection	4
1.1.4	Clinical Presentations of <i>Chlamydia</i> Infections	5
1.1.4.1	Overview of <i>Chlamydia</i> Species Infections in Humans	5
1.1.4.2	Diseases Caused by <i>C. trachomatis</i>	5
1.1.5	Pathogenesis of <i>C. trachomatis</i> Infections	6
1.1.6	Treatment of <i>C. trachomatis</i> Infections	7
1.2	<i>Chlamydia</i> , an Obligate Intracellular Bacterium	7
1.2.1	Microbiological Description of <i>Chlamydia</i>	7
1.2.2	<i>Chlamydia</i> Genetics and Genetic Tools	10
1.2.2.1	The <i>Chlamydia</i> Genome	10
1.2.2.2	The <i>Chlamydia</i> Cryptic Plasmid	11
1.2.2.3	<i>Chlamydia</i> Transformation and Cloning Vectors	11
1.2.2.4	Fluorescent Proteins and Inducible Gene Expression in <i>C. trachomatis</i>	12
1.2.2.5	Mutating the <i>C. trachomatis</i> Genome	12
1.2.3	<i>Chlamydia</i> Effector Proteins	13

1.2.3.1	Type III Secretion System in <i>Chlamydia</i>	13
1.2.3.2	Inclusion Membrane Proteins	20
1.2.4	<i>Chlamydia</i> Interactions with the Host	20
1.2.4.1	Interactions Between the Inclusion and Host Factors	20
1.2.4.1.1	Interactions with the Host Cytoskeleton	24
1.2.4.1.2	Escape from the Endocytic Pathway	24
1.2.4.1.3	Manipulation of the Golgi Apparatus	25
1.2.4.1.4	Direct Contact with the ER	26
1.3	Membrane Contact Sites	30
1.3.1	What is a Membrane Contact Site?	30
1.3.2	Components of MCS	32
1.3.3	Functions of ER-Containing MCS	34
1.3.3.1	Calcium Signaling	34
1.3.3.2	Lipid Exchange	34
1.3.4	Formation and Maintenance of ER-Containing MCS	35
1.3.4.1	Membrane Tethering	35
1.3.4.2	Connecting the ER to Other Organelles Through a Common Protein	35
1.4	Model of ER-Inclusion MCS	38
1.5	Thesis Rationale	40
2	Chapter 2: IncV, a FFAT motif-containing <i>Chlamydia</i> protein, tethers the endoplasmic reticulum to the pathogen-containing vacuole (adapted from Stanhope <i>et al.</i> 2017)	41
2.1	Introduction	42

2.2	Results	45
2.2.1	IncV-VAP Interaction Depends on the FFAT Binding Domain of VAP.	45
2.2.2	IncV Contains Two FFAT Motifs That Mediate IncV-VAP Interaction.	50
2.2.3	The MSP Domain of VAP and the C-terminus of IncV Mediate IncV-VAP Interaction.	53
2.2.4	IncV-VAP Interaction Occurs During <i>C. trachomatis</i> Infection.	53
2.2.5	IncV-mediated Association of VAP With the Inclusion Depends on the FFAT Binding Domain of VAP.	57
2.2.6	Both FFAT motifs of IncV Are Required for VAP Association with the Inclusion.	63
2.2.7	IncV Promotes the Formation of ER-Inclusion MCS in a VAP-Dependent Manner.	63
2.2.8	PM-Targeted IncV Tethers the ER to the PM.	70
2.2.9	An IncV Mutant Displays MCS with Reduced Level of VAP.	73
2.3	Discussion	76
2.4	Conclusion	82
2.5	Materials and Methods	83
2.5.1	Ethics Statement	83
2.5.2	Cell Lines and Bacterial Strains	83
2.5.3	Plasmid Construction	83
2.5.4	Vectors for Expression in Mammalian Cells	83
2.5.5	Vectors for Expression in <i>E. coli</i>	84
2.5.6	Vectors for Expression in <i>C. trachomatis</i>	84

2.5.7	DNA Transfection	84
2.5.8	Co-immunoprecipitation	84
2.5.9	Immunoblotting	85
2.5.10	Antibodies	86
2.5.11	Protein Purification and GST Pull-down	86
2.5.12	Immunofluorescence and Confocal Microscopy	87
2.5.13	<i>C. trachomatis</i> Transformation	87
2.5.14	Inclusion Association Quantification	87
2.5.15	Transmission Electron Microscopy	88
2.6	Acknowledgments	89
3	Chapter 3: IncV, a tether of ER- <i>Chlamydia</i> Inclusion Membrane Contact Site, is phosphorylated by the host Protein Kinase CK2 to promote the IncV-VAP interaction	90
3.1	Introduction	91
3.2	Results	92
3.2.1	IncV is Phosphorylated by a Host Kinase.	92
3.2.2	CK2 is Recruited to the Inclusion in an IncV-Dependent Manner.	96
3.2.3	CK2 is a Novel Member of ER-Inclusion MCS	100
3.2.4	A C-terminal Domain of IncV is Required for CK2 Recruitment to the Inclusion.	103
3.2.5	CK2 Phosphorylates IncV.	106
3.2.6	Phosphorylation of IncV is Necessary and Sufficient to Promote the IncV-VAP Interaction.	110

3.2.7	CK2 Plays a Role in the IncV-VAP Interaction During Infection	114
3.3	Discussion	119
3.3.1	Transient nature of the IncV-CK2 Interaction.	119
3.3.2	Phosphoregulation of VAP-Interacting Proteins	119
3.3.3	Functional Outcomes of Phosphorylation of Inc Proteins by the Host	121
3.3.4	The Role of CK2 in Intracellular Pathogen Lifecycles.	122
3.4	Conclusion	124
3.5	Materials and Methods.	124
3.5.1	Cell Lines and Bacterial Strains.	124
3.5.2	Plasmid Construction.	124
3.5.3	Vectors for Expression in Mammalian Cells.	125
3.5.4	Vectors for Expression in <i>E. coli</i> .	125
3.5.5	Vectors for Expression in <i>C. trachomatis</i> .	125
3.5.6	<i>C. trachomatis</i> Transformation and <i>incV::bla</i> Complementation.	126
3.5.7	DNA Transfection.	126
3.5.8	SDS-PAGE.	126
3.5.9	Immunoblotting.	126
3.5.10	Antibodies.	127
3.5.11	Immunoprecipitation of IncV-3xFLAG From HEK293 Cells Infected with <i>C. trachomatis</i> .	127
3.5.12	Phosphatase assay.	128
3.5.13	DNA Transfections and Infections for Microscopy.	128
3.5.14	Immunofluorescence and Confocal Microscopy.	129

3.5.15	Quantification of YFP-CK2 β and CFP-VAPA Inclusion Association.	129
3.5.16	CK2 Depletion.	130
3.5.17	Protein Purification.	131
3.5.18	<i>In vitro</i> Kinase Assay.	131
3.5.19	<i>In vitro</i> Binding Assay With IncV Dephosphorylation.	132
3.5.20	<i>In vitro</i> Binding Assay With CK2 Phosphorylation of IncV.	133
3.5.21	CK2 Inhibition	134
3.6	Acknowledgments.	134
4	Chapter 4: Discussion, Conclusions, and Future Directions	136
4.1	Summary of Major Findings	137
4.2	Tethering the ER to the Inclusion Membrane	137
4.2.1	Tether definition	137
4.2.2	IncV as a Tether	137
4.2.3	Types of MCS Tethers	138
4.2.4	What Type of Tether is IncV?	139
4.2.5	Tethering redundancy	140
4.2.5.1	IncV is a Redundant Tether	140
4.2.5.2	The IncD-CERT-VAP Complex as a Tether	140
4.2.5.3	STIM1 as a Tether	141
4.2.6	Regulation of the IncV-VAP Tethering Complex	142
4.2.6.1	IncV as a Protein Kinase CK2 Substrate	142
4.2.6.2	Potential IncV phosphorylation sites	143
4.2.6.2.1	Potential phosphorylation in a C-Terminal Domain of IncV	143

4.2.6.2.2	Potential phosphorylation in the IncV serine tracts flanking the FFAT motifs	148
4.2.6.2.3	Additional Kinases Playing a Role in IncV Phosphorylation	150
4.3	Membrane Contact Sites in Host-Pathogen Interactions	151
4.3.1	FFAT Motif-Containing Proteins Encoded by a Pathogen	156
4.3.2	Pathogen-Encoded Proteins That Interact with Eukaryotic FFAT Motif-Containing Proteins	156
4.3.3	FFAT-Independent Pathogen-Mediated Membrane Contact Site Formation	158
4.3.4	Unknown mechanism of interaction between ER and Pathogen-Containing Compartment MCS	158
4.4	Future Directions	160
4.4.1	Dynamics of IncV Phosphorylation	160
4.4.2	IncV Serine Tracts, More Mimicry of Eukaryotic FFAT Motifs?	161
4.4.3	Role of Other Potential Phosphorylated Residues in the IncV-VAP interaction	162
4.4.4	Other Kinases Potentially Phosphorylating IncV	163
4.4.5	Other Possible Roles for IncV	163
4.4.6	Interplay between IncV and other ER-Inclusion MCS components	165
4.4.7	ER-Inclusion MCS and Inclusion Microdomains: One and the Same?	166
4.4.8	Subclasses of ER-Inclusion MCS	167
4.4.9	Dynamics of ER-Inclusion MCS formation	168
4.5	Final Conclusions	169
5	Chapter 5: References	172

Appendix 1	Primers and templates used for generating constructs in chapter 2	209
Appendix 2	Primers and templates used for generating constructs in chapter 3	212

Chapter 1
Introduction

Chapter 1: Introduction

1.1 *Chlamydia, the disease*

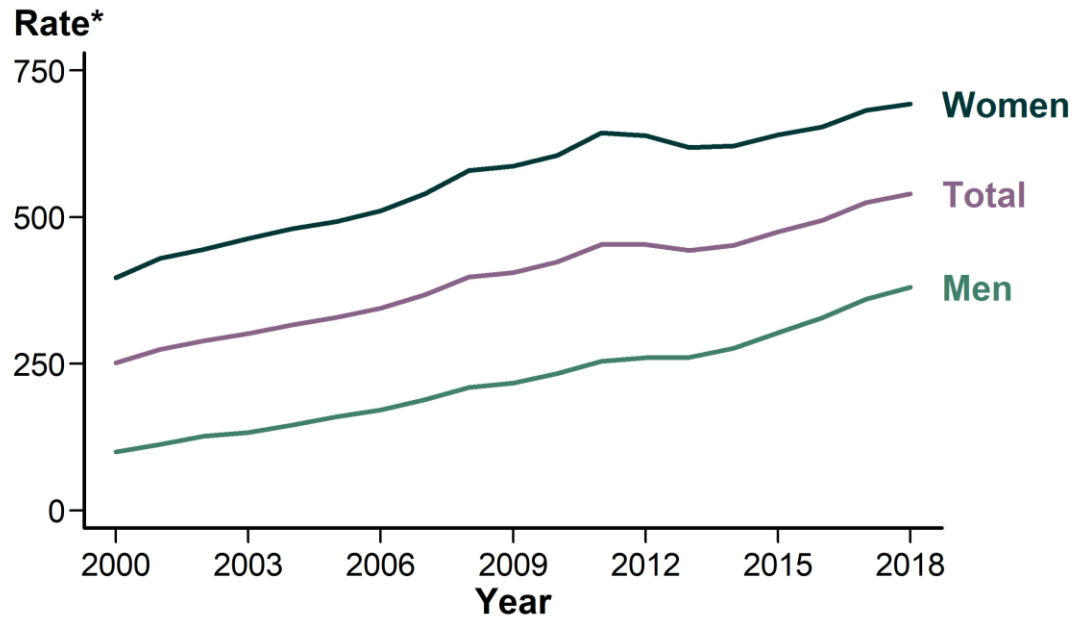
1.1.1 *Epidemiology*

1.1.1.1 *The Incidence of Sexually Transmitted Infections Worldwide*

Over 1 million bacterial sexually transmitted infections are estimated to occur daily around the world.¹ Globally, there are an estimated 376 million new cases in people between ages 15 and 49 every year with the top four non-viral sexually transmitted infections (STIs), *Chlamydia*, gonorrhea, syphilis and trichomoniasis.¹ Over one third (131 million) of these new infections are attributed to *Chlamydia trachomatis*, the causative agent of *Chlamydia*.²

1.1.1.2 *The Incidence of Sexually Transmitted Infections in the United States*

In 2018, there was an increase in reported cases for all three of the notifiable STIs of bacterial origin, *Chlamydia*, gonorrhea, and syphilis, in the United States (US) for the 5th year in a row (Figure 1.1).³ In the US, *C. trachomatis* is the most commonly reported infection, with about 1.8 million cases reported to the CDC in 2018.³ There has been a steady increase in reported *Chlamydia* infections between 2000 and 2018.³ The true incidence of *Chlamydia* infections is unknown because the majority of infections are asymptomatic.⁴ Adjusted to 2010 dollars, *Chlamydia* was the mostly costly sexually transmitted infection of bacterial origin in the US with an estimated \$517 million direct medical cost.⁵



* Per 100,000.

Figure 1.1. Reported cases of *C. trachomatis* sexually transmitted infections in the United States from 2000-2018. Rate is expressed per 100,000 people. Graph was obtained from the CDC website.

1.1.2 *C. trachomatis* Transmission

Most *C. trachomatis* infections affecting adults and teens are transmitted sexually.³ While there are no similar studies in the United States, one Australian study found that among females infected with *C. trachomatis*, 76% of their male partners also tested positive.⁶ A second Australian study assessed transmission rates male same sex couples and found that about half of the partners of those positive for urethral *C. trachomatis* tested positive for rectal *C. trachomatis*.⁷ Their findings suggested that transmission from urethra to rectum, and vice versa, might be less efficient than transmission between male and female genital tracts in heterosexual couples.⁷ However, no data was collected on the number of exposures, so it would be difficult to draw such conclusions. There are also no studies examining transmission rates to and from other anatomical sites such as the pharynx.⁸

1.1.3 Risk Factors for *C. trachomatis* Infection

Young people are more likely to be infected with *C. trachomatis* and those ages 15 to 24 make up nearly 60% of the reported cases in 2018.³ Females are infected at twice the rate of males.³ Having multiple or new sex partners is a risk factor for all sexually transmitted infections (STIs), as is inconsistent condom use.^{9–11} Having a history of previous *C. trachomatis* infection is a risk factor, though it is probably more related to behavior rather than biology.¹² Socioeconomic status and race have also been identified as risk factors.³ In particular, Blacks had a rate of reported infections that was 5.6 times higher than that of Whites in 2018.³ American Indian/Alaska Native and Native

Hawaiian/Other Pacific Islander were also disproportionately represented in the number of reported infections.³

1.1.4 Clinical Presentations of Chlamydia Infections

1.1.4.1 Overview of Chlamydia Species Infections in Humans

There are nine *Chlamydia* species including *C. trachomatis*, *C. pneumoniae*, *C. abortus*, and *C. psittaci* which can all infect humans.¹³ Depending on the anatomical site of infection and with which *Chlamydia* species, there are a diverse range of clinical manifestations of *Chlamydia* infections. *C. pneumoniae* typically infects the lungs and causes pneumonia, an inflammation of air sacs in one or both lungs.¹⁴ *C. abortus* is a pathogen that largely infects ruminants, but occasionally infects humans and can cause abortions their mammalian host.¹⁵ *C. psittaci* typically infects birds and livestock, and sometimes infects humans and causes flu-like symptoms that can progress into life-threatening pneumonia.¹⁶ The major *Chlamydia* species that infects humans is *C. trachomatis*, which causes eye infections, sexually transmitted infections, and rarely, pneumonia.¹⁷

1.1.4.2 Diseases Caused by *C. trachomatis*

C. trachomatis strains, referred to as serovars, are divided into two biovars: 1) the trachoma biovar, which contains ocular and urogenital strains; and 2) the Lymphogranuloma venereum biovar.¹⁸ The ocular serovars in the trachoma biovar (serovars A, B, Ba, and C) are generally known to cause an eye infection called trachoma which is characterized by conjunctivitis, swelling of the eyelids, and eye pain.¹⁹ The urogenital serovars in the trachoma biovar (serovars D, E, F, G, H, I, J, and K) mostly cause

infections of the genital tract which can lead to symptoms including discharge, bleeding, pelvic pain, and pain with urination.²⁰ The serovars in the Lymphogranuloma venereum biovar (L1, L2, L2a, L2b, and L3) cause an infection of the draining lymph nodes close to the site of entry called Lymphogranuloma venereum (LGV).²¹ LGV usually manifests as genital ulcers and swollen lymph nodes in the groin.²¹ Each serovar exhibits a preferred tissue tropism, though it is increasingly appreciated that most serovars are capable of infecting sites other than the preferred tissue.²⁰ For example, a study in Austria demonstrated the presence of serovars E and F in several ocular samples and serovar B in several genital samples.²² Another example is *Chlamydial* neonatal conjunctivitis which occurs when a pregnant woman who is infected with *C. trachomatis* genitally (most commonly serovars D-K) transmits the bacteria during birth.²³

1.1.5 Pathogenesis of *C. trachomatis* Infections

The majority of *C. trachomatis* infections are asymptomatic and thus, often go untreated.^{4,24} If left untreated, infections can progress to lifelong sequelae that interfere with quality of life. Trachoma, the leading cause of non-congenital blindness globally, can lead to severe scarring on the inside of the eyelid, which could then turn eyelashes inward where they continually scratch the eye, including the cornea.¹⁹ Once the cornea is scarred from constant scratching, the infected person can become irreversibly vision impaired or blind.¹⁹ In females, genital tract infections can ascend into the upper genital tract (uterus, fallopian tubes, or ovaries) and cause pelvic inflammatory disease, which can lead to extensive scarring within the upper genital tract.²⁵ This scarring can then

lead to complications such as chronic pelvic pain, infertility, and ectopic pregnancy.²⁵ In males, genital tract infections can extend into the testicles and cause epididymitis, inflammation of the tube that carries sperm, which can ultimately lead to sterility.²⁶ LGV can cause obstruction of the lymphatic system, which can lead to elephantiasis, the enlargement and hardening of body parts.²⁷ There is some evidence that, in some cases, *C. trachomatis* can travel to joints and lead to reactive arthritis.²⁸

1.1.6 Treatment of *C. trachomatis* Infections

Uncomplicated genital tract infections, as well as trachoma, can be treated with a single, large dose of oral azithromycin or oral doxycycline twice daily for seven days.²⁹ Azithromycin is considered safe to use during pregnancy, but doxycycline is not recommended after the 1st trimester.³⁰ Neonatal conjunctivitis is also treated with azithromycin.³⁰ Alternatives to the first-line treatments include quinolones and erythromycins.²⁹ Complicated urogenital infections and LGV are often treated with a combination of oral doxycycline taken for several weeks and an intramuscular injection of a quinolone.²¹

1.2 *Chlamydia*, an Obligate Intracellular Bacterium

1.2.1 Microbiological Description of *Chlamydia*

Chlamydiae are obligate intracellular, gram negative bacteria that replicate most commonly within epithelial cells and sometimes in macrophages and dendritic cells, though it is not currently known if the latter occurs in infected individuals.^{31–33} All *Chlamydiae* share a biphasic developmental cycle, where the bacteria transition to two forms (Figure 1.2).³⁴ The cycle begins when an infectious, non-replicating elementary

body (EB) attaches to a host cell and induces its own endocytosis.³⁵ From this point forward, the bacteria reside exclusively within a membrane-bound vacuole called the inclusion.³⁶ The nascent inclusion, containing one EB, traffics along microtubules until it reaches the microtubule organizing center (MTOC) in a perinuclear region.^{37,38} The EB converts into a replicating, non-infectious reticulate body (RB).³⁵ If more than one EB entered the same cell, the separate inclusions fuse to form a single inclusion.³⁹ As RBs replicate, the inclusion becomes larger to accommodate the increasing number of bacteria.³⁵ Eventually, RBs convert asynchronously into EBs which then exit the cell through host cell lysis or extrusion of the inclusion.⁴⁰

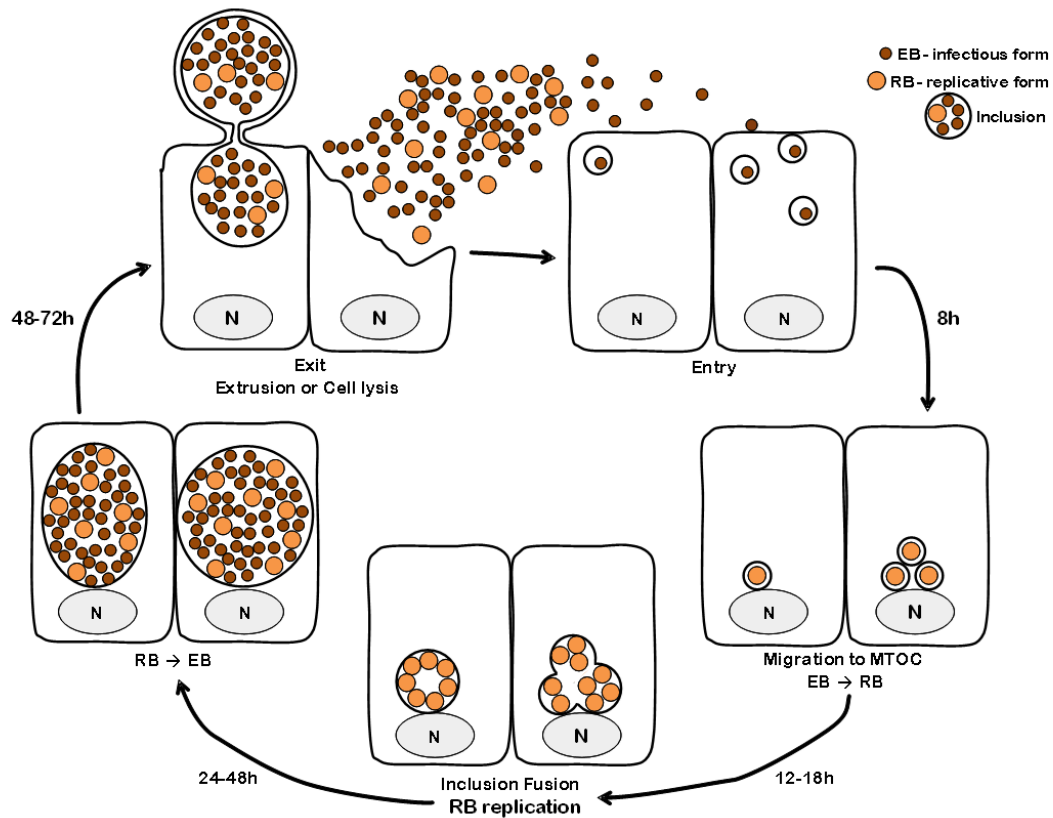


Figure 1.2. *Chlamydia* developmental cycle. Infectious elementary bodies (EB) enter an epithelial cell and are enclosed in a membrane vacuole called the inclusion. Nascent inclusions travel down microtubules until they reach the microtubule organization center (MTOC) next to the nucleus. By 8 hours post-infection, EBs have transitioned into the replicating reticulate bodies (RB). If multiple bacteria enter a cell, the individual inclusions will fuse around 12-18 hours post-infection. RBs replicate until 24 – 48 hours post infection when they begin to transition back into EBs asynchronously. 48-72 hours post infection, bacteria exit the cell through cell lysis or inclusion extrusion. N = nucleus. This figure was adapted from Bastidas *et al.*⁴¹

1.2.2 *Chlamydia* Genetics and Genetic Tools

A common way to determine protein function in many organisms is to mutate or delete the corresponding gene and/or to introduce extrachromosomal DNA, such as plasmids, containing the given gene. It was not until recently that tools to genetically manipulate *Chlamydia* were available and the recent advances have been essential for furthering our understanding of *Chlamydia* biology.⁴²⁻⁴⁴

1.2.2.1 The *Chlamydia* Genome

Over millions of years of co-evolution with the human host, *C. trachomatis* has reduced its genome to about 1 million base pairs that encode about 900 open reading frames (ORFs).¹⁸ There are relatively few examples of recently acquired genes from foreign sources, but the majority of acquired genes bear more similarity to eukaryotic genes than prokaryotic genes.⁴⁵ Because many bacterial metabolic enzymes are missing, the bacteria rely on the host for several metabolic processes.⁴⁵ For example, *Chlamydia* possesses a mostly intact glycolytic pathway missing the gene encoding an enzyme that catalyzes the conversion of fructose bisphosphate into glyceraldehyde-3-phosphate.⁴⁵ As a result, *C. trachomatis* cannot use glucose and must import glucose-6-phosphate from the host. Additionally, *Chlamydia* is auxotrophic for most amino acids, likely due to the considerable lack of amino acid biosynthesis enzymes.⁴⁵ The *Chlamydia* genome lacks homologs encoding enzymes and other proteins involved in the uptake of foreign DNA including transformation, competence, restriction enzymes, phages, or transposons.⁴⁵ However, there is evidence of recombination machinery, including enzymes

involved in DNA repair, replication, and recombination, suggesting *Chlamydia* is at least capable of recombining DNA.⁴⁵ Conversely, the *Chlamydia* genome lacks orthologs of oxidative DNA damage repair enzymes and mismatch repair.⁴⁵

1.2.2.2 The *Chlamydia* Cryptic Plasmid

Chlamydia have an eight ORF plasmid referred to as a cryptic plasmid.⁴⁶ These ORFs play roles in transcriptionally regulating chromosomal genes and virulence *in vivo*.⁴⁷ There are about 10 copies of the plasmid per genome.⁴⁸ The plasmid is apparently not required for *Chlamydia* propagation as there are laboratory strains that have been cured of the plasmid and still replicate efficiently.⁴⁹ However, plasmid-less strains are less virulent during animal infections, highlighting the importance of the cryptic plasmid *in vivo*.^{49,50}

1.2.2.3 *Chlamydia* Transformation and Cloning Vectors

Obligate intracellular pathogens have been notorious for requiring challenging and inefficient genetic tools.⁵¹ The first barrier encountered for transforming any organism is that foreign DNA must be taken up by the cell. In *Chlamydia*, one must consider several factors such as which form of the bacteria to target. EBs have a highly cross-linked outer membrane that could impede foreign DNA delivery.⁵² On the other hand, RBs are not infectious and are contained within an inclusion within the host cell, presenting at least four membranes to cross to get into the bacterial cytosol.³⁵ Multiple lines of evidence demonstrate that transformation of the EB form is more efficient.^{44,49,53–56} The most efficient method of transformation to date is calcium based.⁵³

Another layer of difficulty was added by the *Chlamydia* cryptic plasmid. The origin of replication in the *Chlamydia* plasmid is not functional in *E. coli*.^{44,46,49} To circumvent this challenge, *C. trachomatis*-*E. coli* shuttle vectors were designed such that they contained the necessary *Chlamydia* components to maintain the plasmid, combined with DNA suitable for plasmid maintenance and replication in *E. coli*.^{53,54,57}

1.2.2.4 Fluorescent Proteins and Inducible Gene Expression in *C. trachomatis*

An important tool developed for studying *C. trachomatis* was the introduction of fluorescent protein expression. This allowed for the visualization of *Chlamydia*-infected cells without having to immunostain a bacterial protein and also allowed for straightforward live imaging of the developmental cycle.^{53,54} Not long after fluorescent protein expression was possible in *C. trachomatis*, systems for inducible expression of fluorescent proteins and tagged *C. trachomatis* proteins were developed.^{55,57,58} Inducible expression was an instrumental tool because it allowed for studying protein functions at various times during the developmental cycle.⁵⁷⁻⁶² Inducible expression from a *Chlamydia*-*E. coli* shuttle vector is now widely used and has proved essential for functional studies.⁵⁷⁻⁶²

1.2.2.5 Mutating the *C. trachomatis* Genome

The first instances of generating of a *Chlamydia* null mutant was a complicated process involving chemical mutagenesis combined with the mismatch specific endonuclease CEL I or whole genome sequencing and a collection of mutants was generated.⁶³⁻
⁶⁵ One method relied on the rare event of a single point mutation to generate an early stop codon and the base pair mutated was mostly random.⁶⁵ Another method used high

concentrations of a chemical mutagen which resulted in multiple mutations per genome.⁶³ This meant that screening of many mutants and whole genome sequencing was required to confirm the mutation sites.^{63–65} To optimize generation of null mutants, the TargeTron system was applied to *C. trachomatis* and allowed for site-specific, targeted disruption of genes by the insertion of a Type II intron.⁵⁶ Many *C. trachomatis* genes have been mutated with TargeTron, but it requires a proprietary algorithm to identify suitable insertion sites.^{61,66–72} Even though it is site specific, TargeTron can still lead to the generation of functional, truncated gene products instead of a true null mutant, have off target insertions, or not be inserted at all.⁷³ Fluorescence-Reported Allelic Exchange (FRAEM) was developed to completely replace a given gene with a fluorescent marker and a resistance cassette.⁷⁴ A new version of FRAEM was recently developed, called Floxed-Cassette Allelic Exchange Mutagenesis (FLAEM), that allows for the removal of the fluorescent protein and resistance cassette after FRAEM using a Cre-lox system to generate a marker-less mutant.⁷⁵

1.2.3 *Chlamydia* Effector Proteins

1.2.3.1 Type III Secretion System in *Chlamydia*

Many pathogens utilize a needle-like apparatus, called type III secretion system (T3SS), to inject effector proteins into the target host cell to promote bacterial survival and manipulate host factors to establish the bacterial niche (Figure 1.3 A).⁷⁶ The *Chlamydia* T3SS was first discovered in *C. psittaci* which contains several open reading frames that are homologous to *Yersinia* T3SS genes.⁷⁷ One year later, a T3SS was

identified in *C. trachomatis* when the genome was sequenced.^{45,78} Additionally, all *Chlamydia* species genomes sequenced to date contain T3SS subunit genes.^{79–82} Initially, *Chlamydia* EBs use T3SSs presynthesized by RBs to inject presynthesized effector proteins across the host cell plasma membrane that facilitate bacterial entry into the cell.^{83–85} Once an inclusion is formed, *Chlamydia* establishes an intracellular niche by using the T3SS to translocate effector proteins that manipulate its host cell surroundings and to modify the inclusion.^{36,86} Effectors are categorized based on when they are expressed during the developmental cycle and their expression mostly corresponds with specific stages of the cycle. Early effectors are expressed just after the transition from EB to RB.⁸⁷ Early effectors are proposed to be involved in modifying the inclusion membrane.^{34,87,88} Mid-cycle effectors are expressed during RB replication and are proposed to facilitate nutrient acquisition, inclusion membrane maintenance, and innate immunity modulation.^{34,87,88} Late effectors are expressed as RBs convert to EBs through the end of the cycle and some late effectors are packaged into EBs to facilitate entry into a new cell.^{34,87,88} An overview of T3SS effectors of *C. trachomatis* functions and temporal category are presented in Table 1.1

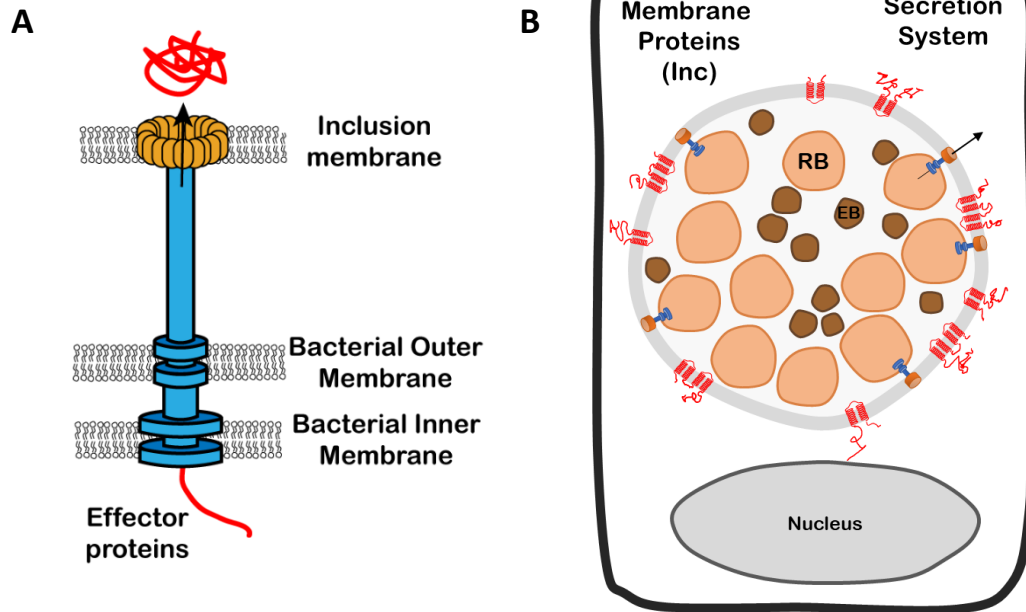


Figure 1.3. Type III secretion system and Inclusion membrane proteins. A) Schematic of generic bacterial type III secretion system (T3SS). The T3SS is embedded into both bacterial membranes and a 3rd membrane that interfaces with the target cell cytosol. Effector proteins are translocated from the bacterial cytosol to the environment on the opposite side of the 3rd membrane. B) Schematic depicting an inclusion in an epithelial cell. The *Chlamydia* T3SS (blue/orange) is inserted through both bacterial membranes and the inclusion membrane and translocates effector proteins into the host cytosol. Inclusion membrane proteins (Inc) (red) are effector proteins that are embedded into the inclusion membrane and have cytosolic tails. RB, *Chlamydia* reticulate body. EB, *Chlamydia* elementary body.

Table 1.1 *C. trachomatis* Type III Secretion System effector proteins

Serovar D/L2 annotations, Common Name	Temporal Class ^{87,89}	Host interacting partner(s)	Proposed role and/or localiza-tion	References
Non-Inc proteins				
CT042/CTL0298, GlgX	No data	None	Glycogen hydrolase in inclusion lumen	90
CT089/CTL0344, CopN	No data	Unknown	Regulates T3SS at inclusion membrane	91
CT105/CTL0360, CteG	mid	Unknown	Modulates host cell vesicular trafficking	92
CT142/CTL0397, None	mid	Unknown	Unknown function in inclusion lumen	93
CT143/CTL0398, None	mid	Unknown	Unknown function in inclusion lumen	93
CT144/CTL0399, None	mid	Unknown	Unknown function in inclusion lumen	93
CT456/CTL0716, TarP	mid	Actin, Abl1, Vav2, PI3K, SHC1	Nucleates actin, promotes host cell survival	94–99
CT529/CTL0791, Cap1	early	Unknown	Associates with lipid droplets and inclusion membrane	100,101
CT620/CTL0884, None	mid	ESCRT	Unknown function in inclusion lumen, host cytosol, nucleus	102
CT621/CTL0885, None	mid	ESCRT	Unknown function in in-clusion lumen, host cyto-sol, nucleus	102
CT622/CTL0886, None	early	Unknown	Promotes bacterial growth in in-clusion lumen and host cytosol	103,104
CT694/CTL0063, TmeA	late	AHNAK	Promotes host cell invasion	75,85,105

CT695/CTL0064, TmeB	late	Unknown	Unknown function in the cytosol	106
CT711/CTL0080, None	mid	ESCRT	Unknown function in the nucleus	102
CT737/CTL0106, NUE	late	Histones	Histone methyltransferase in nucleus	107
CT798/CTL0167, GlgA	late	None	Glycogen synthase in inclusion lumen	108
CT875/CTL0255, TepP	early	CRK, CRKL, PI3K, GSK3	Manipulates host gene expression	71,84
Inc Proteins				
CT005/CTL0260, IncV	early	VAPA/VAPB	ER-Inclusion MCS tether	109
CT006/CTL0261, None	early	Unknown	Unknown	
CT101/CTL0356, MrcA	mid	ITPR3	Promotes inclusion extrusion	61
CT115/CTL0370, IncD	early	CERT	Lipid transfer at ER-Inclusion MCS	58,110
CT116/CTL0371, IncE	early	SNX5/SNX6	Restricts retromer	60,111
CT117/CTL0372, IncF	early	Unknown	Inc-Inc Interactions	59
CT118/CTL0373, IncG	early	14-3-3 β	Unknown	112
CT119/CTL0374, IncA	mid	VAMP3/VAMP7/VAMP8	Homotypic fusion of inclusions, inhibit fusion with endolysosomal system	56,70,113-116
CT134/CTL0389, None	early	Unknown	Unknown	
CT135/CTL0390, None	early	Unknown	Unknown	
CT147/CTL0402, None	early	Unknown	Unknown	
CT179/CTL0431, None	mid	Unknown	Unknown	
CT192/CTL0444, None	early	Unknown	Unknown	

CT222/CTL0475, None	mid	Unknown	Inc-Inc interactions	117
CT223/CTL0476, IPAM	mid	CEP170	Manipulates host microtubules, inhibits host cell cytokinesis	118,119
CT224/CTL0477, None	early	Unknown	Inhibits host cell cytokinesis	119
CT225/CTL0477A, None	early	Unknown	Inhibits host cell cytokinesis	119
CT226/CTL0478, None	early	Unknown	Unknown	
CT227/CTL0479, None	early	Unknown	Unknown	
CT228/CTL0480, None	early	MYPT1	Inhibits inclusion extrusion	66,120
CT229/CTL0481, CpoS	early	RAB GTPases	Inhibits host cell death, modulates host cell vesicular trafficking	67,68,121,122
CT232/CTL0484, IncB	early	Unknown	Unknown	
CT233/CTL0485, IncC	early	Unknown	Unknown	
CT249/CTL500A, None	early	Unknown	Unknown	
CT288/CTL0540, None	early	CCDC146	Inclusion microdomain localization	123
CT345/CTL0599, None	early	Unknown	Unknown	
CT358/CTL0612, None	early	Unknown	Unknown	
CT383/CTL0639, None	early	Unknown	Promotes stability of inclusion membrane	67
CT440/CTL0699, None	early	Unknown	Unknown	
CT442/CTL0701, CrpA	mid	Unknown	Unknown	
CT449/CTL0709, None	early	Unknown	Unknown	
CT483/CTL0744, None	early	Unknown	Unknown	
CT556/CTL0819, None	mid	Unknown	Unknown	

CT565/CTL0828, None	early	Unknown	Unknown	
CT618/CTL0882, None	mid	Unknown	Unknown	
CT813/CTL0184, InaC	mid	14-3-3 proteins, ARF1/ARF4, VAMP7/VAMP8	Post-translational modification of microtubules, actin remodel- ing, promotes Golgi fragmenta- tion	69,124
CT850/CTL0223, None	late	DYNLT1	Inclusion localization at centro- some, inclusion microdomain localization	125

1.2.3.2 Inclusion Membrane Proteins

Some of the T3SS translocated effector proteins become embedded into the inclusion membrane after their translocation and are called inclusion membrane proteins, or Incs (Figure 1.3 B).^{36,116,126–129} Depending on the serovar, *C. trachomatis* has 30 to 60 predicted Incs.^{128,129} Most Incs are expressed early in the developmental cycle and are thought to play roles in establishing the inclusion.⁸⁷ Incs are defined by having one or more bilobed transmembrane domains with one or more tails facing the host cytosol.¹¹⁶ These cytosolic tails are well positioned to interact with host molecules and manipulate host cell processes. Interestingly, Incs do not share sequence homology amongst themselves and only a few share structural homology regions with proteins in other organisms.^{127,128} Thus, characterization of Incs has been challenging. However, much progress was made over the last several years in the field of Incs, in part because of the increasing availability of genetic tools. An overview of Inc protein functions is presented in Table 1.1 and below.

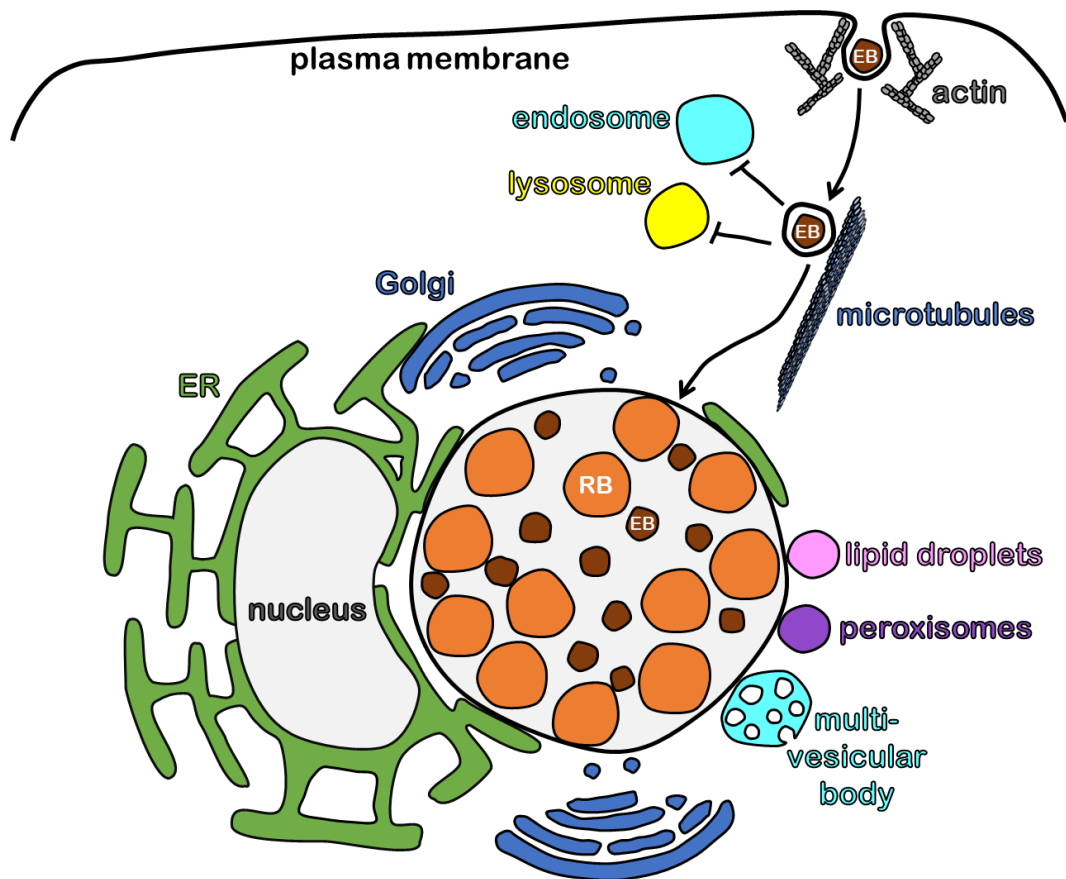
1.2.4 Chlamydia Interactions with the Host

1.2.4.1 Interactions Between the Inclusion and Host Factors

As an intracellular pathogen that relies on the host for many processes to maintain an intracellular niche, *Chlamydia* must interact with host cell components. Since *Chlamydia* resides within the inclusion and does not directly contact host cell components in the cytosol, the inclusion offers a platform through which the bacteria can interact with host cell components. The inclusion has been shown to interact with several

host cell cytoskeletal elements and organelles including multivesicular bodies, the Golgi apparatus, the endoplasmic reticulum, and the plasma membrane.^{34,88} In addition to these interactions, it is now well known that *Chlamydia* require several host lipids, such as phospholipids, sphingomyelin, and cholesterol, to complete the developmental cycle.¹³⁰ A schematic overview of interactions between the inclusion and host cell components is presented in Figure 1.4. Importantly, Inc proteins are a major player in the interactions between host components and the inclusion.

A



B

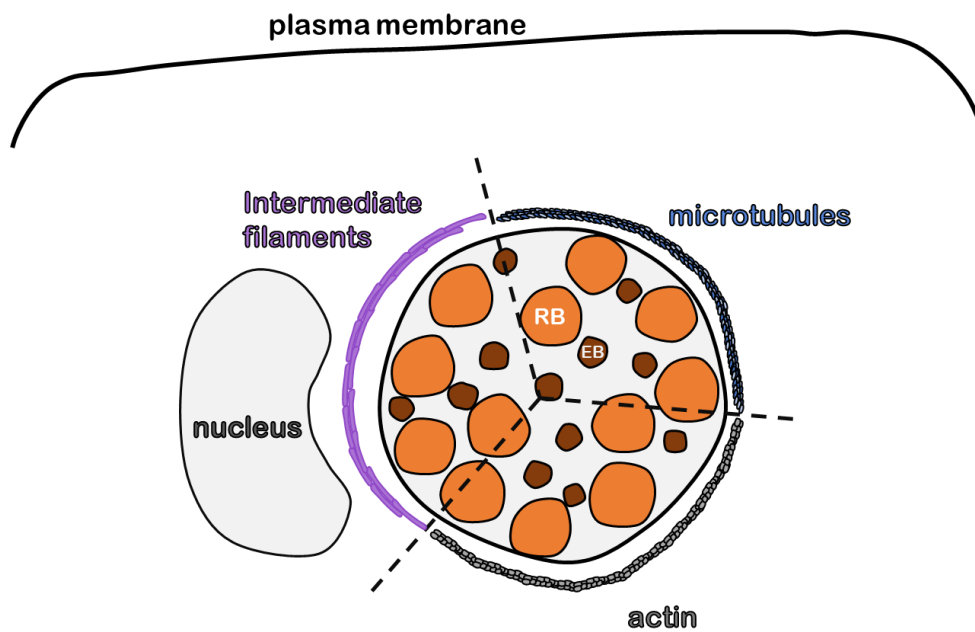


Figure 1.4. *Chlamydia* inclusion interactions with host factors. A) Schematic depicting various interactions between *Chlamydia* and host organelles and molecules. An infectious elementary body (EB, brown) attaches to the plasma membrane and manipulates the host actin cytoskeleton (grey). After entering the cell, the EB is enclosed in a membrane-bound vacuole called the inclusion (black circle encasing EB and RB) and EBs convert to the replicative form of the bacteria, reticulate bodies (RB, orange). The inclusion quickly diverts from the endocytic cycle and does not fuse with endosomes (cyan) or lysosomes (yellow). The inclusion travels down microtubules (blue) until it reaches a region near the nucleus (light grey). Throughout the developmental cycle, the inclusion interacts with several host organelles. Infection induces the fragmentation of the Golgi apparatus (blue) into functional mini-stacks that surround the inclusion. The endoplasmic reticulum (green) directly contacts the inclusion membrane. Multivesicular bodies (cyan with white circles), lipid droplets (pink), and peroxisomes (purple) associate with the inclusion and may translocate into the inclusion lumen. B) The inclusion is surrounded by cages of actin (grey), post-translationally modified microtubules (blue), and intermediate filaments (purple).

1.2.4.1.1 Interactions with the Host Cytoskeleton

The actin cytoskeleton plays a major role in the *Chlamydia* developmental cycle. After EBs attach to the host cell, pre-synthesized effector proteins are translocated into the host cytosol via the T3SS.^{83–85} One of the first effector proteins released is the translocated actin-recruiting phosphoprotein (TarP) which contains actin-binding domains.⁸³ Upon its translocation into the host cell, TarP recruits and nucleates actin, which results in membrane remodeling and internalization of the bacteria.¹³¹ Actin also seems to play a role in stabilizing the inclusion during the rest of the developmental cycle.¹³² Both actin and intermediate filaments form a cage around the inclusion that is thought to maintain the integrity of the inclusion membrane.¹³² Several host factors and one Inc protein, InaC, have been shown to play a role in actin cage formation.^{63,133} Microtubules also play important roles in the *Chlamydia* developmental cycle. Nascent inclusions traffic along microtubules until they reach the Microtubule Organizing Center (MTOC). Several Incs (MrcA, CT222, IPAM, CT224, CT228, IncB, IncC, CT288, and CT850) localize to a region on the inclusion membrane near the MTOC and IPAM, CT288, and CT850 are proposed to facilitate interactions with the MTOC, as well as the actin cytoskeleton.^{37,38,118,120,125,134} In addition to the actin cage, there is also a cage of post-translationally modified microtubules formed around the inclusion and the microtubule cage formation relies on several host and Incs (InaC and IPAM).^{69,118,135,136}

1.2.4.1.2 Escape from the Endocytic Pathway

It has been known for decades that the inclusion rapidly escapes the endocytic pathway after bacterial internalization. The inclusion is negative for late endosome and lysosomal markers and the lumen of the inclusion is not acidified.¹³⁷ Despite its diversion from the endocytic pathway, the inclusion still associates with many endolysosomal pathway components, such as RAB GTPases, sorting nexins, and endocytic SNARE protein.^{60,138–141} For example, IncA contains SNARE motif mimics and IncA, InaC, and IPAM recruit host SNARE proteins which are proposed to inhibit lysosomal fusion with the inclusion.^{114,115,142} Additionally, IncE was shown to sequester retromer (a protein complex that recycles endosome cargo) components and could play a role in preventing lysosomal fusion with the inclusion.⁶⁰ Despite inhibiting several steps in the endolysosomal pathway, an interesting finding was that the contents of multivesicular bodies, a late endocytic organelle, are translocated into the inclusion lumen as a source of host lipids.^{139,143}

1.2.4.1.3 *Manipulation of the Golgi Apparatus*

Partway through the *Chlamydia* developmental cycle, the Golgi apparatus becomes fragmented into “mini-stacks” which are then positioned around the inclusion.¹⁴⁴ Since *Chlamydia* requires host lipids, such as sphingomyelin, to complete its developmental cycle and these lipids are synthesized in the Golgi, mini-stack formation had previously been proposed to facilitate lipid delivery.¹⁴⁴ However, recent studies have demonstrated that Golgi fragmentation is not required for lipid delivery.¹⁴⁵ The Inc protein InaC controls the position of the mini-stacks around the inclusion, but an *inaC*

mutant strain of *C. trachomatis* is not deficient in sphingolipid trafficking.⁶³ Thus, the precise role of Golgi fragmentation is still unclear. Nevertheless, *C. trachomatis* is known to incorporate sphingomyelin into the inclusion membrane and bacterial cell walls.¹⁴⁶ This sphingomyelin acquisition is essential for *C. trachomatis* development.¹⁴⁷ It was shown that Golgi-derived sphingomyelin-containing vesicles fuse with the inclusion. Interestingly, when cells were pretreated with Brefeldin A, an inhibitor of vesicular trafficking, sphingomyelin accumulation in the inclusion was decreased and inclusions were smaller, but Brefeldin A treatment had no effect on infectious progeny production.¹⁴⁶ These data suggested a non-vesicular route of sphingomyelin acquisition.

1.2.4.1.4 Direct Contact with the ER

The inclusion establishes direct contact with the endoplasmic reticulum (ER). First identified over a decade ago, electron micrographs revealed that ER was closely associated with the inclusion membrane.¹⁴⁸ Our lab, concurrently with Elwell *et al*, subsequently confirmed ER and Inclusion association using confocal fluorescence and electron microscopy approaches (Figure 1.5).^{110,149} It was observed that the inclusion was covered in patches of ER and that the ER and inclusion membranes did not fuse.^{110,150} The measured distance between the ER and inclusion membranes was about 10-20nm.^{110,150} Because of their striking resemblance to Membrane Contact Sites (discussed in detail in the following section), we named them ER-Inclusion Membrane Contact Sites.^{110,151} An independent study showed that the *Chlamydia* inclusion contacts the ER in a structure referred to as a pathogen synapse, which contain ordered arrays of bacterial T3SS

connect the bacterial, inclusion, and ER membranes.¹⁵⁰ It is unclear at this point, whether ER-Inclusion MCS and the *Chlamydia* pathogen synapse is referring to the same structure.

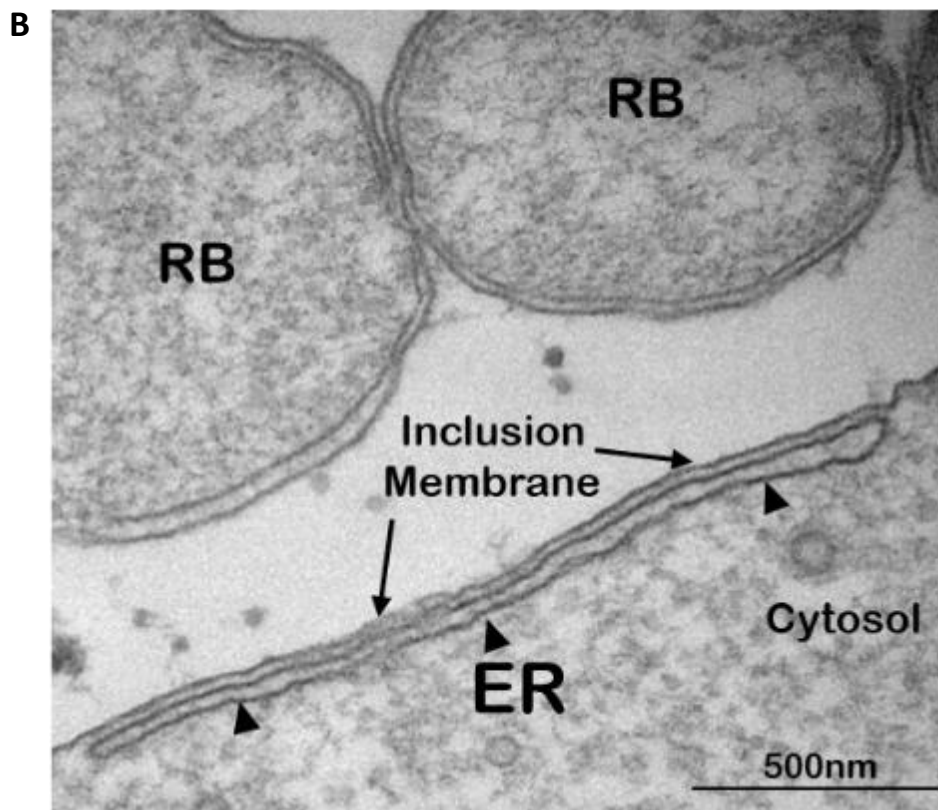
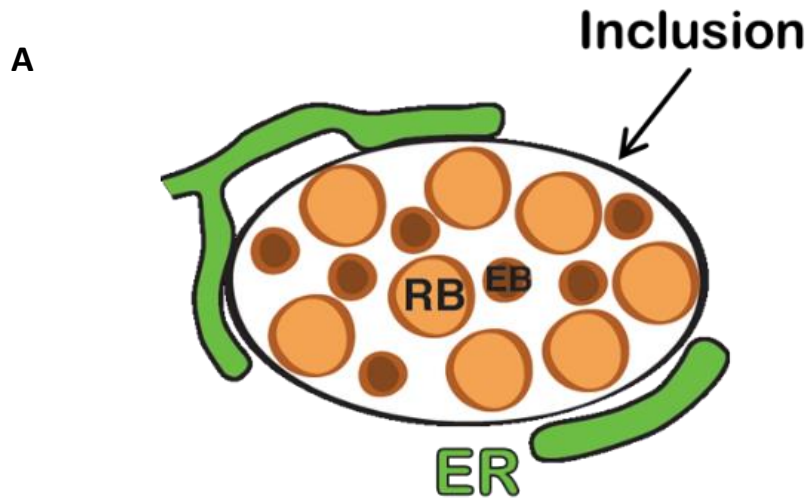


Figure 1.5. ER-Inclusion Membrane Contact Sites. A) Schematic depicting the contact between the endoplasmic reticulum (ER) and the inclusion membrane. RB, reticulate body. EB, elementary body. B) Transmission electron micrograph (TEM) of *C. trachomatis* infected HeLa cell and showing the close contact of the ER (arrowheads) with the inclusion membrane (arrows). The scale bar is 500nm. ER, endoplasmic reticulum. RB, reticulate body. EB, elementary body.

1.3 Membrane Contact Sites

1.3.1 What is a Membrane Contact Site?

The compartmentalization of cells into discrete organelles with a membrane enclosure allows for the spatial concentration of specialized functions. However, this presents a challenge when the different organelles need to talk to each other and/or exchange materials that do not easily diffuse across membrane. Vesicular trafficking is a major means of transporting lipids between different membranes within the cell. However, blocking vesicular trafficking does not cease all lipid trafficking.^{152,153} It is being increasingly appreciated that lipids and small molecules are also transported at sites where membranes of different organelles interface.¹⁵⁴⁻¹⁶¹ These platforms are called Membrane Contact Sites (MCS) and are defined as zones of close apposition, typically about 10-30nm apart, between two membranes with no fusion occurring.¹⁵⁴⁻¹⁶² MCS have been identified between almost all organelle pairings, and the largest membrane bound organelle, the endoplasmic reticulum (ER), is often one of the partnering organelles. A schematic overview of a selection of Membrane Contact Sites is presented in Figure 1.6.

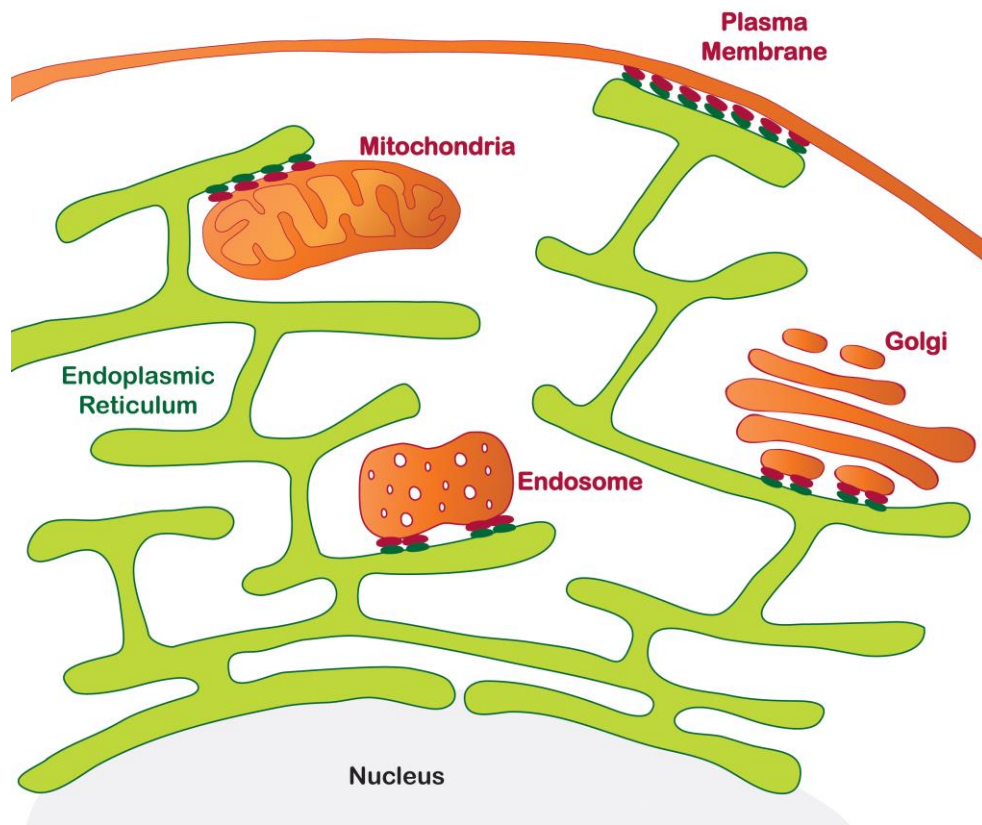


Figure 1.6. Membrane contact sites structure and function. The endoplasmic reticulum (green) contacts most other organelles (orange, shown here are mitochondria, endosome, Golgi) and the plasma membrane. Proteins enriched at each MCS are depicted with green and red ovals.

1.3.2 Components of MCS

There are four subclasses of proteins within MCS: 1) structural, 2) functional, 3) sorting, and 4) regulating (Figure 1.7).¹⁶² Structural proteins bridge the space between the membranes, maintaining a specific distance that allows functional components to perform their functions.^{162,163} For example, junctophilin proteins are anchored into the ER and have a domain with affinity for the plasma membrane (PM).¹⁶⁴ In the absence of junctophilin ER-PM MCS fail to assemble and Ca²⁺ signaling is defective at these sites in excitable cells.¹⁶⁴ Functional proteins play an active role in transferring small molecules such as lipids or ions. The activity of the ceramide transfer protein (CERT) in transferring ceramide from the ER to the Golgi places it in the functional category.¹⁶⁵ Sorting proteins recruit specific proteins or modify membrane lipids to define the molecular components of a given contact site.¹⁶² For example, phosphoinositide kinases localized to certain MCS modify phosphatidylinositol to enrich that contact in specific phospholipids, which then recruit proteins with domains specific to a given phospholipid.¹⁶⁶ Regulating proteins modulate the formation, maintenance, or function of MCS.¹⁶² For example, phosphorylation of a tether protein by an unidentified kinase at mitochondria and vacuole contacts in yeast disrupts vacuole-mitochondria MCS.¹⁶⁷ It is also important to note that tethering proteins at MCS can also be functional components.

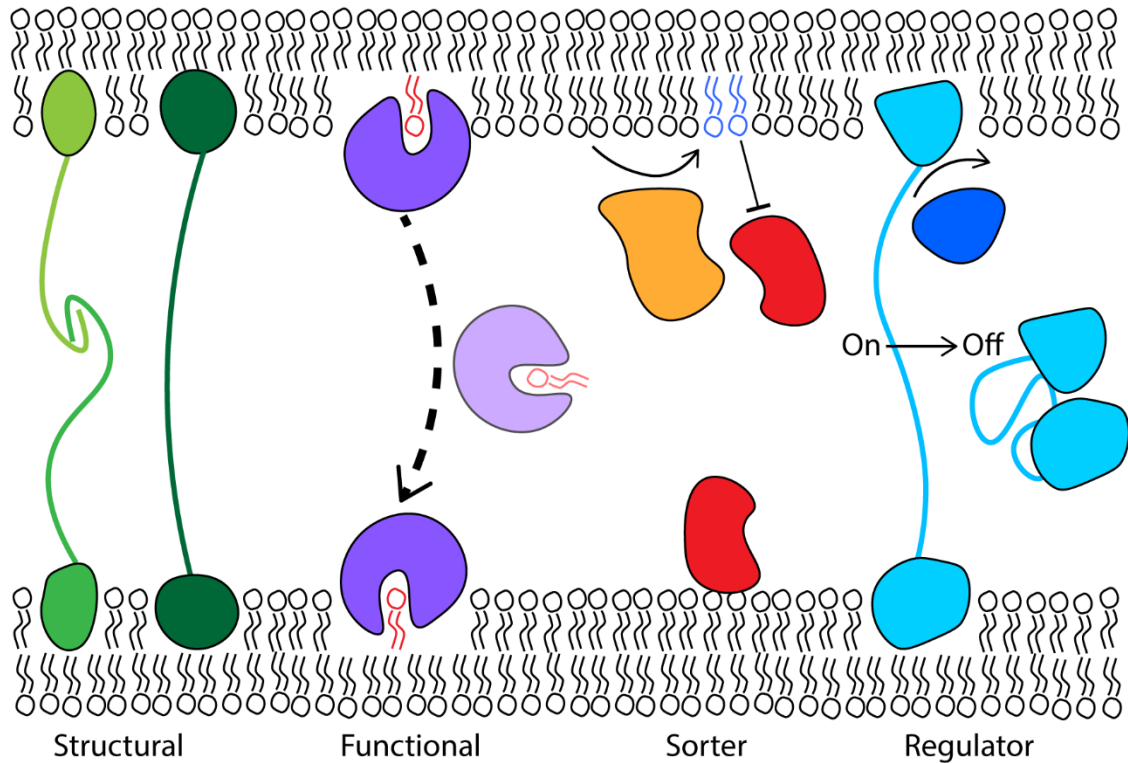


Figure 1.7. Types of Proteins at Membrane Contact Sites. Schematic depicting the different categories of proteins found at Membrane Contact Sites. Structural proteins (light and dark green) tether the opposing organelles together. Functional proteins (purple) perform a specific function such as lipid transfer or ion exchange. Sorter proteins (red) recruit specific proteins and repel other proteins. Regulator proteins (dark blue) control the function or formation of Membrane Contact Sites.

1.3.3 Functions of ER-Containing MCS

1.3.3.1 Calcium Signaling

Calcium (Ca^{2+}) signaling is an important mechanism used by the cell to alert the cell to changes and initiate downstream signaling. The ER maintains a relatively high Ca^{2+} ion concentration within its lumen compared to cytosolic Ca^{2+} concentration.^{168,169} This ER Ca^{2+} store can be released in response to external stimuli to initiate Ca^{2+} signaling in the cytosol or other organelles, such as mitochondria or endosomes.¹⁷⁰ MCS are formed between the ER and mitochondria or endosomes to facilitate efficient and rapid Ca^{2+} transfer from the ER.¹⁷¹ Additionally, once Ca^{2+} stores in the ER have decreased, they must be refilled to maintain ER Ca^{2+} homeostasis.¹⁷¹ The ER-resident Ca^{2+} sensor molecule STIM1 detects low ER luminal Ca^{2+} which induces oligomerization of STIM1 molecules.¹⁷² Clustered STIM1 then interact with the plasma membrane, thus forming ER-plasma membrane MCS, and recruits Ca^{2+} specific Orai channels to stimulate ER Ca^{2+} store refilling.¹⁷³

1.3.3.2 Lipid Exchange

Eukaryotic cells contain lipids that are used to make membranes, store energy, and for communication between cells. Most lipids found in cells are synthesized in the ER and then must be delivered to the correct location.¹⁷⁴ Vesicular trafficking is one way lipids can be delivered, but some organelles, such as peroxisomes, are not connected to the ER via vesicular trafficking.¹⁷⁵ Nonvesicular lipid exchange at MCS provides a source of lipids for many membranes. Lipid transport proteins (LTPs) extract one lipid from a

certain membrane and transfer it to another membrane.¹⁵⁵ Different LTPs localize to certain MCS by binding to lipids and/or proteins enriched at the contact.^{155,158} For example, CERT contains one Golgi-targeting domain and one ER-targeting domain to position it at ER-Golgi MCS.¹⁷⁶ CERT contains a ceramide-binding domain that transfer ceramide from the ER to the Golgi.¹⁷⁶

1.3.4 Formation and Maintenance of ER-Containing MCS

1.3.4.1 Membrane Tethering

For functional components of MCS to perform their functions, the two membranes must be brought together and held in place. Proteins that bridge the two membranes are referred to as tethers.¹⁶³ To be considered an MCS tether, a protein must fulfill the following four criteria: 1) enriched in the MCS, 2) mediates binding to opposing membranes, 3) its overexpression increases the area of the MCS, and 4) its deletion decreases the MCS.^{157,163} The fourth criterium has been challenging to prove because there can be redundancy in tethering. For example, in yeast, six tethers must be deleted before ER-plasma membrane MCS are depleted.¹⁷⁷

1.3.4.2 Connecting the ER to Other Organelles Through a Common Protein

Many MCS formed between the ER and other organelles are enriched in the ER-resident vesicle-associated membrane protein-associated protein (VAP) proteins.¹⁷⁸ There are two VAP proteins (VAPA and VAPB) in vertebrates, and because of their high homology, they are together referred to as VAP.¹⁷⁸ VAP contains a globular domain with homology to major sperm protein (MSP), short linker regions, a predicted coiled-coil

domain, and a transmembrane helix which anchors it to the ER (Figure 1.8A).¹⁷⁹ ER-integral VAP interacts with a broad range of proteins on different organelles.¹⁷⁸ Most VAP-interacting proteins contain one or more phenylalanine-phenylalanine (FF) in an acidic tract (FFAT) motifs that interact with an electropositive face in the MSP domain of VAP.^{179–181} FFAT motifs are defined by a core motif made of seven amino acids with the consensus motif of E¹-F²-F³-D⁴-A⁵-x-E⁷, where x is any amino acid.^{178–182} Several proteins containing FFAT motifs that have been identified and an alignment of their FFAT motif cores demonstrates that there is considerable variation tolerated in any core amino acid except for position 2, which must be a phenylalanine (F) or tyrosine (Y) (Figure 1.8B).^{178,182} The other important component of FFAT motifs is an acidic tract which is an enrichment of acidic residues flanking the core of the motif.¹⁸⁰ Acidic tracts are thought to provide an initial, nonspecific interaction with the electropositive face on the VAP MSP domain before the core of the FFAT motif then binds stably in a hydrophobic pocket.¹⁷⁹ VAP-interacting proteins, which are often lipid transfer proteins, interact with VAP using a FFAT motif and contain at least one other domain targeting the opposing organelle.¹⁵⁸

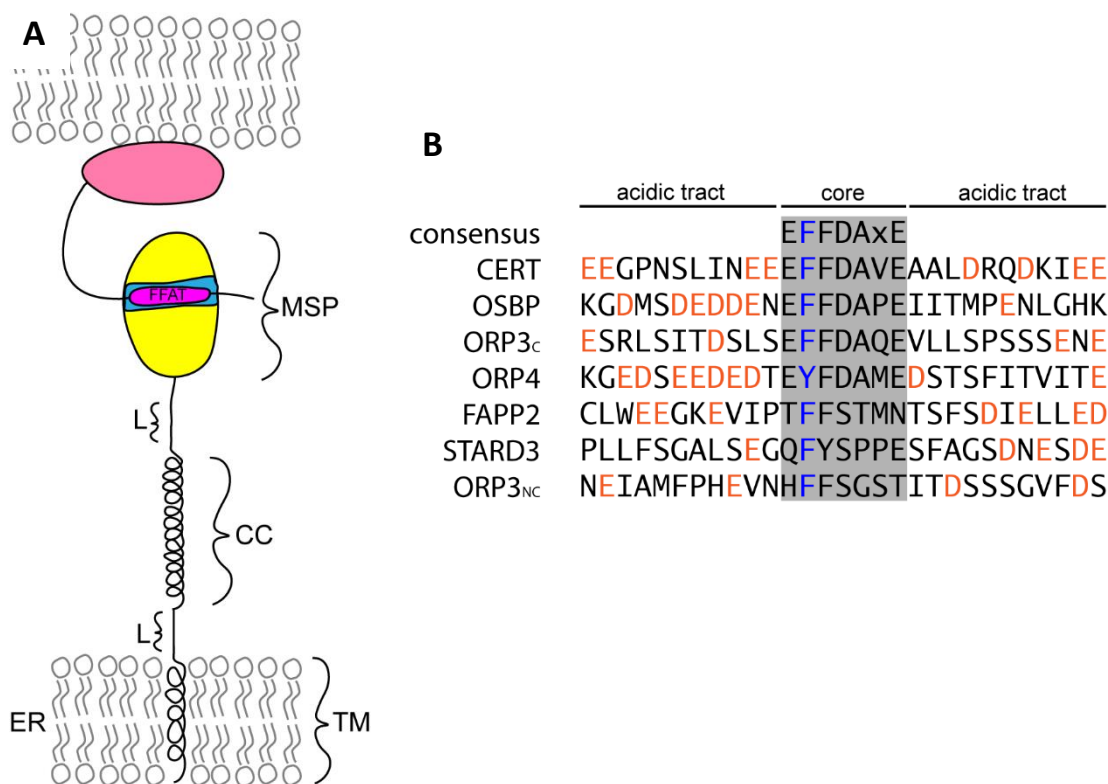


Figure 1.8. VAP binds to proteins with FFAT motifs. A) Schematic depicting the domains of VAP (yellow) and a VAP interacting protein (pink). blue, electropositive face; MSP, Major Sperm Protein domain. CC, predicted coiled coil domain; L, linkers; TM, trans-membrane domain; Magenta, Two Phenylalanines (FF) in an Acidic Tract (FFAT). B) Alignment of experimentally validated FFAT motifs. The grey box highlights the core of the FFAT motif. Acidic residues in orange and essential position 2 of core motif in blue. CERT, ceramide transfer protein. OSBP, oxysterol-binding protein. ORP3, oxysterol-binding protein-related protein 3. ORP4, oxysterol-binding protein-related protein 4. FAPP2, pleckstrin homology domain-containing family A member 8. STARD3, StAR Related Lipid Transfer Domain Containing 3. C, canonical FFAT motif. NC, noncanonical FFAT motif.

1.4 Model of ER-Inclusion MCS

Our lab has identified several molecular components of ER-Inclusion MCS, including both host and bacterial factors (Figure 1.9). *C. trachomatis* expresses the Inc protein IncD which interacts with the FFAT motif-containing ceramide transfer protein (CERT).^{58,110} VAP is also a part of this complex, so the IncD-CERT-VAP complex bridges Inclusion with the ER where it is proposed to function in transferring ceramide from the ER to the inclusion membrane.^{110,149} Depletion of CERT or VAP causes inclusions to be smaller and a reduction in infectious progeny formation, demonstrating their importance during infection.^{110,149} We also identified the host protein STIM1 as a component of ER-Inclusion MCS.¹⁵¹ STIM1 depletion had no effect on inclusion size or infectious progeny production but negatively affected the extrusion mechanism of host cell exit.^{61,151} However, the specific role of STIM1 at ER-Inclusion MCS remains to be defined. Until this point, though we had gained insight into potential functions of ER-Inclusion MCS, it remained unclear how these structures were formed and maintained.

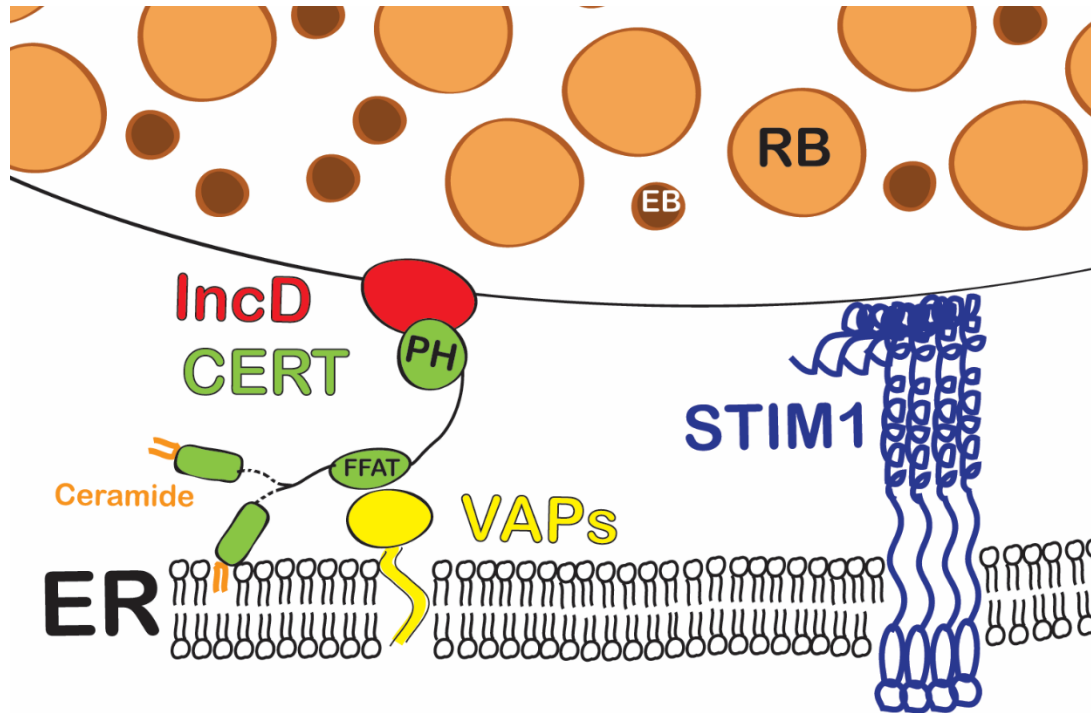


Figure 1.9. Model of molecular components at ER-Inclusion Membrane Contact Sites.

The IncD (red)-CERT (green)-VAP (yellow) complex had been proposed to facilitate lipid acquisition by the bacteria. STIM1 (blue) localizes to ER-Inclusion MCS but has an unknown function at the sites.

1.5 Thesis Rationale

In addition to the machinery contributing to the function of MCS in naïve cells, such as ion and lipid transfer, an important part of MCS biology is that specific tethering molecules must contribute to their formation.^{158,163} A defining feature of such tether molecules is their insertion in the membrane of a given organelle and their interaction with a molecule inserted in the membrane of the opposing organelle.¹⁶³ The typical structure of *Chlamydia* Inc proteins, consisting of a transmembrane domain embedded in the inclusion membrane and cytoplasmic tails facing the cytosol, makes them ideal candidates to act as tether molecules bridging the ER and inclusion membranes by directly interacting with ER-resident proteins. The Inc-Human interactome is a published web of interactions between Incs and host proteins.⁶⁰ The authors expressed tagged versions of 58 of the 62 predicted Incs in HEK293T cells and performed affinity purification coupled to mass spectrometry to identify interacting partners. The interactome predicted an interaction between the Inc protein CT005 (renamed IncV based on our findings), and the ER-resident VAP proteins. An analysis of the amino acid sequence of IncV revealed a conserved FFAT motif. Because of the putative FFAT motif in IncV and the fact that VAP is already a known component of ER-Inclusion MCS, I hypothesized that IncV was a novel component of ER-Inclusion MCS that acts as a tether between the ER and the inclusion membrane.

Chapter 2

IncV, a FFAT motif-containing *Chlamydia* protein, tethers the endoplasmic reticulum to the pathogen-containing vacuole^a

^aStanhope, R., Flora, E., Bayne, C. & Derré, I. IncV, a FFAT motif-containing *Chlamydia* protein, tethers the endoplasmic reticulum to the pathogen-containing vacuole. Proc. Natl. Acad. Sci. 114, 201709060 (2017).

2.1 Introduction

Eukaryotic cells are compartmentalized into intracellular membrane-enclosed organelles (the endoplasmic reticulum (ER), the Golgi apparatus, mitochondria, endosomes etc.), which perform very specific functions essential for cell homeostasis. However, while organelles can be perceived as isolated entities, the proper function of the cell relies on constant inter-organelle communication. This can occur through vesicular trafficking, a process in which the material to be exchanged is packaged into vesicles that bud off of the sending organelles and fuse with the membranes of the receiving organelles to deliver their cargo.¹⁸³⁻¹⁸⁸ In addition, direct organelle contact is emerging as an important way to coordinate cellular activities.^{157,158} Membrane contact sites (MCS) are defined as a zone of close apposition (10-30nm) between the membranes of two organelles, with no fusion occurring. MCS play a role in the non-vesicular trafficking of small molecules such as lipids and calcium (Ca^{2+}) and have been described between the ER and nearly any other organelles or the plasma membrane.

By definition, MCS can only occur, and perform their respective functions, if the two organelles are brought together and maintained in close apposition. This process is proposed to rely on specific tethering molecules that should in theory fulfill the following requirements: 1) be enriched at the point of contact between the two organelles, 2) be part of a molecular complex that bridges the opposing membranes, 3) if not redundant, their deletion should abolish the contact between the two organelles and 4) regardless of redundancy, their overexpression should increase the extent of

contact.^{157,163} Once contacts are established, functional proteins such as lipid transfer proteins or ion channels can initiate the exchange of molecules between the paired organelles. In many instances, however, it is difficult to discriminate between tethering and functional components, as their roles are not mutually exclusive. For example, the lipid transfer protein STARD3 has been implicated in tethering endosomes to the ER and in cholesterol transfer between these two organelles.^{189,190} In addition, because of redundancy, few molecules fulfill all the tethering molecule criteria listed above. This is probably best illustrated by the fact that, in yeast, ER-PM contacts were only lost after deletion of all three classes of tethering molecules (6 proteins total).¹⁹¹

The ER integral proteins VAPA and VAPB (Vesicle-associated membrane protein-associated protein, referred to as VAPs here¹⁹²) are common components of the MCS formed between the ER and various organelles.^{189,193–198} At each of these MCS, VAPs interact with different proteins that have in common a 7 amino acid sequence, known as a FFAT motif (two phenylalanines (FF) in an acidic tract).¹⁸⁰ The binding of the FFAT motif to electropositive residues in the cytosolic MSP (Major Sperm Protein) domain of the VAP proteins mediates the interaction between the FFAT motif-containing proteins and the VAPs.^{179,199} Many of the VAP-interacting proteins are lipid transfer proteins, including CERT (Ceramide transfer protein)²⁰⁰ and OSBP (Oxysterol-binding protein) family members²⁰¹, which can also act as tethering factors through their interaction with the VAPs.

Pathogen-containing vacuoles resemble cellular organelles: they have a unique protein and lipid composition and their maturation requires interaction with other cellular organelles. This is a pathogen-driven process. One common strategy that pathogens employ is to secrete bacterial effector proteins across the vacuolar membrane to manipulate the vesicular trafficking of the host cell.²⁰² In particular, the obligate intracellular bacteria *Chlamydia trachomatis*, which resides in a membrane-bound compartment termed the inclusion, intercepts the vesicular trafficking between the Golgi and the plasma membrane to acquire sphingomyelin, a host lipid that is incorporated into the cell wall of the bacteria and is essential for bacterial replication.^{144,147,203} In addition to vesicular trafficking, we have shown that the *C. trachomatis* inclusion also establishes membrane contact sites with cellular organelles such as the ER.¹¹⁰ These ER-Inclusion MCS are highly enriched in two known components of ER-Golgi MCS, the lipid transfer protein CERT, which mediates the non-vesicular transfer of ceramide from the ER to the Golgi, and the ER integral protein VAP.^{110,149,192,200} IncD, a member of the family of *C. trachomatis* type III secreted effector proteins that are inserted into the inclusion membrane (i.e the Inc proteins),^{36,127,128} also localizes to ER-Inclusion MCS and recruits CERT to the inclusion.¹¹⁰ The IncD/CERT/VAP complex has been proposed to mediate the transfer of lipids to the inclusion, a process necessary for bacterial replication.^{110,149}

Although we have started to gain insight into the functional role of ER-Inclusion MCS in lipid exchange, it is still unclear how the ER is recruited and maintained in close apposition to the inclusion membrane. Here we show that, through molecular mimicry

of a eukaryotic FFAT motif, the *C. trachomatis* protein IncV acts as a molecular tether that mediates the formation of ER-inclusion MCS through interaction with the ER-resident proteins VAPA and VAPB.

2.2 Results

2.2.1 IncV-VAP Interaction Depends on the FFAT Binding Domain of VAP.

C. trachomatis Inc proteins all share a common predicted structure, including at least two to four transmembrane domains¹¹⁶ for insertion into the inclusion membrane and amino- and carboxyl-terminal cytosolic tails. Inc proteins are strategically positioned to mediate inclusion interaction with cellular organelles. For example, IncD mediates the recruitment of the functional component CERT to ER-inclusion MCS.¹¹⁰ However, it is unknown if Inc proteins can also act as structural components to bring and maintain the ER and the inclusion membrane in close apposition. *C. trachomatis* encodes more than 50 putative Incs and only some of them have known functions in *C. trachomatis* infection.^{39,58,60,63,67–69,110–112,121,128,134,141} Recently, Mirrashidi *et al.*⁶⁰ determined the Inc-human interactome from uninfected cells expressing *C. trachomatis* Inc proteins. Interestingly, the Inc protein CT005, that we have renamed IncV (Inc interacting with VAP) based on our findings, was predicted to interact with the ER-resident proteins VAPA and VAPB, which are both enriched at ER-inclusion MCS.^{58,110} To validate that IncV interacts with VAPA and VAPB, we subjected lysates from HEK293 cells expressing IncV-3xFLAG and GFP-VAPA or GFP-VAPB to coimmunoprecipitation (co-IP) using anti-FLAG conjugated beads. VAPAWT coimmunoprecipitated with IncV (Figure 2.1A) and a similar result

was obtained with VAPBWT (Figure 2.2A). The IncV–VAP interaction was specific and not due to aggregation of IncV in the ER (Figure 2.3A). Importantly, mutant forms of VAPA and VAPB, with a defective FFAT binding domain (VAPKFM/DFD), failed to co-IP with IncV (Figure 2.1A and Figure 2.2A). Thus, when expressed in eukaryotic cells, IncV interacts with VAPA and VAPB in a manner that relies on the integrity of the FFAT binding domain of VAP.

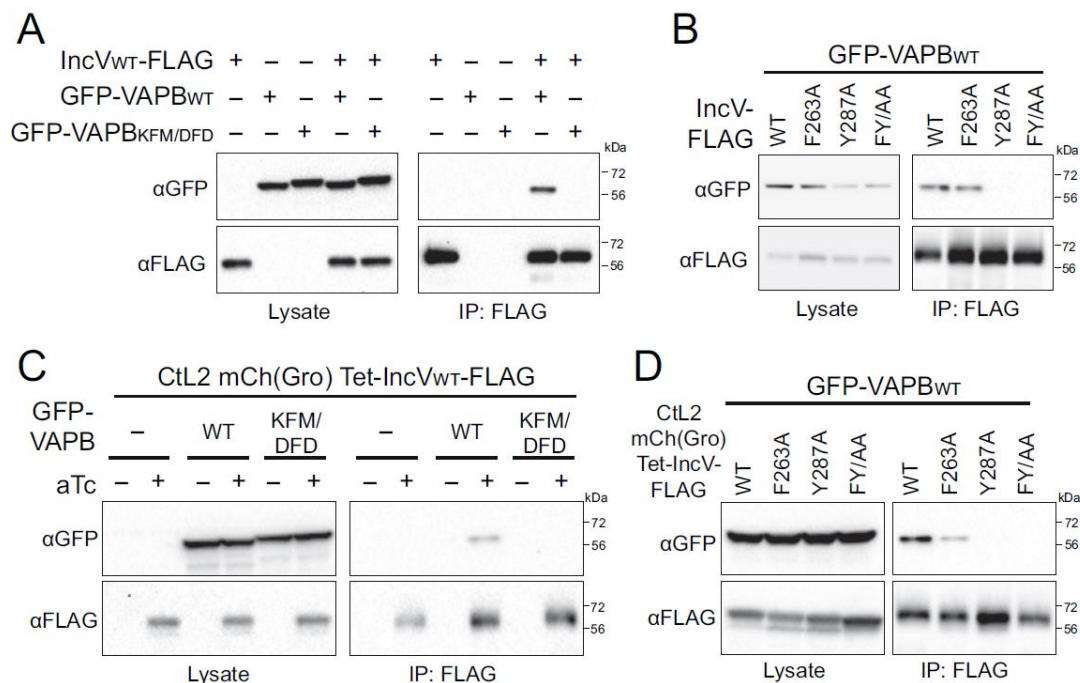


Figure 2.2. IncV–VAPB interaction occurs in cotransfected and *C. trachomatis*-infected cells, and depends on the FFAT binding domain of VAPB and on the FFAT motifs of IncV. (A) Co-IP of IncV-3xFLAG and GFP-VAPB_{WT} from HEK293 lysates coexpressing the two constructs. (B) Co-IP of IncV-3xFLAG (WT, F263A, Y287A, FY/AA) and GFP-VAPB_{WT} from HEK293 lysates coexpressing the indicated constructs. (C) Co-IP of IncV-3xFLAG constructs from lysates of HEK293 cells expressing GFP-VAPB (WT or KFM/DFD) and infected with *C. trachomatis* expressing IncV-3xFLAG WT under the control of an aTc inducible promoter. (D) Same as C with *C. trachomatis* strains expressing IncV-3xFLAG (WT, F263A, Y287A, or FY/AA) and HEK293 cells expressing GFP-VAPB_{WT}.

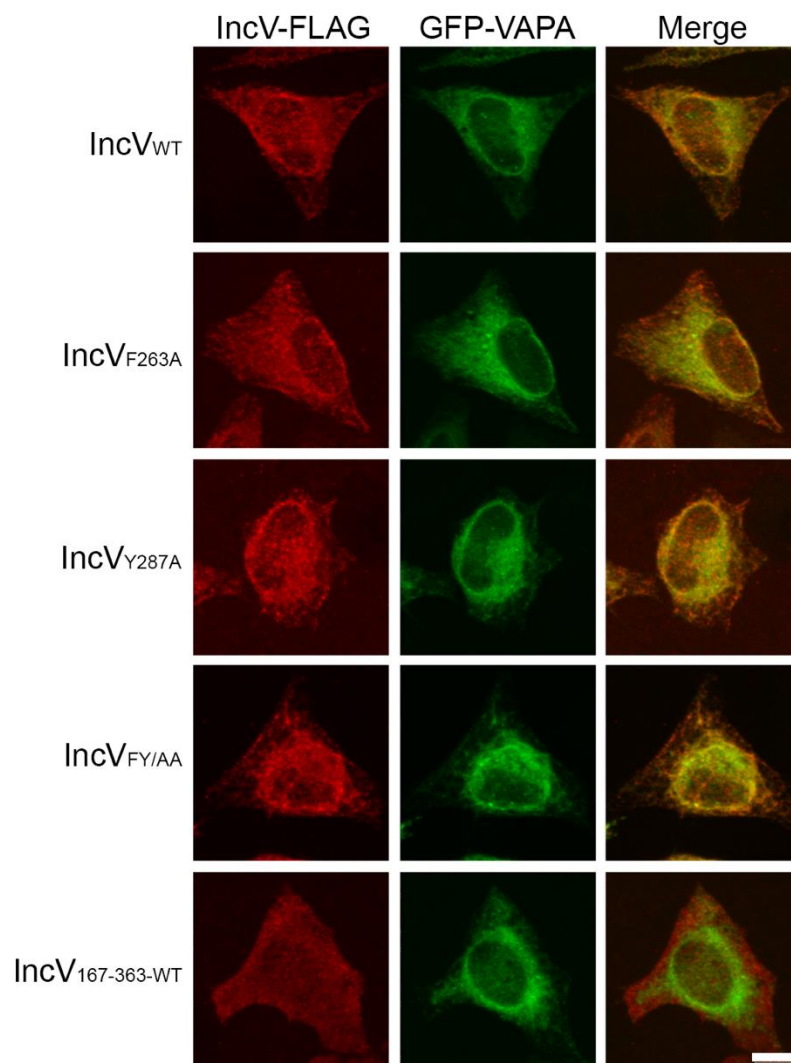


Figure 2.3. The IncV constructs used in this study do not aggregate in eukaryotic cells.

Confocal micrographs of HeLa cells co-expressing GFP-VAPA_{WT} (green) or IncV-3xFLAG (WT, F263A, Y287A, FY/AA), or IncV_{167-363-WT}-3xFLAG (red). The merge is shown on the right. Scale bar = 5 μ m.

2.2.2 *IncV* Contains Two FFAT Motifs That Mediate *IncV*-VAP Interaction.

Based on the hydropathy profile of *IncV* (Figure 2.4), it is predicted that the N-terminal region of *IncV* (amino acids 1–166) contains the type III secretion signal and the hydrophobic domain important for insertion into the inclusion membrane. The C-terminal region of *IncV* (amino acids 167–363) is predicted to face the cytosol. Additionally, analysis of the primary sequence of *IncV* and of the other *C. trachomatis* *Incs*, using an algorithm designed by Murphy and Levine,¹⁷⁸ revealed the presence of two putative FFAT motifs, in the C-terminal (cytosolic) region of *IncV* only (Figure 2.1B, amino acids 252–296 are shown). Both motifs are preceded by a stretch of serine residues which, if phosphorylated, could provide the acidic environment typically located upstream of the consensus FFAT sequence [E¹(F/Y)²(F/Y)³D⁴A⁵X⁶E⁷]. One FFAT motif (SFHTPPN, amino acids 262–268) is quite degenerated compared with the consensus sequence, except for the phenylalanine residue at position 263, and will be referred to as the *IncV* noncanonical FFAT motif (ncFFAT). The other FFAT motif (EYMDALE, amino acids 286–292) is located 17 aa downstream of the ncFFAT. Its sequence is nearly identical to the consensus sequence and will be referred to as the *IncV* canonical FFAT (cFFAT). This result suggests that FFAT motifs present in *IncV* may promote *IncV* interaction with VAPA and VAPB.

While amino acid substitutions are tolerated at most positions in the FFAT motif, a phenylalanine or a tyrosine residue at position 2 is critical for VAP binding.¹⁷⁸ To test the functional importance of the putative FFAT motifs in *IncV*, we introduced alanine substitutions in the essential position 2 of the ncFFAT (F263A), the cFFAT (Y287A), or

both FFAT motifs (F263AY287A, referred to as FY/AA). The ability of GFP-VAP to co-IP with the indicated IncV-3xFLAG constructs was assayed, after confirming that these constructs did not aggregate (Figure 2.3). VAPAWT (Figure 2.1C) and VAPBWT (Figure 2.2B) successfully coimmunoprecipitated with IncV-WT and IncV-F263A, but not with IncV-Y287A and IncV-FY/AA. These results indicate that IncV-VAP interaction requires an intact cFFAT motif, but the ncFFAT is apparently dispensable.

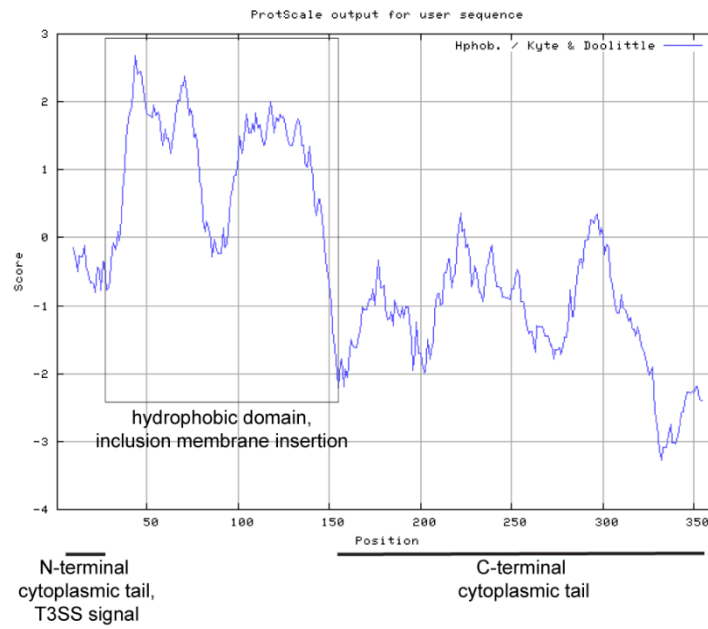


Figure 2.4: Hydropathy profile of IncV as generated using:

<http://web.expasy.org/protscale/>

2.2.3 The MSP Domain of VAP and the C-terminus of IncV Mediate IncV-VAP Interaction.

To demonstrate that IncV interacts with VAPA in an *in vitro* system, we performed GST pull-down assays. The MSP domain of VAPA, which contains the FFAT binding domain, was expressed as a GST-tagged fusion protein in *Escherichia coli*, immobilized on glutathione Sepharose beads, and incubated with cell lysates from eukaryotic cells expressing IncV-3xFLAG full-length (amino acids 1–363) or the C-terminal part of IncV that contains the FFAT motifs (amino acids 167–363) (Figure 2.1D). VAPAMSP-WT successfully pulled down IncV1–363-WT and IncV167–363-WT. However, mutations in either the FFAT binding domain of VAPA (KFM/DFD) or the FFAT motifs of IncV (FY/AA) abolished this interaction. Thus, the MSP domain of VAP and the C terminus of IncV are sufficient to support the IncV–VAP interaction, which neither relies on insertion of the proteins into the inclusion membrane nor requires additional *C. trachomatis* factors. We cannot exclude, however, that additional eukaryotic factors may be required.

2.2.4 IncV-VAP Interaction Occurs During *C. trachomatis* Infection.

To validate our observations in the context of infected cells, we engineered *C. trachomatis* strains expressing mCherry constitutively, and IncV-3xFLAG (WT, F263A, Y287A, or FY/AA) under the control of an anhydrotetracycline (aTc)-inducible promoter. All four IncV constructs were expressed upon the addition of aTc and localized to the inclusion membrane (Figure 2.5 and Figure 2.6). When cells expressing GFP-VAPAWT or GFP-VAPA-KFM/DFD were infected with the IncVWT-3xFLAG-expressing *C. trachomatis*

strain, VAPAWT, but not VAPA-KFM/DFD, coimmunoprecipitated with IncV-WT (Figure 2.5A). Moreover, while VAPA-WT also coimmunoprecipitated with IncV-F263A, it failed to do so with IncV-Y287A or IncV-FY/AA (Figure 2.5B). A similar result was obtained with VAPB (Figure 2.2 C and D). Altogether, these results show that IncV proteins, produced by *C. trachomatis* and inserted into the inclusion membrane, interact with VAPA and VAPB in a manner that relies on the FFAT binding domain of VAP and the cFFAT motif of IncV.

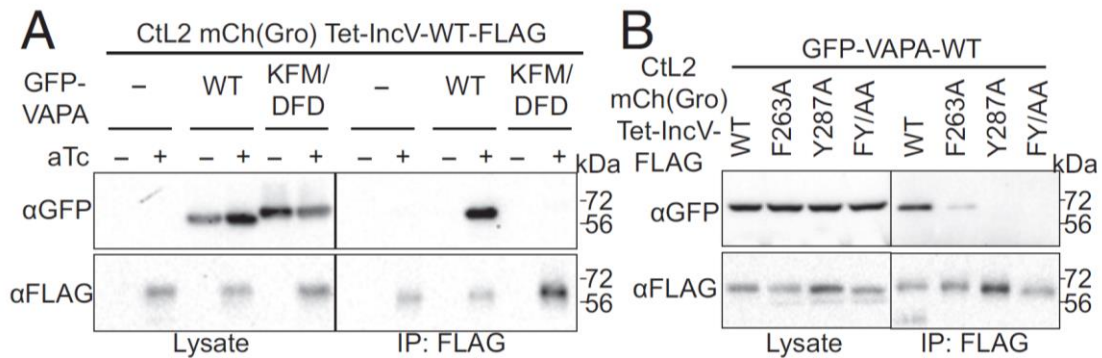


Figure 2.5. IncV–VAPA interaction occurs in *C. trachomatis*-infected cells and depends on the FFAT binding domain of VAPA and on the FFAT motifs of IncV. (A) Co-IP of IncV-3xFLAG constructs from lysates of HEK293 cells expressing GFP-VAPA (WT or KFM/DFD) and infected with *C. trachomatis* expressing IncV-3xFLAG WT under the control of an aTc inducible promoter. (B) Same as A, with *C. trachomatis* strains expressing IncV-3xFLAG (WT, F263A, Y287A, or FY/AA) and HEK293 cells expressing GFP-VAPA-WT.

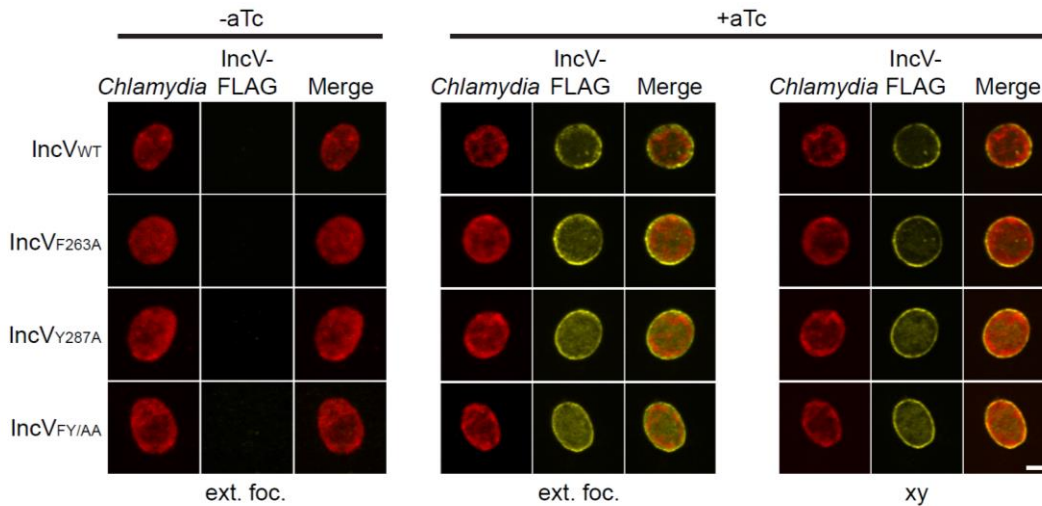


Figure 2.6. The IncV constructs used in this study are aTc inducible and localize to the inclusion when expressed from *C. trachomatis*. Confocal micrographs of HeLa cells infected with a *C. trachomatis* strains expressing mCherry constitutively (red) and IncV-3xFLAG WT, F263A, Y287A or FY/AA (yellow) under the control of an aTc inducible promoter in the absence (-aTc) or the presence (+aTc). The merge is shown on the right. Scale bar = 5 μ m. Ext. foc., extended focus. xy, cross-section through the center of the inclusion.

2.2.5 *IncV*-mediated Association of VAP With the Inclusion Depends on the FFAT

Binding Domain of VAP.

We next investigated the cellular localization of YFP-VAPA in cells infected with a *C. trachomatis* strain expressing the inducible IncVWT-3xFLAG. In the absence of inducer, small patches of VAPAWT were observed in close apposition to the inclusion (Figure 2.7A). Upon the addition of aTc, IncV-WT localized to the inclusion membrane, which correlated with an increased recruitment of VAPAWT to the inclusion and with colocalization of IncV and VAPA on the inclusion (Figure 2.7 A and D). IncV-WT expression, however, did not induce an increase in recruitment of VAPAKFM/DFD to the inclusion (Figure 2.7 B and D). Similar results were observed with VAPB (Figure 2.9 A, B, and D). These results indicate that IncV mediates the recruitment of VAP to the inclusion and that this recruitment requires an intact FFAT binding domain in the VAP molecule.

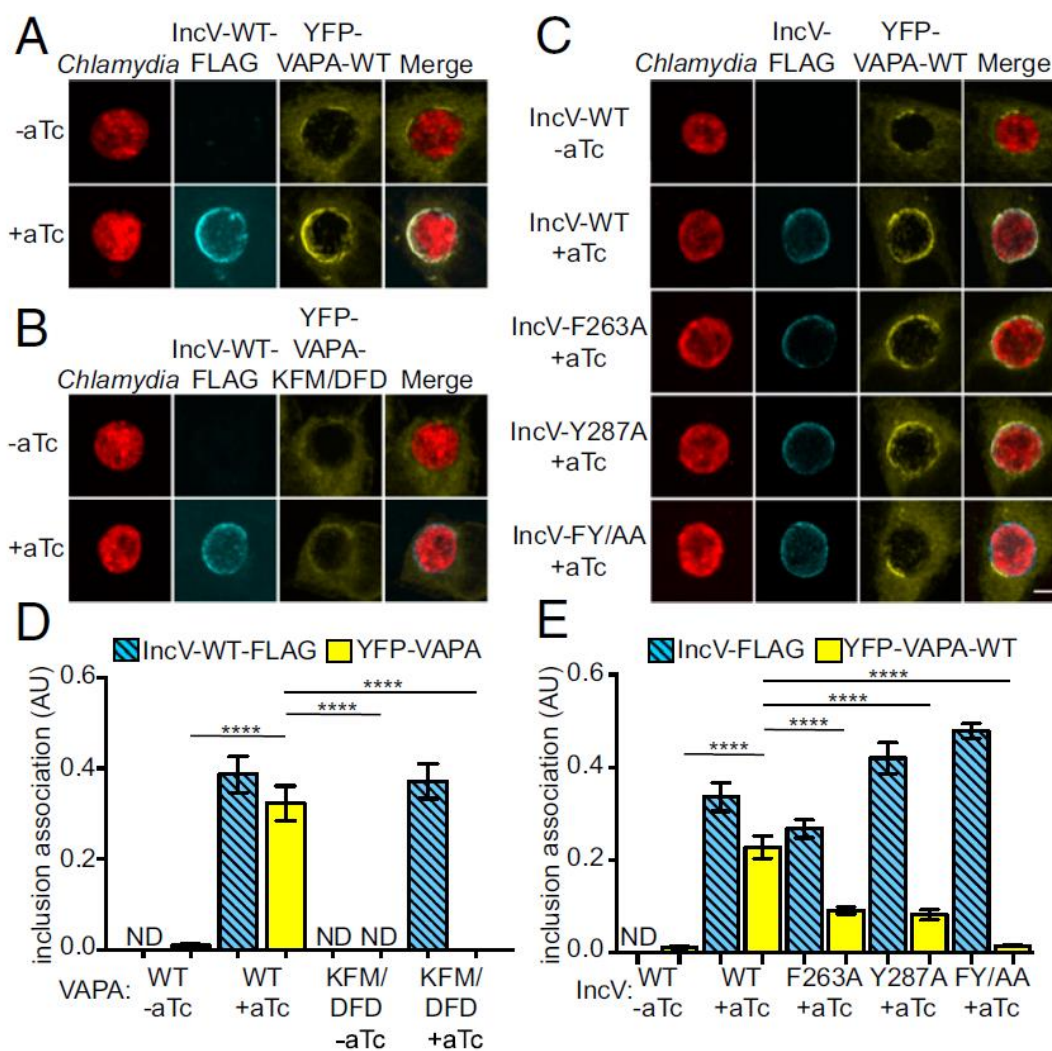


Figure 2.7. The IncV-mediated VAP recruitment to the inclusion depends on the FFAT binding domain of VAPA and on the FFAT motifs of IncV. (A–C) Threedimensional reconstruction of confocal micrographs of HeLa cells expressing YFP-VAPAWT (A and C) or KFM/DFD (B) (yellow) infected with a *C. trachomatis* strain expressing mCherry constitutively (red) and IncV-3xFLAGWT (A and B) or WT, F263A, Y287A, or FY/AA (C) (blue) under the control of an aTc inducible promoter, in the absence (–aTc) or the presence

(+aTc) of aTc. The merge is shown on the Right. (D and E) Quantification of IncV-3xFLAG (blue, hashed bars) and YFP-VAPA (yellow, solid bars) association with the inclusion in arbitrary units (AU). D and E, respectively, correspond to quantification of A and B, and C. The quantification method is described in Figure 2.8A. Error bars are SEM. ****P <0.0001. ND, none detected. (Scale bar, 5 μ m; applies to A–C.)

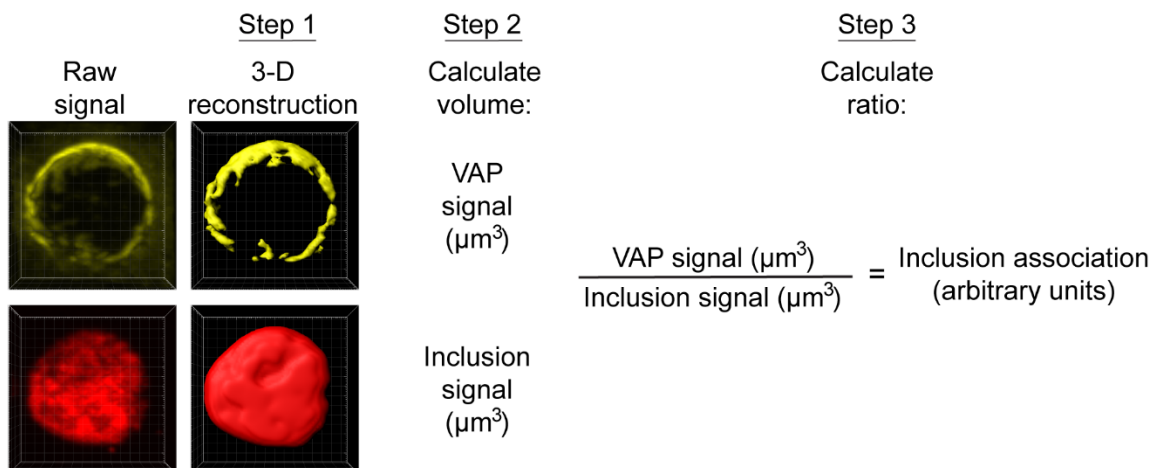


Figure 2.8: Method to quantify the inclusion association of a given marker.

3-dimensional reconstruction of the raw signal corresponding to a given marker was generated using the Imaris imaging software. The volume corresponding to the sum of the pixels, above the threshold corresponding to the signal in the cytosol, was determined for the marker of interest and for the inclusion. The inclusion association of the given marker was determined in arbitrary units by normalizing the volume of the marker of interest with the corresponding volume of the inclusion.

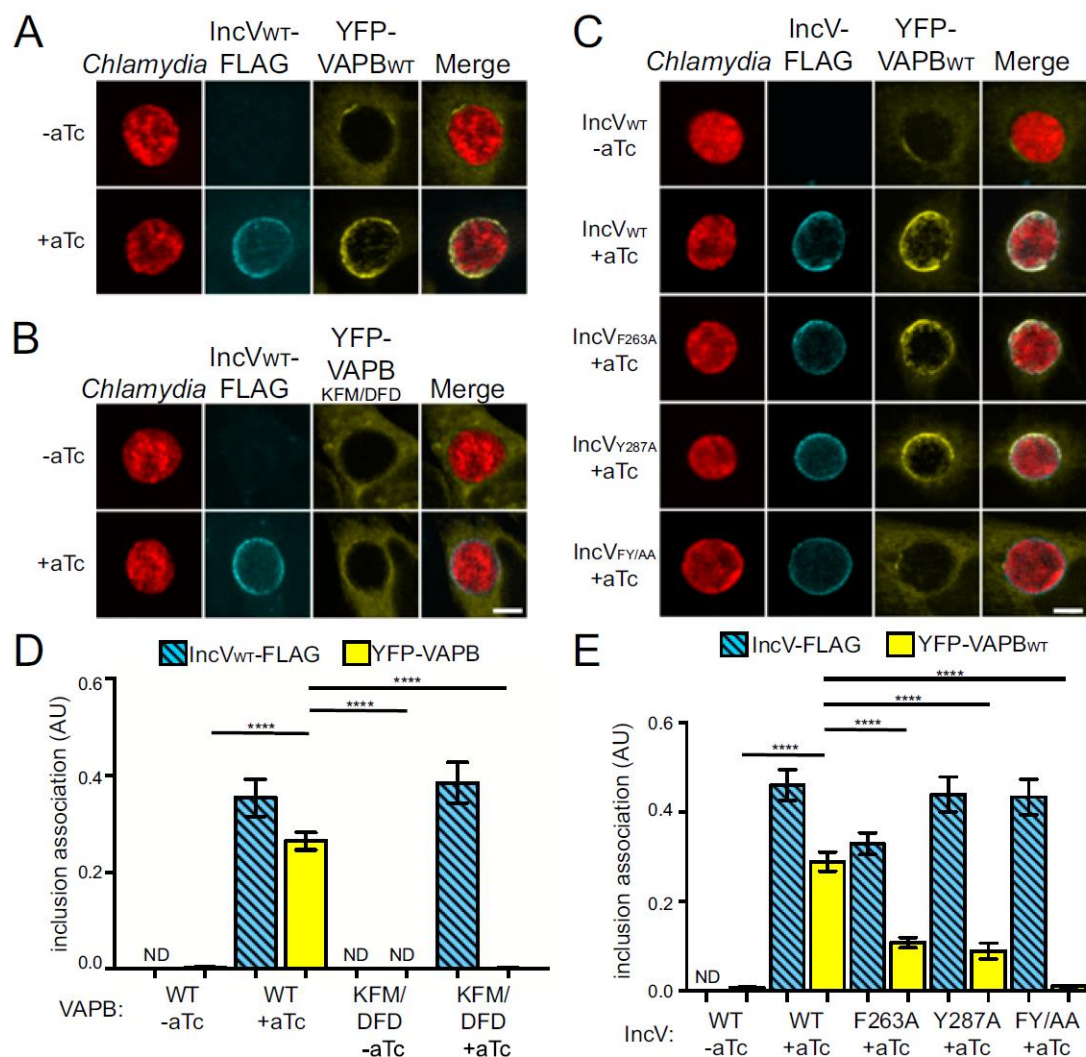


Figure 2.9. The IncV-mediated VAP recruitment to the inclusion depends on the FFAT binding domain of VAPB and on the FFAT motifs of IncV. (A–C) Three dimensional reconstruction of confocal micrographs of HeLa cells expressing YFP-VAPB WT (A and C) or KFM/DFD (B) (yellow) infected with a *C. trachomatis* strain expressing mCherry constitutively (red) and IncV-3xFLAG WT (A and B) or WT, F263A, Y287A, or FY/AA (C) (blue) under the control of an aTc inducible promoter, in the absence (-aTc) or the presence (+aTc) of aTc. The merge is shown on the Right. (Scale bars, 5 μ m; applies to A and B.) (D

and E) Quantification of IncV-3xFLAG (blue, hashed bars) and YFP-VAPB (yellow, solid bars) association with the inclusion in arbitrary units (AU). D and E, respectively, correspond to quantification of A and B, and C. The quantification method is described in Figure 2.9. Error bars are SEM. ****P < 0.0001. ND, None detected.

2.2.6 Both FFAT motifs of IncV Are Required for VAP Association With the Inclusion.

Both FFAT Motifs of IncV Are Required for VAP Association with the Inclusion.

We next tested whether the FFAT motifs of IncV are required for VAP association with the inclusion. As observed with IncVWT, inclusions harboring *C. trachomatis* expressing IncVF263A or IncVY287A displayed increased association with VAPA^{WT}, compared with the uninduced control (Figure 2.7C). Expression of IncVFY/AA, however, did not induce an increase in the association of VAPA with the inclusion. Quantification of the immunofluorescence data revealed that, individually, the introduction of F263A and Y287A mutations reduced VAPA recruitment to the inclusion by 60% compared with their WT counterpart. The combination of these mutations (FY/AA) had an additive effect, leading to a reduction of nearly 95% (Figure 2.7E). A similar result was observed with VAPB^{WT} (Figure 2.9 C and E). Altogether, these results indicate that IncV promotes VAP recruitment to the *C. trachomatis* inclusion and that both IncV ncFFAT and cFFAT motifs contribute to this process.

2.2.7 IncV Promotes the Formation of ER-Inclusion MCS in a VAP-Dependent Manner.

To determine if IncV could recruit the endogenous ER-resident VAP proteins to the inclusion membrane, HeLa cells infected with a *C. trachomatis* strain expressing the inducible IncVWT-3xFLAG construct were immuno-labeled with anti-VAPA antibodies (Figure 2.10A). In the absence of inducer, endogenous VAPA localized to discrete patches in close proximity to the inclusion. However, when the expression of IncVWT was induced, endogenous VAPA strongly accumulated on the surface of the inclusion.

These results indicate that IncV can recruit the endogenous ER-resident protein VAPA to the inclusion membrane and possibly the ER associated with this protein. In support of this notion, qualitative ultrastructural analysis of *C. trachomatis* inclusions harboring the inducible IncVWT-3xFLAG strain, in the absence of inducer, revealed the recruitment of ER-like membrane structures closely apposed to the inclusion membrane (see Figure 2.10B and Figure 2.11 for larger images), as previously described.¹¹⁰ The extent of the ER-like membrane structures was greatly increased when IncVWT expression was induced, with long and continuous membrane tracks tightly apposed to the inclusion membrane. The ER nature of the tracks was further confirmed by analyzing the cellular localization of the ER marker Sec61 β by confocal microscopy. Sec61 β + rings that colocalized with IncV surrounded 80% of the inclusions harboring the inducible IncVWT strain (see Figure 2.10 C and D and Figure 2.12A for larger images of the Sec61 β marker). In cells treated with siRNA against VAPA and VAPB, however, the percentage of inclusions presenting a Sec61 β + ring was reduced by 65%, which also translated into a reduction of the Sec61 β signal associated with IncV (Figure 2.11E). Taken together, these results indicate that IncV promotes the formation of ER-inclusion MCS and that VAPA and VAPB are required for this process.

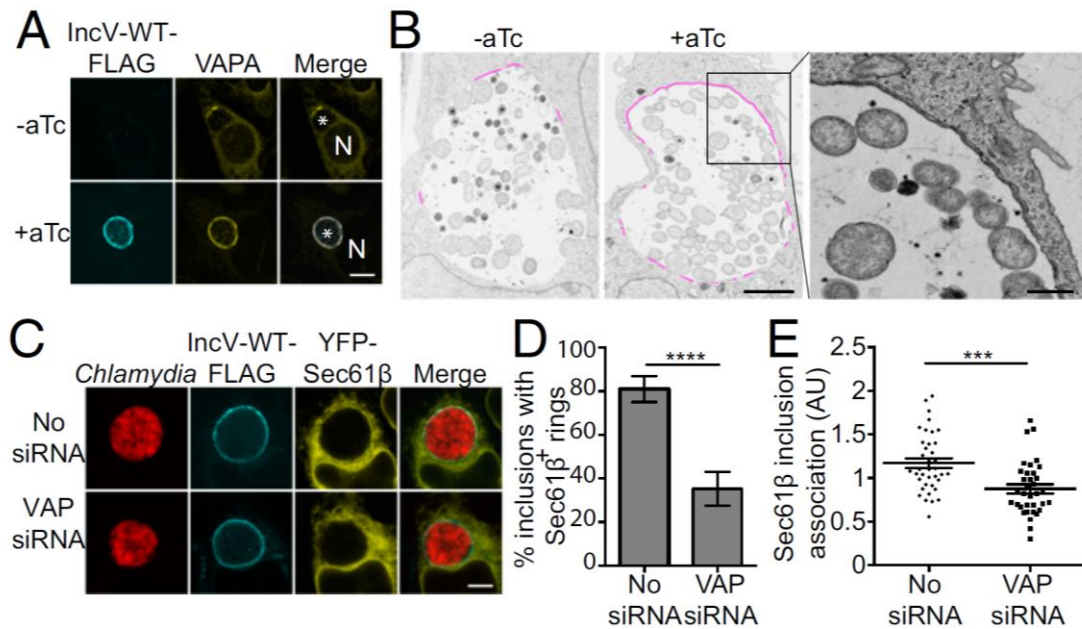


Figure 2.10. IncV induces the formation of ER-Inclusion MCS in a VAP-dependent

manner. (A) Three-dimensional reconstruction of confocal micrographs of HeLa cells infected with a *C. trachomatis* strain expressing mCherry constitutively and IncV-WT-3xFLAG under the control of an aTc-inducible promoter in the absence (-aTc) or presence (+aTc) of aTc and stained with antibodies against FLAG (blue) and endogenous VAPA (yellow). The merge is shown on the Right. (Scale bar, 10 μ m.) (B) Transmission electron micrographs of HeLa cells infected as described in A. ER patches are highlighted in pink and a higher magnification of the +aTc image is shown on the Right. (Scale bars, 2.5 μ m.) (C) XY plane confocal micrographs of HeLa cells, depleted (VAP siRNA) or not (No siRNA) of VAPA and VAPB, expressing YFP-Sec61 β (yellow) and infected with a *C. trachomatis* strain expressing mCherry (red) and IncV-3xFLAG WT (blue). The merge is shown on the Right. (Scale bar, 5 μ m.) (D and E) Quantification of inclusions presenting a

Sec61 β + ring (D) and of the Sec61 β signal associated with IncV in arbitrary units (AU) (E) in cells as described in C. The quantification method used for E is described in Figure S6C. Error bars are SEM. ****P < 0.0001, ***P < 0.001.

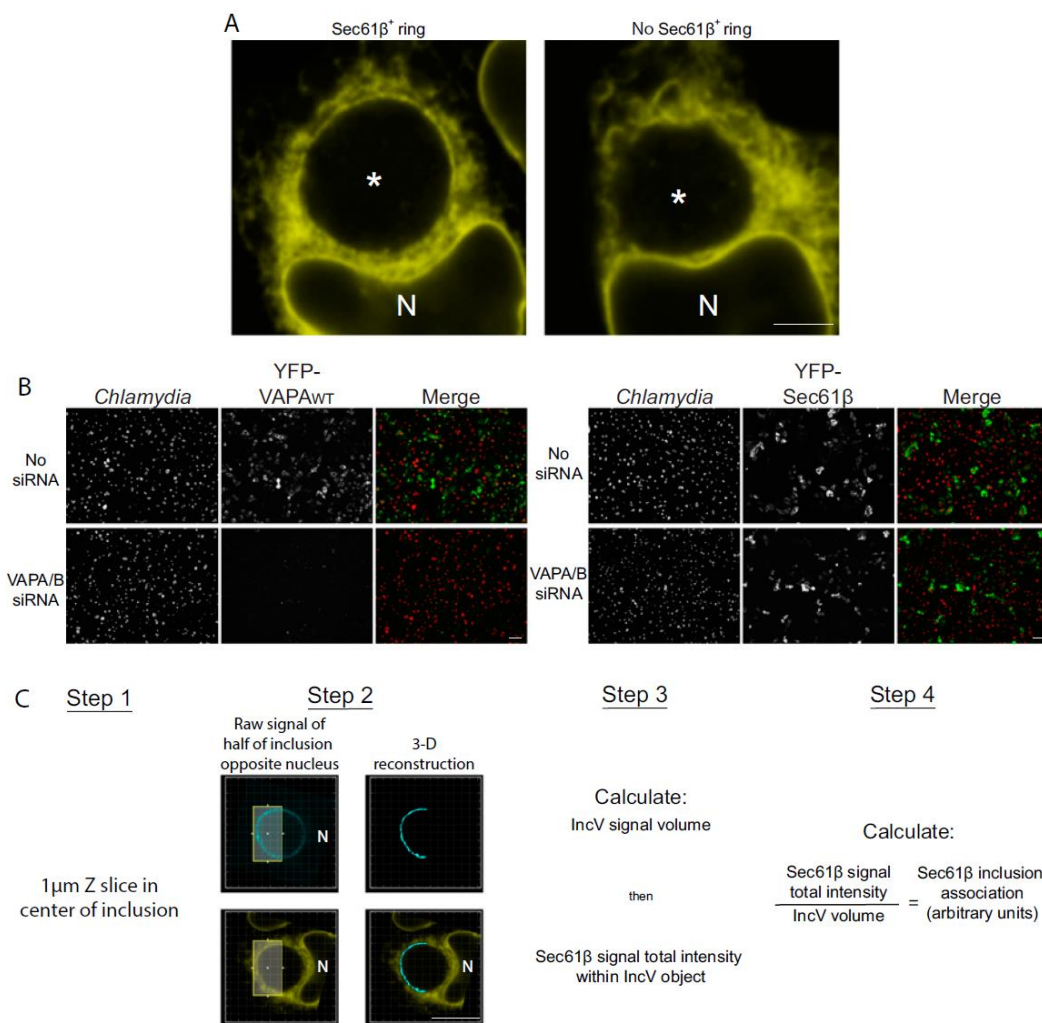


Figure 2.12. Quantification of YFP-Sec61β association with the inclusion. (A) Larger representation of the images presented in Figure 2.10C to visualize the Sec61β⁺ ring. (Scale bar, 5 μm.) (B) VAPA/B siRNA treatment prevents YFP-VAPA but not YFP-Sec61β expression. Fluorescence micrographs of VAPA/B siRNA treated or untreated HeLa cells transfected with YFP-VAPAWT or YFP-Sec61β (green) infected with a *C. trachomatis* strain expressing mCherry constitutively (red) and IncVWT-3xFLAG under the control of an aTc inducible promoter, in the presence of aTc. The merge is shown on the Right.

(Scale bars, 50 μm .) (C) Quantification method. Step 1: 1 μm z-slices in the center of the inclusion were used for quantification of Sec61 β inclusion association. Step 2: A three-dimensional object from the raw IncV signal was generated using the Imaris imaging software. The object was restricted to the half of the inclusion opposite the nucleus to limit the background due to the signal from the bulk of the ER present between the nucleus and the inclusion. Step 3: First, the volume corresponding to the sum of the pixels was determined for IncV. Then the total intensity of the Sec61 β signal within the IncV+ object was determined. Step 4: The inclusion association of Sec61 β was determined in arbitrary units by normalizing the YFP-Sec61 β total intensity within the IncV-positive object with the corresponding volume of the IncV object. (Scale bar, 10 μm .)

2.2.8 PM-Targeted IncV Tethers the ER to the PM.

To determine if IncV is sufficient to mediate the formation of MCS between the ER and other cellular membranes in the absence of *Chlamydia* infection, we targeted the C-terminal cytosolic tail of IncV to the PM, by fusion of a C-terminal CAAX motif (PM-IncV167–363-3xFLAG) (Figure 2.13A). In cells expressing the cytosolic IncV167–363-WT, VAPAWT displayed the typical reticulate pattern of the ER (Figure 2.14A, Top). A similar VAPA pattern was observed upon expression of a PM-targeted red fluorescent protein (Figure 2.13B). Expression of PM-IncV167–363-WT, however, dramatically affected the cellular localization of VAPAWT and induced the formation of large sheets that were plastered against the PM and highly enriched in VAP and PM-IncV (Figure 2.14, Middle). The sheets were positive for the ER marker CFP-ER (Figure 2.14B), but were not observed when the FFAT motifs of IncV were mutated (FY/AA) (Figure 2.14A, Bottom). Altogether, these results indicate that, independent of the lipid and protein environment of the inclusion membrane, expression of PM-targeted IncV induces the formation of ER–PM MCS.

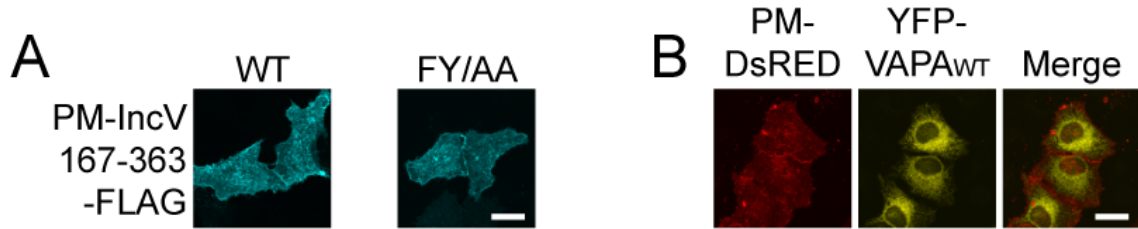


Figure 2.13. PM targeting of IncV and effect of PM-dsRed on VAPA cellular localization.

Confocal micrographs of HeLa cells expressing PM-IncV₁₆₇₋₃₆₃-WT-3xFLAG or PM-IncV₁₆₇₋₃₆₃-FY/AA-3xFLAG (blue) (A) or co-expressing PM-dsRed (red) and YFP-VAPA WT (yellow) (B). Scale bar = 5 μ m.

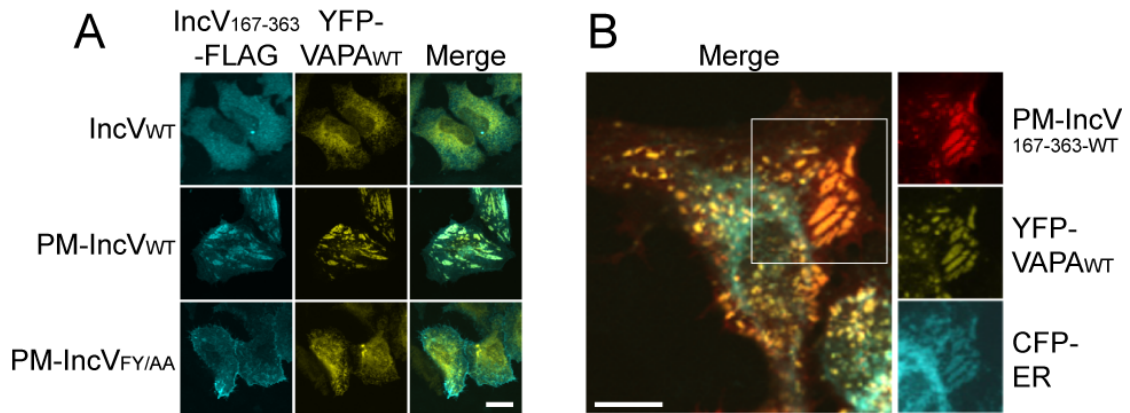


Figure 2.14. PM targeting of IncV induces the formation of ER-PM MCS. (A) Confocal micrographs of HeLa cells coexpressing YFP-VAPAWT (yellow) and IncV167–363-WT-3xFLAG, PM-IncV167–363-WT-3xFLAG, or PM-IncV167–363-FY/AA-3xFLAG (blue). The merge is shown on the Right. (Scale bar, 10 μm .) PM targeting was achieved by fusion of a C-terminal CAAX motif. (B) Confocal micrograph of HeLa cells coexpressing PM-IncV167–363-WT-3xFLAG (red), YFPVAPAWT (yellow), and CFP-ER (blue). The merge is shown on the Left and individual channels to the Right. (Scale bars, Left, 10 μm ; Right, 5 μm .) In A and B, XY cross-sections corresponding to the cell glass coverslip interface are shown.

2.2.9 An *IncV* Mutant Displays MCS with Reduced Level of VAP.

Finally, we tested if *IncV* is required for the formation of ER-inclusion MCS by using an *incV::bla* mutant.⁶⁷ We confirmed that the mutant harbors an intron insertion between nucleotide position 99 and 100 of the *incV* ORF, which is predicted to lead to the production of a truncated peptide containing the first 33 aa of *IncV* (Figure 2.15 A and B). Moreover, as previously shown by Weber *et al.*, the *incV::bla* mutant did not display a growth defect (Figure 2.14C). VAP+ ER-inclusion MCS of similar volumes were observed in close apposition to inclusions harboring the *incV::bla* mutant or its WT counterpart (Figure 2.16 A and B); however, the mutant displayed a significant, albeit moderate, reduction in the levels of YFP-VAP enrichment at the MCS (Figure 2.16C). In sum, our data indicate that *IncV* is sufficient, but not necessary, for the formation of ER-inclusion MCS, suggesting the existence of redundant mechanisms.

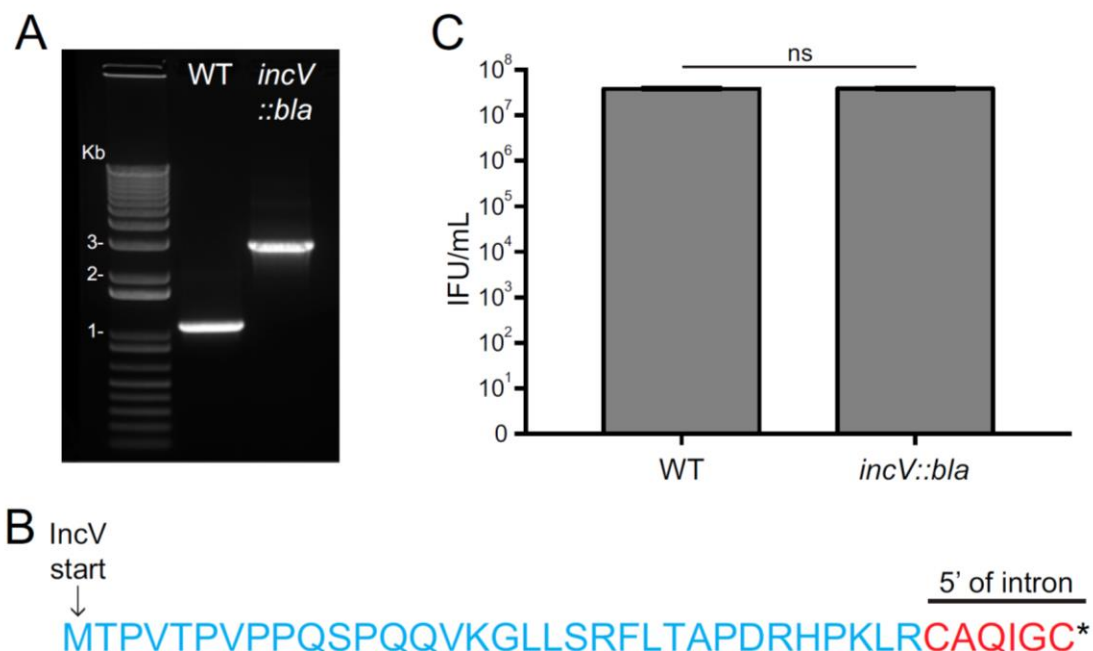


Figure 2.15. Characterization of the *C. trachomatis incV::bla* mutant. (A) PCR analysis of the *incV::bla* mutant. The *incV* ORF was amplified from genomic DNA extracted from WT *C. trachomatis* (WT) or the *incV::bla* mutant and the corresponding PCR products were resolved on a 1% DNA agarose gel stained with ethidium bromide (lane 2: WT; lane 3: *incV::bla* mutant). Lane 1: molecular weight marker. The marker sizes are listed in kilo base pairs to the left. (B) The site of insertion of the group II intron was determined by Sanger sequencing. A translation of the resulting IncV truncated peptide is presented. The asterisk denotes the early stop codon introduced by insertion of the group II intron. Blue: IncV, Red: group II intron. (C) HeLa cells were infected with *C. trachomatis* WT or the *incV::bla* strain and infectious forming units (IFUs) were measured 48 h postinfection. ns, not significant.

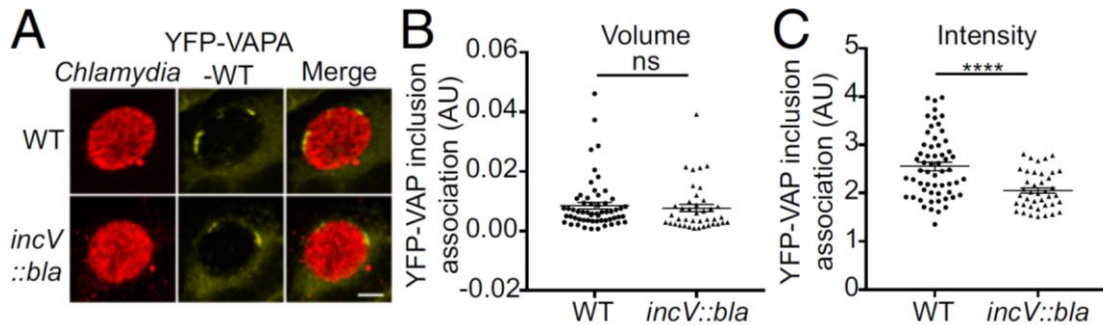


Figure 2.16. An *incV* mutant displays diminished VAP association with the inclusion.

(A) Three-dimensional reconstruction of confocal micrographs of HeLa cells expressing YFP-VAPAWT (yellow), infected with *C. trachomatis* WT or an *incV* mutant (*incV::bla*) and stained with anti-major outer membrane protein (anti-MOMP) antibodies (red). The merge is shown on the Right. (Scale bar, 5 μm .) (B and C) Quantification of the volume (B) and intensity normalized to the bulk of the ER (C) of the YFP-VAP signal associated with WT (•) or *incV* mutant (*incV::bla*, ▲) inclusions in arbitrary units (AU). Each circle or triangle represents one inclusion. The quantification method is described in Figure 2.8. Error bars are SEM. ns, not significant. **** $P < 0.0001$.

2.3 Discussion

Here, we report the first bacterial factor containing eukaryotic FFAT motifs and we present evidence that both motifs are required for IncV interaction with the ER-resident proteins VAPA and VAPB.

FFAT motifs were first described as a 7 amino acid sequence (EFFDaxE) that target eukaryotic proteins to the ER through interaction with the ER-resident VAP proteins.¹⁸⁰ The sequence of IncV cFFAT (EYMDALE) is nearly identical to the consensus FFAT motif and key residues that have been shown to mediate the FFAT/VAP interaction are conserved.^{179,181,199} It includes the invariable aromatic residue (phenylalanine or tyrosine) at position 2, which has been shown to establish van der Waals interaction with VAPA residue methionine 89. Accordingly, mutation of this critical aromatic residue at position 2 of the cFFAT motif of IncV was sufficient to abolish the IncV-VAP interaction. Moreover, substitution of methionine 89 (and lysine 87) in VAP_{KFM/DFD} abolishes VAP interaction with FFAT-containing proteins, including IncV. The cFFAT of IncV also displays the conserved aspartate residue at position 4. Structure analysis of VAP bound to the FFAT motif of OSBP revealed that this aspartate residue formed an electrostatic interaction with lysine 34 and lysine 45 present in the electropositive face of the MSP domain of VAPA.¹⁹⁹ In addition, alanine substitution of aspartate residue at position 4 in the FFAT motif of Osh1, CERT and protrudin abolished the interaction of each protein with VAP,^{180,193,204} further illustrating the importance of these conserved residues for FFAT-VAP interaction. As previously described for the FFAT-like motif of ORP3 (HFFSGST) and

STARD3 (QFYSPPE), the ncFFAT of IncV (SFHTPPN) is more divergent from the canonical sequence.^{189,201} Nevertheless, it displays the aromatic residue at position 2 and, like in ORP3 and STARD3, position 4 harbors a serine or threonine residue that could be phosphorylated and therefore mimic the aspartate residue present in the canonical sequence. Altogether, the level of mimicry displayed by the FFAT motifs of IncV is striking and each motif, especially the cFFAT, contains the key residues that have been experimentally confirmed to promote interaction with the VAP proteins.

Another hallmark of the FFAT motif is the presence of upstream acidic residues, such as aspartate, glutamate or negatively charged residues such as phosphorylated serine and threonine residues.¹⁸⁰ On average, four acidic residues are present upstream of any given FFAT motif,^{178,201} but strikingly, IncV ncFFAT and cFFAT motifs are each directly preceded by multiple serine residues, which, if phosphorylated and combined with the acidic residues also present upstream of the FFAT motifs, would offer unprecedented tracts of nine and eight consecutive negatively charged residues, respectively (Figure 2.1B). If, as proposed, the acidic tract plays a role in increasing VAP binding by mediating the formation of intermediate FFAT-VAP complex *via* electrostatic interactions,¹⁹⁹ it would suggest that the molecular mimicry displayed by *C. trachomatis* goes beyond the presence of FFAT motifs and also includes an accessory mechanism that ensures strong binding to VAP.

Many of the FFAT motif-containing proteins characterized to date are lipid transfer proteins of the CERT and QSBP-related proteins (ORP) family. Until recently, it was

assumed that each of these proteins harbor a single canonical FFAT motif that interacts with the electropositive face of the MSP domain of the VAP proteins, thus mediating the interaction with the ER. However, Weber-Boyvat *et. al.* identified and characterized a second FFAT-like motif upstream of the canonical FFAT motif in ORP3.²⁰¹ This observation led to the identification of many more putative FFAT-like motifs upstream of the canonical FFAT motif of known VAP interacting proteins.^{178,201} Although the functionality of these FFAT-like motifs remains to be tested experimentally, data gathered for ORP3 validated the importance of the FFAT-like motif, by demonstrating that although mutation of the FFAT motif abolished VAP binding by 40%, mutation of both the FFAT and the FFAT-like motifs of ORP3 were required to completely abolish ORP3-VAP interaction, indicating that both motifs acted in synergy for VAP binding.²⁰¹ Similarly, the results presented here with IncV show that although the ncFFAT of IncV was dispensable for IncV-VAP interaction in a Co-IP experiment *in vitro*, both motifs were required for VAP association with the inclusion *in vivo*. Altogether, these results reinforce the idea that cooperation of two FFAT motifs may be a common mechanism dictating the interaction of proteins with the VAP proteins.

At MCS, the membranes of the contacting organelles are brought and kept in close proximity by molecular tethers that meet the following criteria: 1) are enriched at the point of contact between the two organelles, 2) are part of a molecular complex that bridges the opposing membranes, 3) if not redundant, their deletion abolishes the contact between the two organelles and 4) regardless of redundancy, their

overexpression increases the extent of contact.^{157,163} Our work demonstrates that the *C. trachomatis* inclusion membrane protein, IncV, fulfills at least three of the four criteria of a MCS tether. 1) IncV localizes to ER-Inclusion MCS. 2) IncV is inserted into the inclusion membrane and interacts with the ER-resident protein VAP. The IncV-VAP interaction therefore offers a molecular bridge that connects the inclusion membrane to the ER. 3) An IncV insertion mutant and a ChxR null strain, which display diminished levels of IncV mRNA and protein, were recently described.^{67,205} It would therefore be interesting to assay if these strains are deficient in ER-Inclusion MCS. However, although depletion of the IncV interacting partners, VAPA and VAPB, leads to a reduction in *C. trachomatis* intracellular replication,¹¹⁰ IncV depletion did not affect *Chlamydia* replication in tissue culture.^{67,205} These results suggest that, in addition to IncV, additional bacterial factors may participate in maintaining the ER in close proximity to the inclusion membrane. 4) IncV over-expression in *C. trachomatis* leads to a massive association of VAP with the inclusion, which correlates with an increase in the extent of the contacts between the inclusion membrane and the ER. Importantly, this occurs with endogenous level of VAP. Moreover, IncV could also mediate the recruitment of the ER when targeted to the plasma membrane. The latter indicates that IncV can act independently of the lipid and protein environment, thus providing strong evidence that IncV is sufficient to mediate the formation of ER-Inclusion MCS.

Although the *incV* mutant was partially impaired in VAP recruitment, *incV* deletion did not abolish the formation of ER-inclusion MCS, suggesting that additional

factors may be involved in MCS formation. Interestingly, we have shown that at ER-inclusion MCS, VAP also interacts with the lipid transfer protein CERT, which is recruited to the inclusion via interaction with IncD.⁵⁸ Thus, the IncD/CERT/VAP interaction could also provide some stability to the contacts, while being involved in lipid transfer (Figure 2.17). This would be analogous to the STARD3/VAP interaction occurring at ER-endosome MCS, where the lipid transfer protein STARD3 mediates both the tethering of endosomes to the ER and the transfer of cholesterol between these two organelles.^{189,190} We note, however, that co-overexpression of all three components of the IncD/CERT/VAP complex was required for increased recruitment of VAP to the inclusion.⁵⁸ This is different from the present IncV–VAP interaction, which did not require VAP overexpression, suggesting a potent and direct role for IncV in VAP recruitment to the inclusion. Taking all of this together, we propose a model in which IncV is one of the primary tethers that contributes to the recruitment and association of the ER with the inclusion membrane.

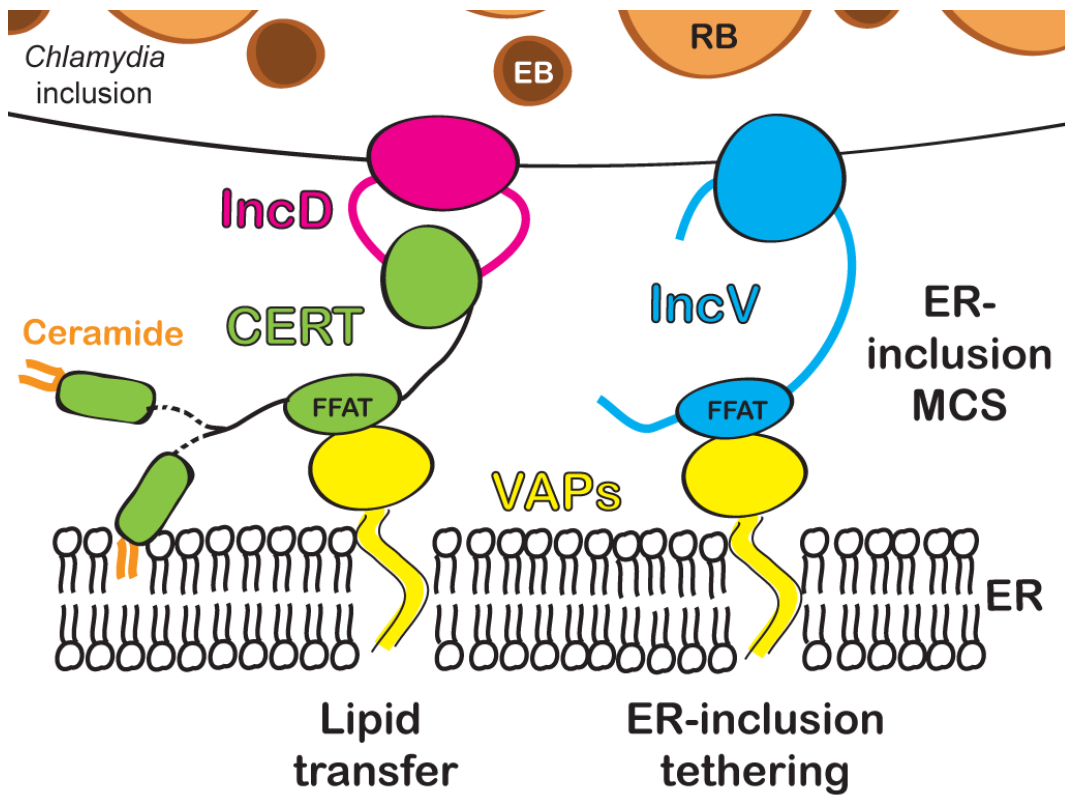


Figure 2.17: Schematic representation and proposed role of IncV/VAP and IncD/CERT/VAP at ER-inclusion MCS. EB, elementary body; RB, reticulate body.

2.4 Conclusion

Direct organelle contact, with no fusion occurring, is emerging as an important mechanism involved in inter-organelle communication, and also in host–pathogen interactions. MCS are complex structures with a specific molecular signature that depends on the organelles involved, and deciphering the molecular components that control their formation and function is important to better understand their overall biology. The work presented herein illustrates how intracellular, vacuolar pathogens have evolved molecular mimicry of these components, thereby mediating the direct contact of the pathogen-containing vacuole with cellular organelles. Specifically, our data demonstrate that *C. trachomatis* displays on the surface of its inclusion a bacterial factor, IncV, that contains eukaryotic FFAT motifs required for the recruitment of the ER-resident protein VAP to the inclusion. Interestingly, as this report was under revision, it was shown that norovirus NS1-2 protein, a known VAP-interacting protein, also contains a FFAT motif.²⁰⁶ Although the role of the NS1-2/VAP interaction remains to be determined, these observations suggest that viral and bacterial pathogens have coopted molecular mimicry of FFAT motifs to exploit the ER and establish their replication niche. Further characterization of the *Chlamydia* IncV–VAP system may not only shed light on the role of ER-inclusion MCS during *Chlamydia* pathogenesis, but also contribute to our understanding of the mechanism underlying organelle communication through formation of membrane contact sites.

2.5 Materials and Methods

2.5.1 Ethics Statement

All genetic manipulations and containment work were approved by the UVA Biosafety Committee and are in compliance with the section III-D-1-a of the National Institute of Health guidelines for research involving recombinant DNA molecules.

2.5.2 Cell Lines and Bacterial Strains

HeLa cells (ATCC CCL-2) or HEK293 cells (ATCC CRL-1573) were cultured at 37°C with 5% CO₂ in DMEM high glucose (Gibco) supplemented with 10% heat inactivated FBS (Gibco). *C. trachomatis Lymphogranuloma venereum, Type II* (ATCC L2/434/Bu VR-902B) propagation and infection were performed as previously described.²⁰⁷

2.5.3 Plasmid Construction

Restriction enzymes and T4 DNA ligase were obtained from New England Biolabs (Ipswich, MA). PCR was performed using Herculase DNA polymerase (Stratagene). PCR primers were obtained from Integrated DNA Technologies. The primers and cloning strategies are listed in Appendix 1.

2.5.4 Vectors for Expression in Mammalian Cells:

PM-DsRed was obtained from Invitrogen. GFP-VAPA_{WT} and GFP-VAPB_{WT} plasmids were previously described.¹¹⁰ GFP-VAPA_{KFM/DFD} and GFP-VAPB_{KFM/DFD} were kind gifts from Dr. Alpy (IGBMC, France) and were previously described.¹⁸⁹ YFP-VAP constructs were generated by cloning of the VAP ORFs into the *AgeI* and *HindIII* (VAPA) and *EcoRI* and *AgeI* (VAPB) restriction sites of pCMV-N1-YFP (Invitrogen). For IncV expression in eukaryotic

cells, DNA fragments corresponding to the IncV ORF either WT or containing the mutations F263A, Y287A and FY-AA were amplified by PCR and cloned into the *XhoI* and *BamHI* restriction sites of pCMV-IE-N2-3xFLAG. The same approach was used to generate the IncV₁₆₇₋₃₇₃3xFLAG WT and FY-AA constructs and the corresponding plasma membrane targeted constructs.

2.5.5 Vectors for Expression in *E. coli*:

GST-VAPA fusion constructs WT or KFM/DFD were generated by cloning the MSP domain of VAPA into the *BamHI* and *EcoRI* restriction sites of pGEX-KG.

2.5.6 Vectors for Expression in *C. trachomatis*:

The p2TK2-SW2 mCh(Gro) Tet-IncV-3F plasmids are derivatives of p2TK2-SW2 mCh(Gro) plasmid and were constructed as described for p2TK2-SW2 mCh(Gro) TetIncD3F.⁵⁸ Briefly, each Tet-IncV-3F fragment was amplified by overlap PCR, using the primers and templates listed in Appendix 1, and cloned into the *KpnI* and *NotI* restriction sites of p2TK2-SW2 mCh(Gro). The resulting plasmids allow for constitutive expression of mCherry under the control of the *groESL* promoter and terminator and the inducible expression of the IncV-FLAG variants (WT, F263A, Y287A and FY-AA) under the control of the anhydrotetracyclin inducible promoter.

2.5.7 DNA Transfection

DNA transfection was performed using X-tremeGENE™ 9 DNA Transfection Reagent (Roche) according to the manufacturer's recommendations.

2.5.8 Co-immunoprecipitation

For co-transfection experiments, 8×10^5 HEK293 cells seeded in 6-well tissue culture plates and transfected for 48 h were washed once with 1xPBS and lysed in 250 μ L of lysis buffer (20mM Tris pH 7.5, 150mM NaCl, 2mM EDTA, 1% Triton X-100, protease inhibitor cocktail EDTA-free (Roche)) for 20 minutes at 4°C, rotating. All subsequent steps were performed at 4°C. The lysates were centrifuged at 13,000 rpm for 10 min and a 10 μ L aliquot of the pre-cleared lysates was collected (Lysate). The pre-cleared lysates were incubated with 10 μ L of anti-FLAG M2 affinity beads (Sigma) for 2 h, rotating. The protein-bound beads were washed three times with wash buffer (20mM Tris pH 7.5, 150mM NaCl, 2mM EDTA, 1% Triton X-100) and proteins were eluted in 20 μ L of elution buffer (20mM Tris pH 7.5, 150mM NaCl, 2mM EDTA, 100 μ g/mL 3xFLAG peptide (Sigma)) and 15 μ L of the elution fraction was collected (IP). For transfection/infection experiments, the cells were transfected for 24h prior to *C. trachomatis* infection (MOI of 5). Infected cells were incubated in the presence of 2ng/ml of aTc starting 8h post infection and the samples were processed as described above 24h post infection.

2.5.9 Immunoblotting

Protein samples were separated by SDS-PAGE and transferred to nitrocellulose membranes. The membranes were stained with a Ponceau S solution, to ensure for even transfer, and rinsed with dH₂O before blocking in blocking buffer (5% nonfat milk in 1xPBS, 0.05% Tween) for 1h at room temperature. Primary and HRP-conjugated secondary antibodies were diluted in blocking buffer and incubated with the membranes overnight at 4°C and 1h at room temperature, respectively. HRP-conjugated secondary

antibodies were detected with the Amersham ECL Western blotting detection reagent according to the manufacturer's recommendations and a BioRad ChemiDoc imaging system.

2.5.10 Antibodies

The following antibodies were used for immunofluorescence microscopy (IF) and immunoblotting (WB): rabbit polyclonal anti-GFP (1:2,000 (WB), Invitrogen), mouse monoclonal anti-FLAG (1:1,000 (IF); 1:10,000 (WB), Sigma), rabbit anti-VAPA (1:200 (IF), kind gift of Dr. DeMatteis, TIGEM, Italy), HRP-conjugated goat anti-rabbit IgG (1:10,000 (WB), Jackson), HRP-conjugated goat anti-mouse IgG (1:10,000 (WB), Jackson), AlexaFluor 594, 514 or Pacific Blue conjugated goat anti-mouse IgG (1:500 (IF), Molecular Probes).

2.5.11 Protein Purification and GST Pull-down

GST, GST-VAPAMSP-WT, GST-VAPAMSP-KFM/DFD constructs were expressed by IPTG induction of a 5ml culture of *E. coli* (BL21IDE3). Bacterial pellets resuspended in 800µl of sonication buffer (20mM Tris pH 7.5, 300mM NaCl, 2mM EDTA, 1mM MgCl₂, 1% Triton X-100, 1mM DTT, 1mM PMSF) were sonicated using 5 pulses at 40% power. The samples were centrifuged for 10 min at 12,000 rpm, 4°C. All subsequent steps were performed at 4°C. The pre-cleared lysates were incubated with 40µl glutathione sepharose beads (GE healthcare), equilibrated with sonication buffer, for 2h, rotating. The protein-bound beads were washed three times in sonication buffer, then resuspended in GST pull down buffer (20mM Tris pH 7.5, 150mM NaCl, 1mM MgCl₂, 1% Triton X-100, protease inhibitor cocktail EDTA-free (Roche)). Equal amount of protein-bound glutathione beads were

incubated overnight, rotating, with 400 μ l of pre-cleared lysate corresponding to a third of a confluent 10cm² dish of HEK293 cells expressing the indicated constructs and lysed in GST pull down buffer. 10 μ l aliquots of the respective lysates were also collected (Lysate). The beads were washed 3 times with 500 μ l of GST pull down buffer and resuspended in SDS sample buffer. The samples were separated by SDS-PAGE and analyzed by Ponceau S staining and immunoblot.

2.5.12 Immunofluorescence and Confocal Microscopy

All steps were performed at room temperature. At the indicated times, HeLa cells seeded on glass coverslips were fixed with 4% paraformaldehyde in 1xPBS for 30 min. Coverslips were sequentially incubated with primary and secondary antibodies diluted in 0.1% Triton X-100 in 1xPBS for 1 h. Coverslips were washed with 1xPBS and mounted with DABCO antifade containing mounting media. For endogenous VAPA staining, the cells were fixed for 5 min in ice-cold methanol (resulting in the loss of the mCherry signal) and the antibodies were diluted in 1xPBS. Imaging was performed using a spinning disc confocal microscope equipped of an Andor CCD camera and running the IQ software.

2.5.13 *C. trachomatis* Transformation

Our calcium-based transformation protocol was previously described.⁵⁴

2.5.14 Inclusion Association Quantification

HeLa cells were transfected with the indicated YFP-VAP construct 24h prior to *C. trachomatis* infection. The expression of the respective IncV constructs was induced for 4h by

addition of 20ng/ml of aTc 20h post *C. trachomatis* infection. The samples were processed for confocal microscopy and 3-dimensional reconstructions of the raw signal corresponding to each marker (IncV-3xFLAG, YFP-VAP and mCherry positive inclusion) were generated using the Imaris imaging software. For each marker, the volume corresponding to the sum of the pixels, above the threshold corresponding to the signal in the cytoplasm, was determined. The IncV and VAP volumes were normalized to the corresponding inclusion volume to determine the inclusion association of the respective markers in arbitrary unit. A graphic representation of the method is presented in Figure. 2.7. 10-30 inclusions were analyzed per condition. The graphs were generated using GraphPad Prism. Average and SEM from one representative experiment are shown. Student's t-test was performed and statistical significance was set to $P < 0.0001$.

2.5.15 Transmission Electron Microscopy

HeLa cells were infected with a strain of *C. trachomatis* expressing IncV-FLAG under the control of the aTc inducible promoter. 18h post infection cells were incubated or not in the presence of 20ng/ml of aTc. 24h post infection, the samples were fixed in 2% paraformaldehyde + 2.5% glutaraldehyde in 0.1M cacodylate buffer (pH 7.4) for 60 min on ice. After several washes with cacodylate buffer, cells were scraped off and pelleted. The cells were resuspended in 2% ultra-low temperature gelling agarose (in 0.1M cacodylate, 37°C) and then quickly pelleted and cooled on ice for the agarose to solidify. The pellet were cut out into small pieces and post-fixed in 1% reduced OsO₄ on ice for 60 min. After post-fixation, the pellet pieces were washed with H₂O and en block stained

with 2% uranyl acetate (in H₂O). The pellet pieces were then dehydrated through an ethanol series, infiltrated and embedded in Epon. 70nm-thick sections were cut from the embedded sample using a Leica EM UC7 ultramicrotome and contrast stained with uranyl acetate and lead. Finally, images were acquired with a JEOL 1230 TEM.

2.6 Acknowledgments

We thank Ted Hackstadt (NIH-Rocky Mountain Laboratories) and Mary Weber (University of Iowa) for sharing the *incV::bla* strain; Antonella DeMatteis (Telethon Institute of Genetics and Medicine) for providing the anti-VAPA antibodies; Fabien Alpy (Institut de Génétique et Biologie Moléculaire et Cellulaire) for the GFP-VAP constructs; Tom-Rapoport (Harvard Medical School) for the Sec61 β DNA; Yalin Wang for the electron microscopy (University of Virginia); And Hervé Agaisse, Dave Kashatus, Jim Casanova, Maria-Eugenia Cortina, and Rachel Ende (University of Virginia) for critical reading of the manuscript. This work was supported by NIH Grants R01AI101441 (to I.D.) and T32AI007046 (to R.S.).

Chapter 3

**IncV, a tether of ER-*Chlamydia* Inclusion Membrane Contact Site,
is phosphorylated by the host Protein Kinase CK2 to promote the
IncV-VAP interaction^b**

^bStanhope, R., Ende, R. & Derré, I. IncV, a tether of ER-*Chlamydia* Inclusion Membrane Contact Site, is phosphorylated by the host Protein Kinase CK2 to promote the IncV-VAP interaction. Manuscript in preparation.

3.1 Introduction

Emerging evidence suggests that MCS are regulated through post-translational modifications.¹⁶² For example, CERT lipid transfer function and binding to VAP proteins are both modulated through two distinct phosphorylation events on CERT.^{208,209} In another example, the formation of Yeast vacuole-Mitochondria MCS is regulated through the phosphorylation of the tether protein Vps39.¹⁶⁷ Given the dynamic nature of many MCS, I hypothesize that phosphorylation or other post-translational modifications play a role in more MCS.

The current model of ER-inclusion MCS includes both functional and structural components from the host and bacteria. The Inc protein IncD interacts with the Pleckstrin homology (PH) domain of the host ceramide transfer protein CERT.^{58,110,210} In both *Chlamydia*-infected and naïve cells, CERT interacts with VAP proteins.^{110,149,165} The IncD/CERT/VAP complex has been proposed to function in bacterial acquisition of host lipids.^{110,149} The ER calcium sensor protein STIM1 was also identified as a component of ER-inclusion MCS and has an unknown interacting partner there.¹⁵¹ Most recently, we have described a tethering complex at ER-inclusion MCS that is composed of the Inc protein IncV which interacts directly with VAP (Chapter 2).¹⁰⁹ The c-terminal, cytoplasmic tail of IncV contains two FFAT motifs that mediate the interaction with VAP.

Though we have gained insight into the function and formation of ER-inclusion MCS, it is still unclear if or how their formation is regulated. Here, we describe the role of a host kinase, Protein Kinase CK2, in phosphorylating IncV to promote the IncV-VAP

interaction *in vitro* and during infection. We demonstrate that a specific region in the C-terminus of IncV mediates the recruitment of CK2 to the inclusion membrane during infection. We show that IncV is phosphorylated by CK2 and inhibition of CK2 prevents phosphorylation of IncV and that IncV-dependent VAP recruitment to the inclusion depends on the function of CK2. We present evidence that CK2 is a new member of ER-Inclusion MCS and discuss the implications for these findings in the broader context of infection and VAP-mediated MCS biology.

3.2 Results

3.2.1 IncV is Phosphorylated by a Host Kinase.

We had previously observed that IncV-3xFLAG protein expressed by *Chlamydia trachomatis* migrated as a protein band doublet in Western blot. This observation led us to hypothesize that IncV was post-translationally modified. To determine whether host factors played a role in modifying IncV, we assessed the apparent molecular weight of IncV-3xFLAG expressed in *C. trachomatis*-infected cells, HEK293 cells, or *E. coli* by anti-FLAG Western blot analysis of whole cell lysates (Figure 3.1A). For inducible expression of IncV in *C. trachomatis*, we utilized a strain of wild type *C. trachomatis* serovar L2 transformed with our p2TK2-SW2 mCh(gro) *C. trachomatis*/*E. coli* shuttle vector containing IncV-3xFLAG under an anhydrotetracycline (aTc)-inducible promoter and mCherry under a constitutive promoter (hereafter referred to as *C. trachomatis* wildtype + pTet-IncV-3xFLAG). IncV-3xFLAG that was expressed in *C. trachomatis* appeared as a protein band doublet, with bands at approximately 60kD and 50kD (Figure

3.1A, middle lane, 293 + *Ct*). For transient expression in eukaryotic cells, we generated a plasmid containing the *incV* open reading frame (ORF) with a c-terminal 3xFLAG tag in a eukaryotic vector. IncV-3xFLAG that was expressed in HEK293 cells had an apparent molecular weight that was more similar to the top band of the doublet (Figure 3.1A, left lane, 293). In contrast, IncV-3xFLAG expressed in *E. coli* had an apparent molecular weight equivalent to the lower band of the doublet (Figure 3.1A, right lane, *Ec*). The data presented in Figure 3.1A suggest a eukaryotic enzyme, and not an enzyme found in *E. coli*, plays a role in modifying IncV.

A common post-translational modification is phosphorylation and the cytosolic tail of IncV is enriched in phosphorylatable residues (Serine, Threonine, and Tyrosine). Thus, we tested whether IncV was phosphorylated by performing a phosphatase assay. IncV-3xFLAG was immunoprecipitated, using anti-FLAG-conjugated Sepharose beads, from lysates of HEK293 cells infected with *C. trachomatis* that expressed IncV-3xFLAG. Following the release of IncV-3xFLAG from the beads by FLAG peptide competition, the eluate was treated with lambda (λ) phosphatase or phosphatase buffer alone, and subsequently subjected to anti-FLAG Western blot analysis (Figure 3.1B). In the absence of λ phosphatase, the apparent molecular weight of IncV-3xFLAG was approximately 60kD (Figure 3.1B, left lane). Upon phosphatase treatment, we observed a decrease in the apparent molecular weight of IncV-3xFLAG to approximately 50kD similar to what is observed in *E. coli*, indicating that phosphate groups had been removed and

demonstrating that IncV is phosphorylated (Figure 3.1B, right lane). Altogether, these results suggest that a eukaryotic kinase plays a role in the phosphorylation of IncV.

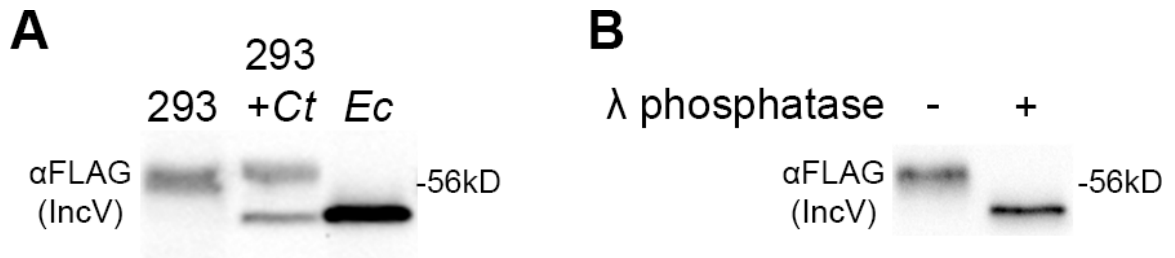


Figure 3.1. IncV is phosphorylated by a host factor. A) Western blot of IncV-3xFLAG in lysates of HEK293 cells expressing IncV-3xFLAG (293), in HEK293 cells infected with *C. trachomatis* expressing IncV-3xFLAG (293 + Ct), or *E. coli* (Ec). B) Western blot of IncV-3xFLAG purified from lysates of HEK293 cells infected with *C. trachomatis* expressing IncV-3xFLAG and treated with lambda (λ) phosphatase (+) or phosphatase buffer alone (-).

3.2.2 CK2 is Recruited to the Inclusion in an IncV-Dependent Manner.

We next focused on identifying the host kinase responsible of phosphorylating IncV at the inclusion. Interestingly, all three subunits of Protein Kinase CK2, formerly known as casein kinase 2, were identified as potential interactors of IncV in an Inc-Human interactome that originally predicted the IncV-VAP interaction.⁶⁰ The Inc-Human interactome is a web of predicted interactions between Inc proteins and host proteins generated by transfecting cells with DNA encoding tagged Inc proteins then performing affinity purification coupled with mass spectrometry.⁶⁰ The C-terminal, cytosolic tail of IncV contains 38 predicted CK2 recognition motifs identified using the canonical CK2 recognition motifs $(S/T)^1x^2x^3(D/E/pS/pY)^4$ and $(S/T)^1x^2(D/E/pS/pY)^3$, where x is any amino acid.²¹¹ To confirm that CK2 is associated with IncV on the inclusion membrane, we used confocal immunofluorescence microscopy to visualize HeLa cells expressing YFP-CK2 α or YFP-CK2 β and infected with *C. trachomatis* wildtype + pTet-IncV-3xFLAG (Figure 3.2). In the absence of IncV induction, YFP-CK2 α and YFP-CK2 β were not detected at the inclusion membrane (Figure 3.2A and 3.2B, -aTc). However, upon induction of IncV-3xFLAG, YFP-CK2 α and YFP-CK2 β were recruited to the inclusion membrane where they colocalized with IncV (Figure 3.2A and 3.2B, +aTc). To confirm that this phenotype was not the result of overexpression of CK2 subunits, we detected CK2 with an antibody that recognized endogenous CK2 β . As was the case for CK2 overexpression, endogenous CK2 β was not detected on the inclusion in the absence of IncV-3xFLAG induction (Figure 3.2C, -aTc). When IncV-3xFLAG expression was induced, endogenous CK2 β was recruited to

the inclusion (Figure 3.2C, +aTc). Together, these results demonstrate that CK2 is recruited to the inclusion in an IncV-dependent manner and that overexpression of CK2 is not required to observe this phenotype.

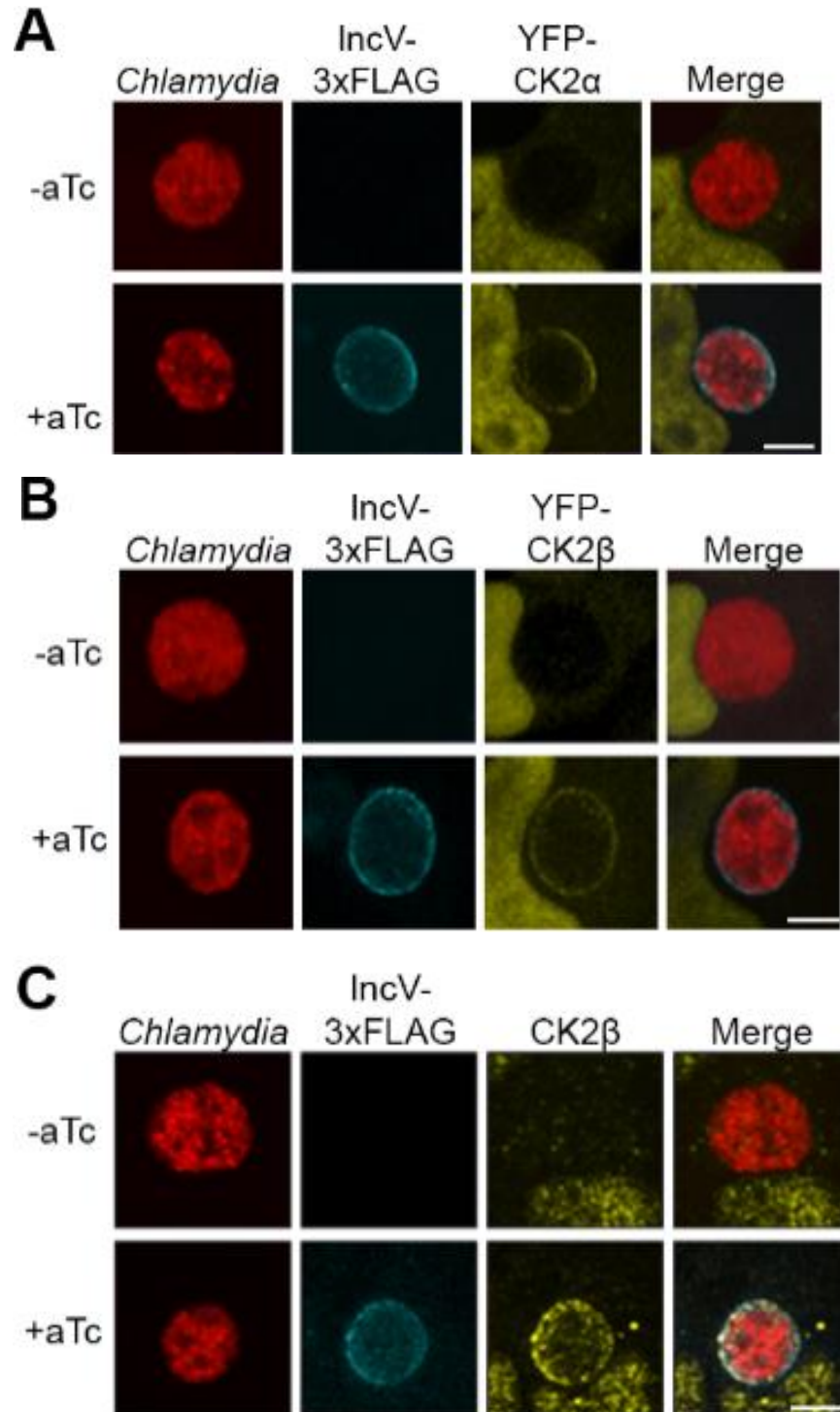


Figure 3.2. CK2 is recruited to the inclusion in an IncV-dependent manner. (A-B) 3-dimensional reconstruction of confocal images of HeLa cells overexpressing YFP-CK2 α (A,

yellow) or YFP-CK2 β (B, yellow) and infected with *C. trachomatis* expressing mCherry constitutively (red) and IncV-3xFLAG (blue) under the control of an anhydrotetracycline (aTc)-inducible promoter in the absence (-aTc) or presence (+aTc) of aTc. (C) Same as B except that endogenous CK2 β (Yellow) is detected instead of YFP-CK2 β . The merge is shown on the right. Scale bar is 5 μ m.

3.2.3 CK2 is a Novel Member of ER-Inclusion MCS

CK2 was recruited by the known ER-Inclusion MCS tether IncV (Figure 3.2A). Thus, we determined whether CK2 was also a component of ER-Inclusion MCS using confocal immunofluorescence microscopy to visualize the co-localization of CK2 and VAP upon IncV-3xFLAG overexpression (Figure 3.3A). HeLa cells were co-transfected with CFP-VAPA and YFP-CK2 α or YFP-CK2 β then infected with *C. trachomatis* wildtype + pTet-IncV-3xFLAG. In the absence of IncV-3xFLAG induction, YFP-CK2 α and YFP-CK2 β were not detected at the inclusion membrane and CFP-VAPA was enriched in small patches (Figure 3.3A and 3.3B, -aTc). However, upon IncV-3xFLAG expression, YFP-CK2 α and YFP-CK2 β colocalized with CFP-VAPA on the inclusion membrane (Figure 3.3A and 3.3B, +aTc). These results demonstrate that CK2 is a new factor in ER-Inclusion MCS.

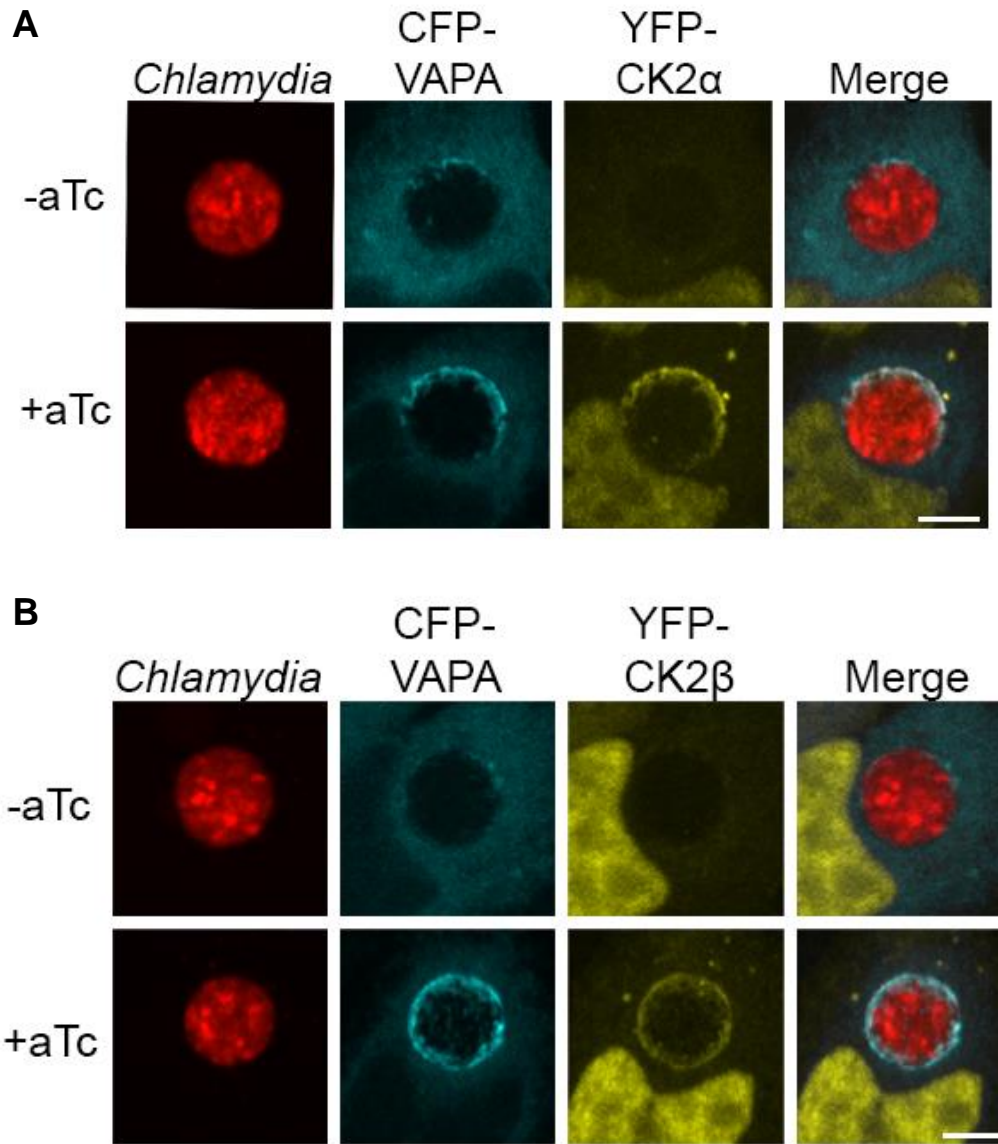


Figure 3.3. CK2 is a novel member of ER-Inclusion MCS. (A-B) 3-dimensional reconstruction of confocal images of HeLa cells overexpressing YFP-CK2 α (A, yellow) or YFP-CK2 β (B, yellow) and CFP-VAPA (blue) and infected with *C. trachomatis* expressing mCherry constitutively (red) and IncV-3xFLAG (not shown) under the control of an aTc-inducible

promoter in the absence (-aTc) or presence (+aTc) of aTc. The merge is shown on the right. Scale bar is 5 μ m.

3.2.4 A C-terminal Domain of IncV is Required for CK2 Recruitment to the Inclusion.

Since IncV mediated the recruitment of CK2 to the inclusion membrane, we next determined which regions of IncV were important for this recruitment by generating truncated IncV constructs (Figure 3.4A). To determine the contribution of specific regions of IncV without the endogenous IncV protein present, we utilized a previously characterized *incV* mutant strain of *C. trachomatis*, (referred to as *incV::bla*).^{67,109} We complemented the *incV::bla* strain with the pTet-IncV-3xFLAG containing either the full length (FL) or the truncated versions of IncV (1-305, 1-341, and 1-356). HeLa cells expressing YFP-CK2 β were infected with *C. trachomatis incV::bla* complemented with Tet-IncV-3xFLAG (FL, 1-356, 1-341, or 1-305) and IncV-3xFLAG expression was induced. Confocal micrographs were acquired and inclusion association of IncV-3xFLAG and YFP-CK2 β was quantified using the Imaris imaging software. All IncV constructs were displayed on the inclusion at similar levels, with IncV₁₋₃₅₆-3xFLAG inclusion localization modestly increased compared to wild type IncV-3xFLAG (Figure 3.4D). Compared to when IncV_{FL}-3xFLAG was expressed, YFP-CK2 β recruitment to the inclusion was significantly reduced when IncV₁₋₃₀₅-3xFLAG or IncV₁₋₃₄₁-3xFLAG were expressed by *C. trachomatis* (Figure 3.4B C, FL, 1-341, 1-305). We observed a partial rescue of YFP-CK2 β recruitment upon expression of IncV₁₋₃₅₆-3xFLAG (Figure 3.4B C, FL, 1-356). These results suggest that a c-terminal domain between amino acids 342 and 356 is required for IncV-dependent CK2 recruitment to the inclusion.

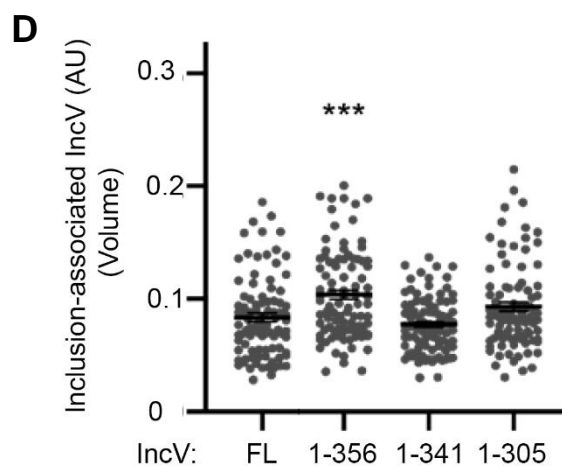
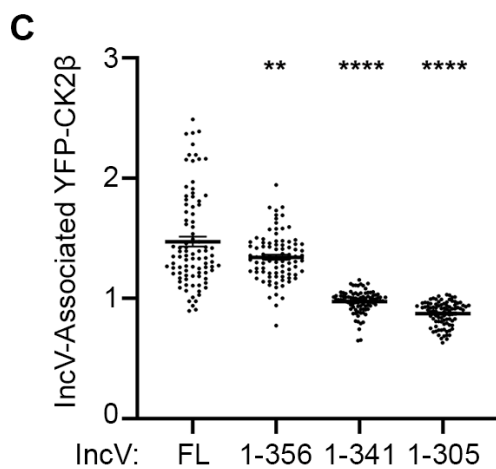
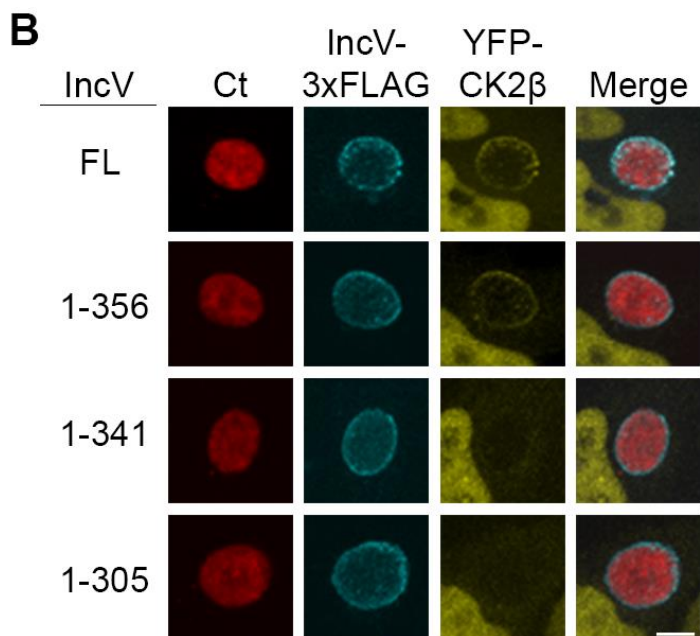
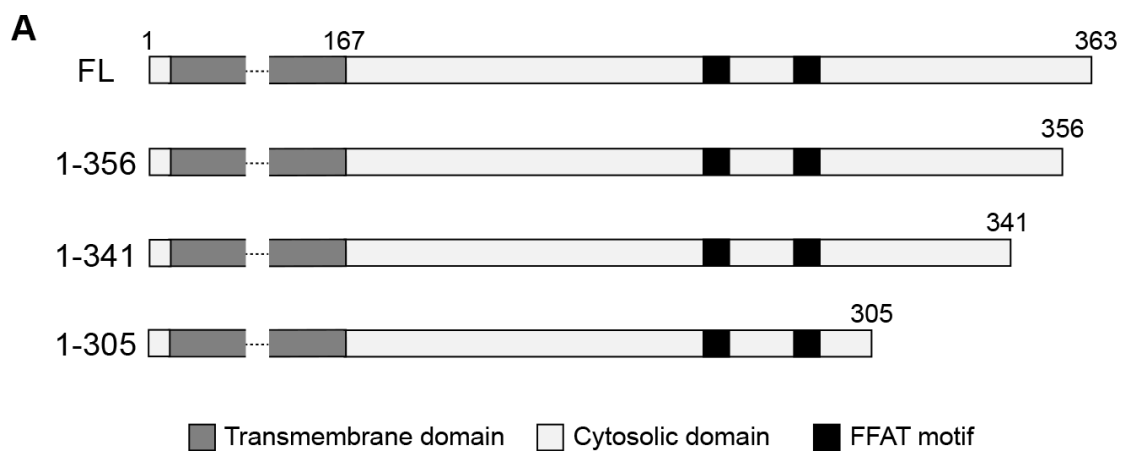


Figure 3.4. A C-terminal domain of IncV is required for CK2 recruitment to the inclusion. A) Schematic depicting truncated IncV constructs. The numbers represent a specific amino acid site in the protein sequence. B) 3-dimensional reconstruction of confocal micrographs of HeLa cells overexpressing YFP-CK2 β (yellow) and infected with *C. trachomatis incV* mutant expressing mCherry constitutively (red) and IncV-3xFLAG (full length (FL) or truncated (1-305, 1-341, or 1-356)) (blue) under the control of an aTc-inducible promoter in the presence of aTc. The merge is shown on the right. Scale bar is 5 μ m. C) Quantification of the mean intensity of YFP-CK2 β within an object generated from the IncV-3xFLAG signal and normalized to the mean intensity of YFP-CK2 β in the cytosol. Each dot represents one inclusion. Student's t-test was performed comparing truncations to full length. Error bars are SEM. ** $p < 0.01$, **** $p < 0.0001$. $n = 90$ inclusion D) Quantification of the volume of an object generated from the IncV-3xFLAG signal associated with the inclusion normalized to the volume of an object generated from the mCherry signal of the bacteria. Each dot represents one inclusion. Student's t-test was performed comparing truncations to full length. Error bars are SEM. *** $p < 0.001$. $n = 90$ inclusions.

3.2.5 CK2 Phosphorylates IncV.

We next tested if CK2 phosphorylates IncV. We performed an *in vitro* kinase assay using recombinant CK2, ATP γ S, and the cytosolic tail of IncV fused to GST (GST-IncV₁₆₇₋₃₆₃) or GST alone purified from *E. coli*. ATP γ S can be utilized by kinases to thiophosphorylate a substrate and an alkylation reaction of the thiol group generates an epitope that is detected using an antibody that recognizes thiophosphate esters.²¹² When the GST protein alone was provided as a substrate, there was no detectable phosphorylation, regardless of the presence of CK2 and ATP γ S (Figure 3.5A, lanes 1 and 2). When GST-IncV₁₆₇₋₃₆₃ was provided as a substrate, phosphorylation was not detected in the absence of CK2 and/or ATP γ S (Figure 3.5A, lanes 3 - 5). Conversely, when both ATP γ S and CK2 were present, GST-IncV₁₆₇₋₃₆₃ was phosphorylated (Figure 3.5A, lane 6). These results demonstrated that CK2 directly and specifically phosphorylates IncV *in vitro*

We next determined whether CK2 played a role in the post-translational modification of IncV during infection using RNA interference. Lysates of HeLa cells treated with siRNA targeting *CSNK2B* to deplete CK2 β and infected with *C. trachomatis* *incV::bla* + pTet-IncV-3xFLAG were subjected to Western blot. We confirmed *CSNK2B* knockdown efficiency at the protein level and observed a range of expression from 9.3% to 53.3% of the control expression levels of CK2 β (Figure 3.5B, middle blot). In control cells, as previously observed in Figure 1A, IncV_{FL}-3xFLAG appeared as a doublet with bands on either side of the 56kD marker (Figure 3.5B, top blot, left lane). A line scan analysis was

performed on each lane of the FLAG Western blot. The graph in Figure 3.5C is a graphical representation of the line scan analysis and depicts two major peaks that are representative of the upper band, which is the hyperphosphorylated species of IncV (left peak, black square) and the lower band which is the unphosphorylated species of IncV (right peak, black circle) (Figure 3.5C). Hypophosphorylated species of IncV are denoted by the open triangle above the line scan graph (Figure 3.5C) Consistent with the *in vitro* phosphorylation of IncV by CK2, depletion of CK2 using individual siRNA duplexes (A, B, C, or D) or a pool of all four siRNA duplexes (pool) led to a shift of the top band of the IncV-3xFLAG doublet down in apparent molecular weight, indicating CK2 plays a role in post-translational modification of IncV during infection (Figure 3.5B, top blot, pool, A, B, C, D lanes). The line scan plot illustrates the different species of hypophosphorylated IncV with peaks between the left (closed square) and right peaks (open circle) (Figure 3.5C). Moreover, knockdown efficiency mostly correlated with a larger shift in apparent molecular weight when CK2 expression was decreased (Figure 3.5B). Together, these data indicate that CK2 is involved in the post-translational modification of IncV *in vitro* and during infection.

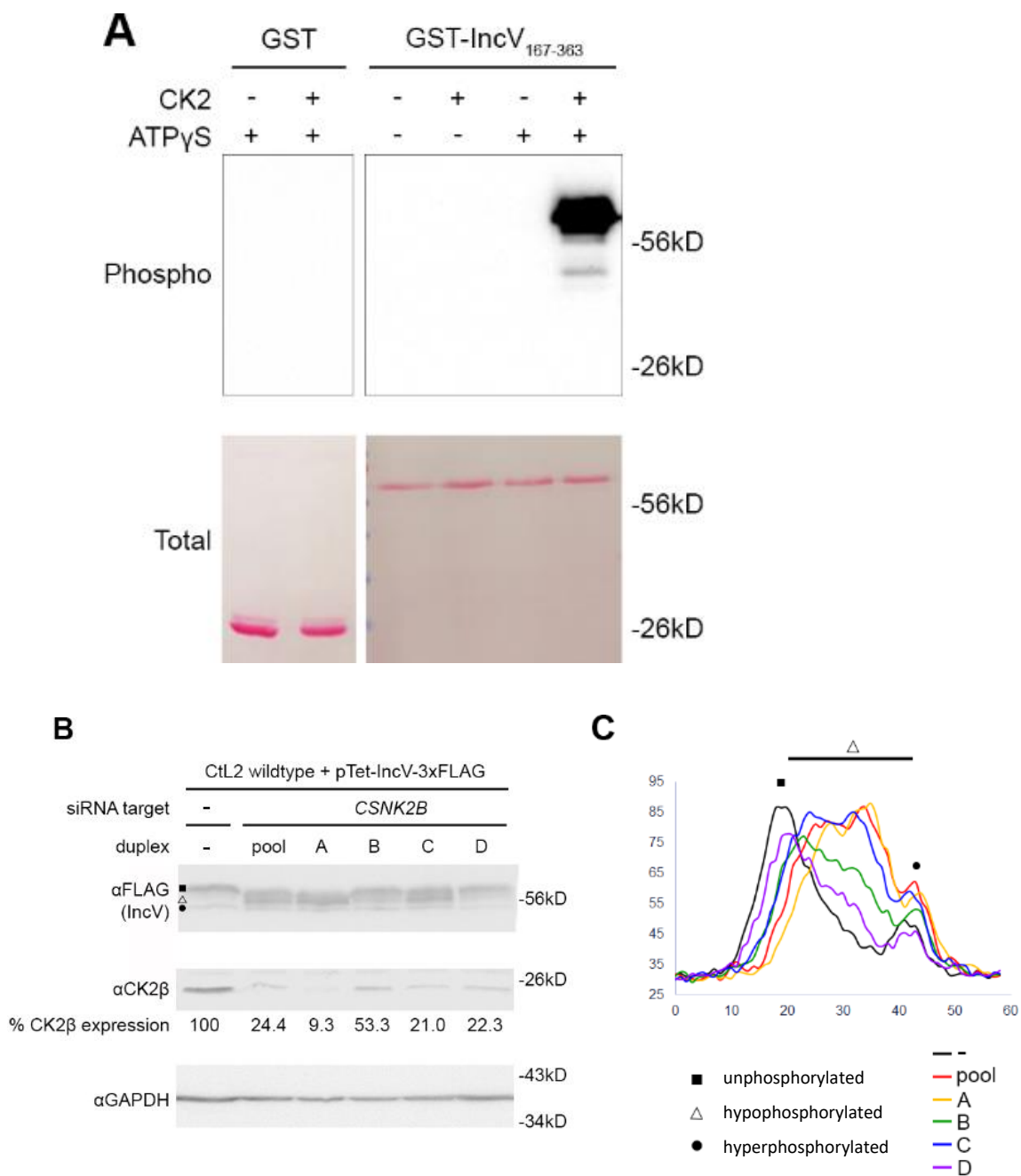


Figure 3.5. IncV is phosphorylated by CK2. A) *In vitro* kinase assay using GST or GST-IncV₁₆₇₋₃₆₃ purified from *E. coli* as a substrate in the presence or absence of recombinant CK2 and in the presence or absence of ATP γ S. The top panel shows phosphorylated

proteins detected with anti-Thiophosphate antibodies and the bottom panel is the same membrane stained with Ponceau S to detect total protein. B) Western blot of lysates of HeLa cells infected with *C. trachomatis* expressing IncV-3xFLAG and treated with siRNA buffer alone (-) or with siRNA duplexes targeting *CSNK2B* (pool of 4 duplexes or individual duplexes A, B, C, or D). The top panel was probed with anti-FLAG. The middle panel was probed with anti-CK2 β . The bottom panel was probed with anti-GAPDH. Relative expression levels of CK2 β normalized to GAPDH loading controls are shown as a percentage of no siRNA control expression. C) Line scan analysis of FLAG signal detected in (B). The black square points out the top band in the Western blot in B and corresponds to the hyperphosphorylated species of IncV, and the black circle denotes the bottom band in the same lane and corresponds to the hypophosphorylated species of IncV. Intermediately phosphorylated species are denoted by the open triangle and correspond to any band between the top and bottom bands. Each line represents a different condition: Control, black; siRNA pool of duplexes A-D, red; siRNA duplex A, yellow; siRNA duplex B, green; siRNA duplex C, blue; siRNA duplex D, purple.

3.2.6 Phosphorylation of IncV is Necessary and Sufficient to Promote the IncV-VAP Interaction.

We have previously shown that the IncV-VAP interaction *in vitro* required factors present in eukaryotic cells,¹⁰⁹ which led us to question whether the phosphorylation status of IncV could be important. We assessed the role of phosphorylation of IncV in the IncV-VAP interaction by performing lambda phosphatase dephosphorylation of IncV coupled with a GST pull-down assay (Figure 3.6A). IncV-3xFLAG was immunoprecipitated from lysates of HEK293 cells expressing IncV-3xFLAG using anti-FLAG-conjugated Sepharose beads. IncV-3xFLAG was released from the beads using FLAG peptide competition and treated with lambda phosphatase or buffer alone. Treated and untreated IncV-3xFLAG samples were then incubated with the cytosolic Major Sperm Protein (MSP) domain of VAPA tagged with GST (GST-VAP_{MSP}) or GST alone bound to glutathione Sepharose beads. The protein-bound beads were subjected to Western blot and the membranes were probed with anti-MBP to determine if IncV-3xFLAG was pulled down by treated or untreated GST or GST-VAP_{MSP} (Figure 3.6B). Untreated IncV-3xFLAG was pulled down by GST-VAP_{MSP}, and not by GST alone, demonstrating a specific interaction between IncV and VAP (Figure 3.6B, lanes 1 - 3). When the eluate containing IncV-3xFLAG was treated with lambda phosphatase prior to incubation with GST-VAP_{MSP}, it was no longer pulled down (Figure 3.6B, lane 4), indicating phosphorylation of IncV is necessary for the IncV-VAP interaction *in vitro*.

We next determined if IncV phosphorylation by CK2 was sufficient to promote

the IncV-VAP interaction in an *in vitro* binding assay (Figure 3.6C). MBP-tagged VAP_{MSP} (MBP-VAP_{MSP}) and GST-IncV₁₆₇₋₃₆₃ were expressed separately in *E. coli* and purified using amylose resin and glutathione Sepharose beads, respectively. GST-IncV₁₆₇₋₃₆₃ was left attached to glutathione Sepharose beads and was phosphorylated by incubation with recombinant CK2 and ATP before combining with purified MBP-VAP_{MSP}. GST-IncV₁₆₇₋₃₆₃ and any associated proteins were pulled down and the samples were subjected to Western blot. The MBP blot was evaluated to determine if MBP-VAP_{MSP} was pulled down by glutathione beads alone, GST alone, or GST-IncV₁₆₇₋₃₆₃ (Figure 3.6C). Regardless of the presence of CK2 and ATP, beads alone, or GST attached to beads did not pull down MBP-VAP_{MSP} (Figure 3.6D, lanes 1 - 4). In the absence of CK2 and ATP, we observed minimal binding of MBP-VAP_{MSP} to GST-IncV₁₆₇₋₃₆₃ (Figure 3.5B, lane 5). When GST-IncV₁₆₇₋₃₆₃ was treated with CK2 and ATP prior to GST-pull down, there was a strong signal of MBP-VAP_{MSP} bound to GST-IncV₁₆₇₋₃₆₃, indicating phosphorylation of IncV by CK2 is sufficient to promote the IncV-VAP interaction *in vitro*. Altogether, these results demonstrate that IncV phosphorylation is necessary and sufficient for the IncV-VAP interaction *in vitro*.

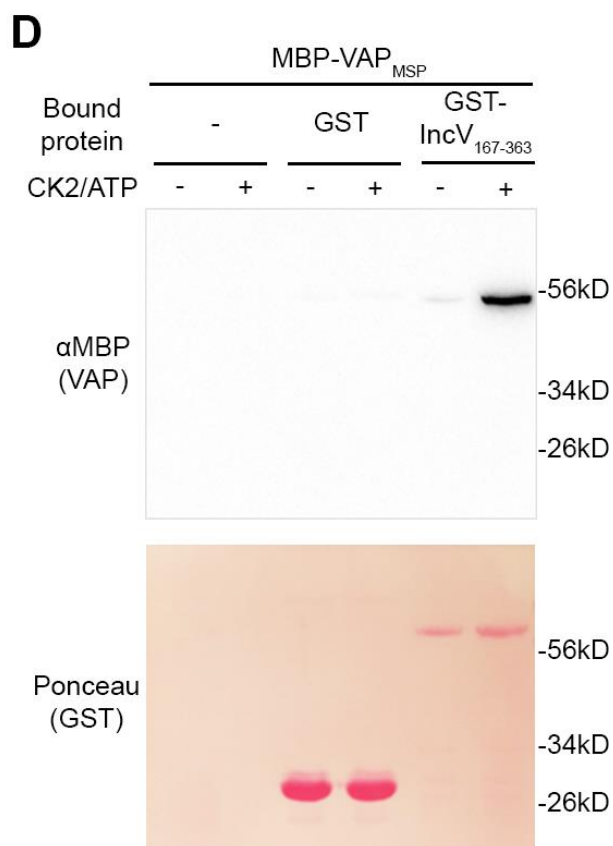
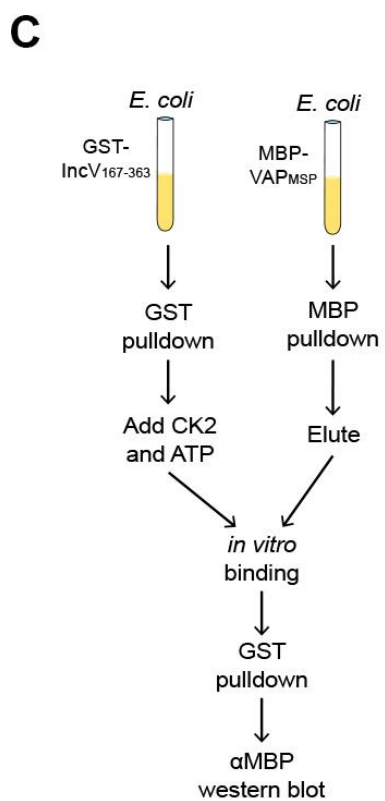
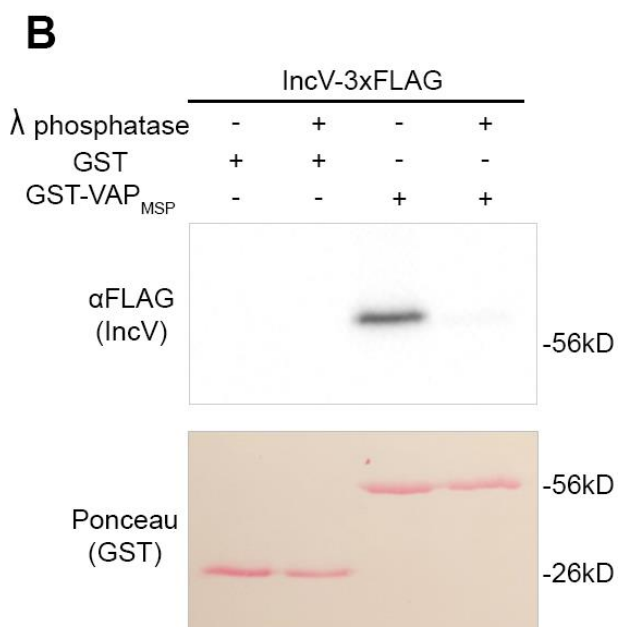
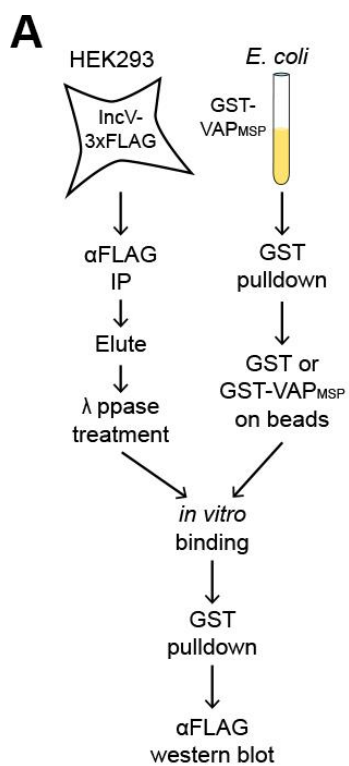
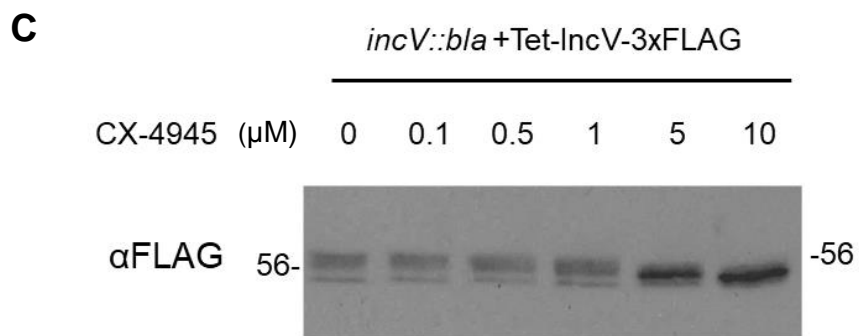
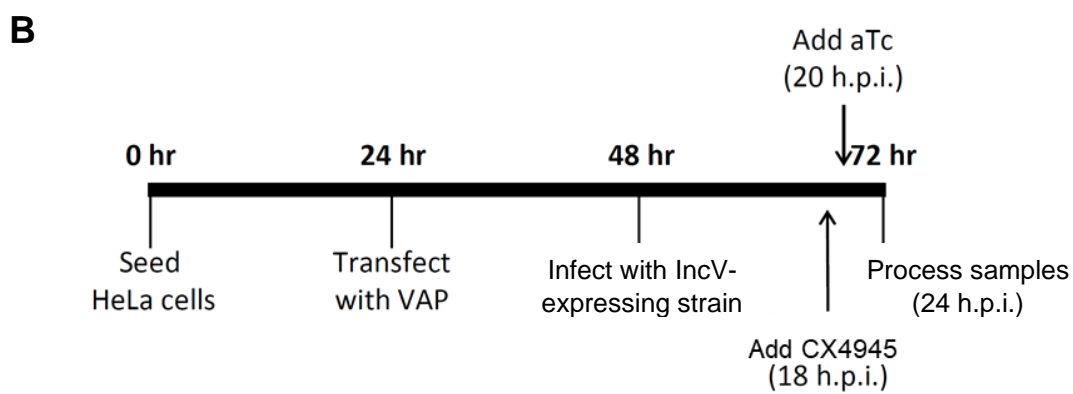
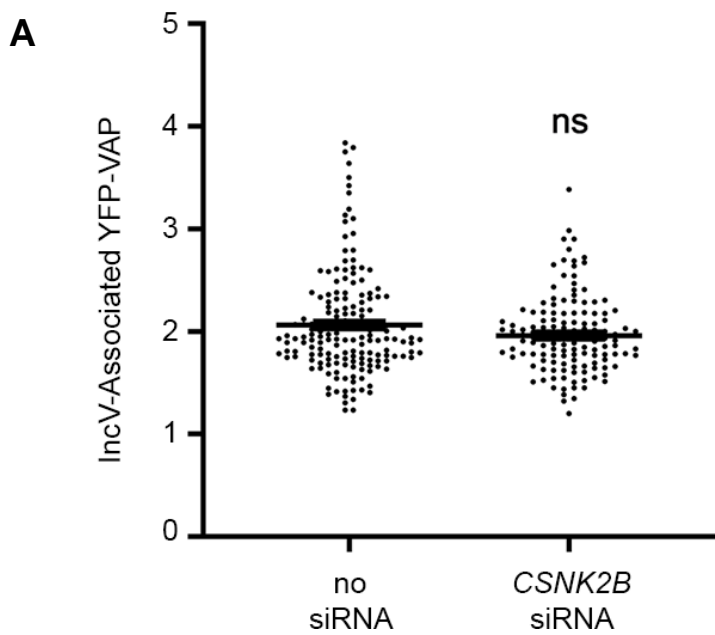


Figure 3.6. Phosphorylation of IncV by CK2 is necessary and sufficient to promote the IncV-VAP interaction *in vitro*. A) Schematic depicting the experimental setup for results in B. B) *In vitro* binding assay using IncV-3xFLAG purified from HEK293 lysates and treated with lambda (λ) phosphatase (+) or phosphatase buffer alone (-) combined with GST or GST-VAP_{MSP} purified from *E. coli* and immobilized on glutathione beads. The top panel shows proteins detected with anti-FLAG anti-bodies and the bottom panel is the same membrane stained with Ponceau S to detect total protein. C) Schematic depicting the experimental setup for results in D. D) *In vitro* binding assay using GST or GST-IncV₁₆₇₋₃₆₃ purified from *E. coli*, and immobilized on glutathione beads, as a substrate for CK2 in the presence (+) or absence (-) of CK2 and ATP, combined with MBP-VAP_{MSP} purified from *E. coli*. The top panel was probed with anti-MBP and the bottom panel was the same membrane stained with Ponceau to detect the GST construct.

3.2.7 CK2 Plays a Role in the IncV-VAP Interaction During Infection.

To assess if CK2 played a role in the IncV-VAP interaction during infection, we utilized both siRNA and inhibitor approaches and monitored VAP recruitment to the inclusion membrane. First, we used a pool of four siRNA duplexes to deplete cells of CK2 β and quantified YFP-VAP association with the inclusion as previously described.¹⁰⁹ There was no significant difference in YFP-VAP recruitment between the control and the CK2-depleted conditions (Figure 3.7E) which could be explained by incomplete knockdown of CK2 (Figure 3.5B) and the fact that we could still observe significant association of CK2 with the inclusion membrane even in CK2 siRNA treated cells (data not shown). We next used the CK2-specific inhibitor CX-4945 to assess the requirement for CK2 activity in IncV phosphorylation and IncV-dependent VAP recruitment to the inclusion (Figure 3.7B-D).^{213,214} Cells expressing CFP-VAPA were infected with *C. trachomatis incV::bla* + pTet-IncV-3xFLAG and treated with a DMSO control or CX-4945 prior to IncV-3xFLAG expression and subsequent Western blot or confocal microscopy analysis (Figure 3.7B). Lysates from cells infected with *C. trachomatis incV::bla* + pTet-IncV-3xFLAG and treated with increasing concentrations of CX-4945 (0, 0.1, 0.5, 1, 5, 10 μ M) were subjected to Western blot to determine the effect of CK2 inhibition on the apparent molecular weight of IncV (Figure 3.7C). In the control lane 1, IncV-3xFLAG migrated as a protein band doublet as observed previously (Figure 3.7C, left lane). As the dose of CX-4945 increased, the apparent molecular weight of IncV decreased and at the 10 μ M concentration of CX-4945, all IncV-3xFLAG molecules exhibit an apparent molecular weight

corresponding to the bottom band, which is the hypophosphorylated species of IncV (Figure 3.7C, lanes 2-6). We next determined whether inhibition of CK2 affected VAP recruitment to the inclusion using the same experimental setup as for the Western blot, except only the no-drug control and 10 μ M CX-4945 conditions were used. Confocal micrographs of infected cells were analyzed by the quantification of VAP associated with the IncV signal on the inclusion membrane. Compared to the DMSO control, CFP-VAPA recruitment to the inclusion was significantly decreased when cells were treated with 10 μ M CX-4945, indicating that active CK2 plays a role in IncV-dependent VAP recruitment during infection. Altogether, these data demonstrate that phosphorylation of IncV in a CK2-dependent manner is required for IncV-dependent VAP recruitment to the inclusion.



N=1

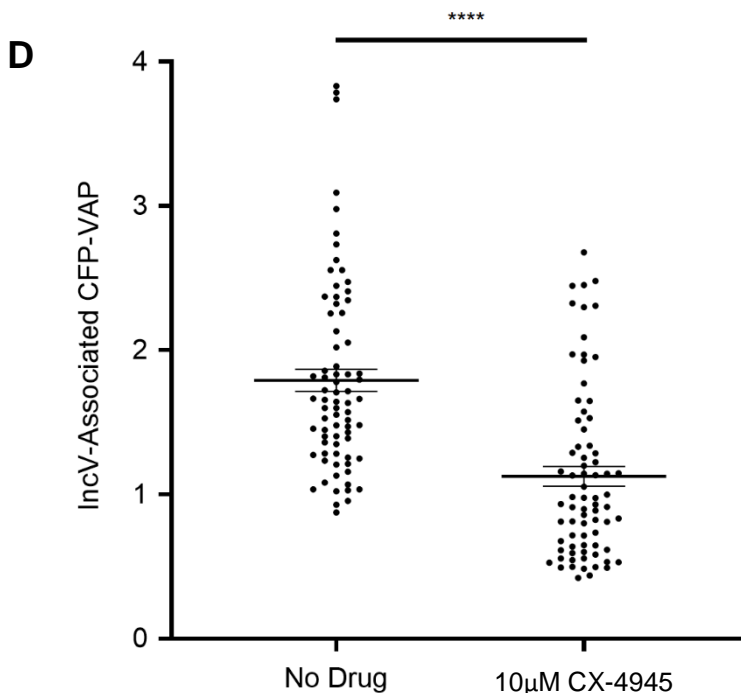


Figure 3.7. CK2 plays a role in the IncV-VAP interaction during infection.

A) Quantification of the mean intensity of the YFP-VAP signal within an object generated from the YFP-VAPA signal at the inclusion and normalized to the mean intensity of YFP-VAP signal in the cytosol. Quantification was performed on 3-dimensional reconstructions on confocal micrographs of HeLa cells depleted of CK2B using siRNA targeting *CSNK2B*, transfected with YFP-VAP, and infected with a strain of *C. trachomatis* expressing mCherry constitutively. Error bars are SEM. Student's t-test was performed comparing *CSNK2B* siRNA to no siRNA control. ns = not significant. B) Schematic of the experimental setup for the experiments in C and D. C) Western Blot of lysates of HeLa cells

infected with *C. trachomatis* expressing IncV-3xFLAG and treated with increasing concentrations of CX-4945 (0, 0.1, 0.5, 1, 5, 10 μ M). The membrane was probed with anti-FLAG antibodies to detect IncV-3xFLAG. D) Quantification of the mean intensity of the CFP-VAPA signal within an object generated from the IncV-3xFLAG signal and normalized to the mean intensity of CFP-VAPA signal in the cytosol. Quantification was performed on 3-dimensional reconstructions of confocal micrographs of HeLa cells treated with 10 μ M CX-4945 or DMSO control, transfected with CFP-VAP, and infected with a strain of *C. trachomatis* expressing IncV-3xFLAG. The CFP-VAPA association number was then normalized to the mean intensity of IncV-3xFLAG within the IncV-3xFLAG object. Student's t-test comparing 10 μ M CX-4945 to DMSO control. Error bars are SEM. ****
p<0.0001.

3.3 Discussion

Here, we describe Protein Kinase CK2 as a novel component of ER-Inclusion MCS. We demonstrated that CK2 is recruited to the inclusion membrane by the Inc protein IncV, a known tether of ER-Inclusion MCS.¹⁰⁹ We provide evidence that CK2 phosphorylates IncV and plays a role in the regulation of the IncV-VAP interaction.

3.3.1 Transient nature of the IncV-CK2 Interaction.

As with many enzyme-substrate interactions, CK2 transiently associates with its target proteins.^{215,216} The transient nature of the interaction could mean that rare events are easily missed with a single snapshot in time. Consistent with this line of thought, IncV must be overexpressed to detect CK2 associated with the inclusion membrane (Figure 3.3B). Additionally, co-immunoprecipitation assays failed to detect a stable IncV-CK2 interaction, which is in contrast with the results from the Inc-Human Interactome.⁶⁰ However, in that situation, the Inc protein bait was overexpressed ectopically in eukaryotic cells, as opposed to overexpressed and localized to the inclusion membrane in our experiments. This could increase the occurrence of IncV-CK2 interactions and increase the probability of detecting a transient interaction and the sensitivity of mass spectrometry allows for the detection of rare events.⁶⁰

3.3.2 Phosphoregulation of VAP-Interacting Proteins

Most protein interactions with VAP are mediated by FFAT motifs. These are defined by a core motif of 7 amino acids with the consensus sequence E-F-F-D-A-x-E, where x is any amino acid, and an enrichment of acidic residues flanking the

core.^{178,180,199} IncV contains two FFAT motifs and mutating two essential amino acids within the IncV FFAT motifs is sufficient to disrupt the IncV-dependent VAP recruitment to the inclusion.¹⁰⁹ Interestingly, we observed a similar defect in VAP recruitment when the C-terminus of IncV was truncated (not shown), which suggests that the IncV-VAP interaction relies on more than simply the FFAT motifs. There are several examples of VAP-interacting proteins being regulated via phosphorylation. For example, the ceramide transfer protein CERT has a serine-repeat motif (SRM) that is ~200 amino acids upstream of the FFAT motif. The phospho-SRM form of CERT is conformationally closed such that the lipid transfer activity of CERT is severely inhibited.²⁰⁸ Since CK2 recruitment to the inclusion depends on a region in the C-terminus of IncV, it is possible that residues in that region are phosphorylated by CK2 to modulate the IncV-VAP interaction by changing conformation of IncV. Alternatively, it is also feasible that the C-terminal domain in IncV recruits CK2 so that CK2 can phosphorylate distal regions that enhance VAP binding, rather than phosphorylating the region itself. In addition to the SRM in CERT, a serine residue six amino acids upstream of the CERT FFAT motif (S315) enhances the CERT-VAP interaction when it is phosphorylated.²⁰⁹ Perhaps not surprising is that dephosphorylation of the CERT SRM, and the resulting open conformation of CERT, promotes the phosphorylation of CERT S315.²⁰⁹ It would be interesting to determine if there is any interplay between IncV phosphorylation sites that enhance or inhibit IncV-VAP binding in different situations. For example, one scenario could be that CK2

phosphorylates the C-terminal tail of IncV to unveil additional kinase-regulated residues in IncV to modulate the IncV-VAP interaction.

3.3.3 Functional Outcomes of Phosphorylation of Inc Proteins by the Host

The functional consequences of Inc phosphorylation by host kinases is not known for any Incs, so far. To date, two Inc proteins (IncA and IncG) are known to be tyrosine phosphorylated by unknown host kinases.^{112,217} IncA from *C. psittaci* was shown to be phosphorylated, but whether the *C. trachomatis* IncA homolog is phosphorylated remains to be confirmed.¹⁴⁶ A recent study characterized the *Chlamydia* infection phosphoproteome of both host and *Chlamydia* proteins using post-translational modification analysis of mass spectrometry to identify host and *Chlamydia* proteins, including IncV, that are phosphorylated differentially during infection.²¹⁸ The study identified an additional 12 phosphorylated Inc proteins and proposed that they could be phosphorylated by host kinases based on phosphorylation recognition site prediction algorithms, but further characterization remains to be done and is discussed in Chapter 4.²¹⁸

Several host kinases including Active Src family kinases (SFks), Myosin light-chain kinase (MLCK), and Protein Kinase C (PKC) are recruited to inclusion microdomains, which are structures on the inclusion membrane enriched in specific *Chlamydia* and host proteins. There, they are proposed to form localized phosphorylation centers on the inclusion membrane.^{125,128,219,220} At microdomains, active SFks, MLCK, and PKC recruit and phosphorylate their respective host substrate proteins (Lutter *et al.* 2013; Shaw 2018). Microdomains also include Inc proteins (IncB, IncC, MrcA, CT222, CT223,

CT224, CT228, CT288, and CT850) which play roles in extrusion (CT228 and MrcA), inclusion positioning through interactions with microtubules (CT850 and CT223), and associations with centrosomes (CT223).^{61,62,118,120,125,134} The Zadora *et al* phosphoproteome study identified several phosphorylated inclusion microdomain Incs and predicted that they were phosphorylated by host kinases.²¹⁸ However, whether or not microdomain Incs are phosphorylated by the microdomain-associated kinases has not been described. Additionally, the role of phosphorylation of inclusion microdomain Incs is unknown. Conversely, our data demonstrates that IncV is phosphorylated to promote the IncV-VAP interaction. Given the currently known examples of phosphorylated Incs (IncA, IncG, and IncV) and the enrichment of many host kinases on the inclusion membrane, it would not be surprising if there are additional examples of host kinase phosphorylation of Incs.

3.3.4 The Role of CK2 in Intracellular Pathogen Lifecycles.

In addition to playing a role in *Chlamydia* infection, CK2 associates with other intracellular pathogens and play a variety of roles during infection. CK2 was shown to phosphorylate the *Listeria monocytogenes* protein ActA which then recruits the actin-related proteins-2/3 (ARP2/3) complex through the molecular mimicry of the actin nucleating host proteins WASP/WAVE to promote actin tail formation and cell-to-cell spread.²²¹ This parallels our findings in the present study in which CK2 phosphorylates IncV which then recruits VAP, suggesting that mimicry of host protein motifs that are phosphorylated by CK2 might be a common mechanism found in many pathogens.

Interestingly, *L. monocytogenes* was still able to replicate in CK2-depleted cells, despite displaying a cell-to-cell spreading defect. At this point, however, it is unclear if CK2 is required for infectious progeny production because the inclusion size at 24 hours post infection did not seem to be affected when CK2 was inhibited. There are several examples of CK2 involvement in either promoting or inhibiting viral replication. Like *L. monocytogenes*, Vaccinia virus requires CK2 for both actin tail formation and cell-to-cell spread.²²² CK2 is packaged into the Human Cytomegalovirus virion and immediately after infection, CK2 enhances the NFκB signaling that positively regulates viral immediate early gene expression.²²³ The structural NS2 protein of Bluetongue virus is phosphorylated by CK2 to promote the formation of cytoplasmic viral inclusion bodies, which are the site of viral replication.²²⁴ Conversely, CK2 positively regulates the stability of the E1 protein and negatively affects viral replication of certain Human Papillomavirus subtypes.²²⁵ CK2 also plays a role in Hepatitis C virus (HCV) infection by phosphorylating the HCV NS2 protein and targeting it for proteasome degradation.^{226,227} Though it is not clear whether CK2 activity promotes *C. trachomatis* infection, it does not seem to be inhibitory because inhibition of CK2 did not result in an increase in inclusion size as one might expect if a suppressive factor in infection was removed. CK2 plays a role in phosphorylating several different proteins expressed by pathogens and each example to date describes a unique downstream effect of that phosphorylation. Our studies presented here add *Chlamydia* to the growing list of intracellular pathogens that co-opt CK2. CK2 has been

demonstrated to regulate many cellular functions and it is remarkable that pathogens have evolved to take advantage of the pleiotropic and ubiquitous nature of CK2.

3.4 Conclusion

In this study, we demonstrated that CK2 is recruited to the inclusion in an IncV-dependent manner that depends on a C-terminal domain of IncV. We showed that CK2 phosphorylates IncV and plays a role in the IncV-VAP interaction *in vitro*. We demonstrated that CK2 is involved in regulating the IncV-VAP tethering interaction during infection. Together, the data presented here begin to uncover a means by which the formation of ER-inclusion MCS is regulated. Further characterization of mechanisms of ER-Inclusion MCS formation and maintenance is important to understand how *C. trachomatis* manipulates its host to establish an intracellular niche.

3.5 Materials and Methods.

3.5.1 Cell Lines and Bacterial Strains.

HeLa cells (ATCC CCL-2) and HEK293 cells (ATCC CRL-1573) were maintained in DMEM high glucose (Gibco) containing 10% heat-inactivated fetal bovine serum (Gibco) at 37degC and 5% CO₂. *Chlamydia trachomatis* Lymphogranuloma venereum, type II (ATCC L2/434/Bu VR-902B) was propagated in HeLa cells as previously described²⁰⁷. The *incV::bla* (also known as *CT005::bla*) strain of *C. trachomatis* was obtained from Ted Hackstadt (NIH, Rocky Mountain Laboratories).⁶⁷

3.5.2 Plasmid Construction.

Plasmids were constructed using the primers (IDT) and templates listed in Appendix 2, restriction enzymes (NEB), and T4 DNA ligase (NEB), Herculase DNA polymerase (Stratagene).

3.5.3 Vectors for Expression in Mammalian Cells.

The IncV-3xFLAG construct cloned in the pCMV-IE-N2-3xFLAG vector was previously described.¹⁰⁹ The YFP-CK2 α and YFP-CK2 β plasmids were kind gifts from Claude Cochet and Odile Filhol-Cochet (Institut Albert Bonniot Departement Reponse et Dynamique Cellulaires) and were previously characterized.²²⁸ The CFP-VAPA plasmid was constructed by cloning the VAP open reading frame (ORF) into pCMV-N1-CFP using AgeI and HindIII restriction sites.

3.5.4 Vectors for Expression in *E. coli*.

The GST-VAPAMSP plasmid was previously described.¹⁰⁹ MBP-VAPMSP was constructed by cloning the MSP domain of VAPA using NotI and BamHI into pMAL. The GST-IncV₁₆₇₋₃₆₃ plasmid was constructed by cloning the base pairs corresponding to amino acids 167-363 of IncV using BamHI and XhoI.

3.5.5 Vectors for Expression in *C. trachomatis*.

Full length and truncated versions of IncV were cloned into the p2TK2_{Spec}-SW2 mCh(Gro) vector as previously described.²²⁹ Briefly, TetRTetAP promoter and 3xFLAG *incD* terminator fragments were appended onto either end of the Full Length IncV fragment using overlap PCR to generate TetRTetAP-IncV-3xFLAG-IncDterm (Tet-IncV-3xFLAG for short) fragments. Truncated IncV constructs (DNA corresponding to amino acids 1-

305, 1-341, and 1-356) were generated using overlap PCR to truncate the IncV ORF. All versions of Tet-IncV-3xFLAG were cloned into p2TK2Spec-SW2 mCh(gro) using KpnI and NotI. mCherry is expressed constitutively from the groESL promoter and IncV-3xFLAG (Full length, 1-356, 1-341, or 1-305) is expressed under the aTc-inducible promoter.

3.5.6 *C. trachomatis* Transformation and *incV::bla* Complementation.

Either wild type *C. trachomatis* or an *incV* mutant (*incV::bla*) was transformed with pTet-IncV-3xFLAG using our previously described calcium-based *Chlamydia* transformation procedure.²²⁹ The resulting strains are called *C. trachomatis* L2 wild type + pTet-IncV-3xFLAG and *C. trachomatis* L2 *incV::bla* + pTet-IncV-3xFLAG.

3.5.7 DNA Transfection.

Cells were transfected with mammalian construct DNA according to manufacturer instructions with X-tremeGENE 9 DNA Transfection Reagent (Roche).

3.5.8 SDS-PAGE.

Cells were either directly lysed in 2x Laemmli buffer with 10mM DTT or IncV was purified as described in the immunoprecipitation and protein purification sections then suspended in a final concentration of 1x Laemmli buffer with 10mM DTT. Protein samples were separated using PAGE on SDS/polyacrylamide gels.

3.5.9 Immunoblotting.

After SDS/PAGE, proteins were transferred onto nitrocellulose membranes (GE Healthsciences). Prior to blocking, membranes were stained with Ponceau S in 5% Acetic acid and washed in dH₂O. Membranes were then incubated for 1 hour with shaking at

room temperature in blocking buffer (5% skim milk in 1xPBS with 0.05% Tween). Membranes were then incubated with primary and secondary (HRP-conjugated) antibodies diluted in blocking buffer overnight at 4degC and 1 hour at room temperature, respectively, with shaking. ECL Standard Western blotting detection reagents (Amersham) were used to detect HRP-conjugated secondary antibodies on a BioRad ChemiDoc imaging system. CK2 β was detected using secondary antibodies conjugated to Alexafluor 800 on Li-Cor Odyssey imaging system.

3.5.10 Antibodies.

The following antibodies were used for immunofluorescence microscopy (IF) and immunoblotting (Western blot): mouse monoclonal anti-FLAG [1:1,000 (IF); 1:10,000 (Western blot); Sigma], HRP-conjugated goat anti-rabbit IgG [1:10,000 (Western blot); Jackson], HRP-conjugated goat anti-mouse IgG [1:10,000 (Western blot); Jackson], AlexaFluor 514, 800, or Pacific Blue-conjugated goat anti-mouse IgG [1:500 (IF); 1:10,000 (Western blot); Molecular Probes]; rabbit polyclonal anti-CK2 β [1:200 (IF); 1:1,000 (Western blot); Bethyl Antibodies]; rabbit polyclonal anti-GAPDH [1:10,000 (Western blot);], rabbit polyclonal anti-Thiophosphate ester antibody [1:2000 (Western blot); Abcam].

3.5.11 Immunoprecipitation of IncV-3xFLAG From HEK293 Cells Infected With *C. trachomatis*.

800,000 HEK293 cells were seeded into one well of a six-well plate (Falcon) and infected the following day with *C. trachomatis* at a multiplicity of infection (MOI) of 5. 8

hours post-infection, media containing 2ng/mL anhydrotetracycline (aTc) was added to the infected cells for 16 hours. 24 hours post-infection, culture media was removed from the cells and 500 μ L of lysis buffer (20 mM Tris pH 7.5, 150 mM NaCl, 2 mM EDTA, 1% Triton X-100, protease inhibitor mixture EDTA-free (Roche)) was added per well. Cells were lysed for 20 minutes at 4degC with rotation. Lysates were centrifuged at 16,000xg for 10 minutes at 4degC to pellet nuclei and unlysed cells. Cleared lysates were incubated with 10 μ L of anti-FLAG M2 affinity beads (Sigma) for 2 hours at 4degC with rotation. The beads were washed with lysis buffer three times. Proteins were eluted with 50 μ L of 100ug/mL 3xFLAG peptide (Sigma) in 1x Tris-buffered saline. For cells transfected with pCMV-IE-N2-IncV-3xFLAG, cells were not infected, and the remainder of the protocol remained the same starting with removal of media and lysing.

3.5.12 Phosphatase assay.

Immunoprecipitation was performed as described above with the following changes: The beads were washed with 1x Tris-buffered saline (TBS) three times and proteins were eluted with 55 μ L of 100ug/mL 3xFLAG peptide (Sigma) in 1x TBS. 20 μ L of eluate was combined with 2.5 μ L of 10mM MnCl₂, 2.5 μ L of 10x PMP buffer (NEB), and 400 units of Lambda (λ) phosphatase (NEB) for 24 hours at 4degC. The assay was halted by adding 5 μ L of 6x Laemmli buffer with 10mM DTT. Samples were boiled and 10 μ L of samples were then used in SDS-PAGE.

3.5.13 DNA Transfections and Infections for Microscopy.

HeLa cells were seeded onto glass coverslips and transfected with YFP-CK2 (α or β) and/or CFP-VAPA the following day. 24 hours post-transfection, cells were infected with the indicated strain of *C. trachomatis* at a MOI of 1. 20 hours post-infection, media containing 2ng/mL aTc (final concentration) was added for 4 hours to induce expression of IncV-3xFLAG.

3.5.14 Immunofluorescence and Confocal Microscopy.

HeLa cells seeded on glass coverslips and infected with *C. trachomatis* were fixed 24 hours post-infection with 4% paraformaldehyde in 1x PBS for 20 minutes at room temperature then washed with 1x PBS three times. The coverslips were sequentially incubated with primary and secondary antibodies in 0.1% Triton X-100 in 1x PBS for 1 hour at room temperature. For coverslips stained with anti-CK2 β , antibodies were diluted in 0.5% Triton X-100 and 5% BSA in 1x PBS. Coverslips were washed with 1x PBS three times then mounted with glycerol containing DABCO and Tris pH 8.0. Confocal images were obtained using an Andor iXon ULTRA 888BV EMCCD camera and a Yokogawa CSU-W1 Confocal Scanner Unit attached to a Leica DMI8 microscope. 1 μ m thick Z slices covering the entirety of the cell were captured.

3.5.15 Quantification of YFP-CK2 β and CFP-VAPA Inclusion Association.

Quantification of YFP-CK2 β or CFP-VAPA association with IncV-3xFLAG on the inclusion membrane was performed using the Imaris imaging software. First, three-dimensional (3D) objects were generated from the raw signal of IncV-3xFLAG on the inclusion membrane. Objects were edited such that IncV-3xFLAG colocalizing with the

mCherry bacteria was removed. Within the resulting IncV object, the mean intensity of YFP-CK2 β or CFP-VAPA was calculated by the Imaris software and normalized to the mean intensity of YFP-CK2 β or CFP-VAPA within the cytosol surrounding the inclusion. Quantification of the IncV-3xFLAG volume was performed to ensure there was no defect in inclusion localization. Using the Imaris imaging software, the sum of the voxels corresponding to the IncV-3xFLAG signal above the threshold set by the signal within the cytosol was calculated for IncV-3xFLAG and mCherry. The IncV-3xFLAG volume was normalized to its corresponding inclusion volume.

Each experiment was performed in triplicate with at least 30 inclusions analyzed per condition per replicate. Data from 3 independent replicates are combined into a single graph. Each point on the graph represents a single inclusion with the average value and SEM shown. Student's t tests were performed.

3.5.16 CK2 Depletion.

CK2 was depleted from cells using a pool of four siRNA duplexes or each duplex individually that was transfected with Dharmafect 1 transfection reagents. On day 0, one volume of 200nM siRNA in siRNA buffer was incubated with one volume of 5 μ L/mL of Dharmafect 1 transfection reagent in DMEM High Glucose in a well for 20 minutes at room temperature. Two volumes of DMEM High Glucose supplemented with 20% FBS and 200,000 HeLa cells per mL were added to the well. Cells were incubated at 37degC with 5% CO₂ for 3 days. The total volume in 96 wells (used for western blot) was 120 μ L. The total volume in a 24 well (used for immunofluorescence) was 400 μ L. On day 1, the

cells in a 24 well were split evenly onto 3 coverslips. On Day 2, the cells in a 24 well was transfected with YFP-VAPA or CFP-VAPA. The CSNK2B target sequence for each individual siRNA duplex was: A, CAACCAGAGUGACCUGAUU; B, GACAAGCUCUAGACAUGAU; C, CAGCCGAGAUGCUUUAUGG; D, GCUCUACGGUUUCAAGAUC.

3.5.17 Protein Purification.

Expression of GST, GST-VAP_{MSP}, GST-IncV₁₆₇₋₃₆₃, or MBP-VAP_{MSP} was induced for 2 hours by isopropyl- β -D-thiogalactopyranoside addition (0.1mM, final concentration) to a 10 mL culture of *E. coli* BL21-DE3 at OD 0.8. Bacterial pellets were frozen at -80degC overnight. Frozen pellets were thawed and resuspended in 800 μ L sonication buffer (20 mM Tris pH 7.5, 300 mM NaCl, 2 mM EDTA, 1 mM MgCl₂, 1% Triton X-100, 1mM DTT, 1mM PMSF). The samples were sonicated using five 5-second pulses at 40% power then centrifuged at 13,000 x g for 10 minutes at 4degC. 40 μ L of glutathione Sepharose beads (GE) for GST-tagged constructs and 40 μ L of Amylose resin for MBP-tagged constructs were washed three times with sonication buffer then added to the cleared lysate and incubated for 2 hours at 4degC with rotation. The beads were washed three times in TBS.

3.5.18 In vitro Kinase Assay.

Protein bound glutathione Sepharose beads were resuspended in 1x NEBuffer™ for Protein Kinases supplemented with 1mM ATP γ S and 10 units of CK2 (NEB) and incubated at 30degC for 45 minutes. P-Nitrobenzyl mesylate (PNBM) was added to the kinase reaction at a final concentration of 2.4mM for 2 hours at room temperature, in the

dark. The PNBM alkylation reaction was quenched by adding an equal volume of 2x Laemmli buffer. Proteins were separated using SDS-PAGE on a 12% acrylamide gel then transferred to a nitrocellulose membrane. The membrane was stained with Ponceau S in 5% acetic acid to detect total protein then washed in dH₂O. The membrane was then probed with anti-Thiophosphate ester antibodies to detect phosphorylated proteins which were detected with HRP-conjugated secondary antibodies.

3.5.19 In vitro Binding Assay With IncV Dephosphorylation.

First, the phosphatase assay was performed with the following changes: 1,000,000 HEK293 cells stably transfected with pCMV-IE-N2-IncV-3xFLAG were seeded per 6 well. 6 wells were lysed in 500 μ L lysis buffer each and lysates from two wells were combined. 10 μ L of anti-FLAG beads were added per 1000 μ L cleared lysate for 2 hours at 4degC with rotation. All beads were combined after the first wash and proteins were eluted in 150 μ L elution buffer (130 μ L eluate collected).

Next, GST and GST-VAP_{MSP} were purified as described in protein purification. Per phosphatase assay tube: 1.5ug of GST or GST-VAP_{MSP} attached to beads (determined empirically by comparison of Coomassie stained gel to BSA standard curve) were suspended in 500 μ L lysis buffer then added to tubes containing the IncV-3xFLAG-containing eluate (+/- phosphatase treatment). Binding was allowed to occur overnight at 4degC with rotation.

To confirm that IncV dephosphorylation was successful, a set of control tubes were incubated with beads alone (no GST construct) in lysis buffer to mimic experimental conditions.

24 hours after binding, beads were washed three times in 1x TBS. After the final wash, all liquid was removed from the beads which were then suspended in 20 μ L 2x Laemmli buffer. The entire sample was separated by SDS-PAGE, proteins transferred to a nitrocellulose membrane which was stained with Ponceau S to detect the GST construct then probed with anti-FLAG to detect IncV-3xFLAG.

3.5.20 In vitro Binding Assay With CK2 Phosphorylation of IncV.

First, GST, GST-IncV₁₆₇₋₃₆₃, and MBP-VAP_{MSP} were purified as described in protein purification. MBP-VAP_{MSP} was eluted from amylose resin using 100 μ L 1x TBS supplemented with 10mM Maltose Monohydrate. 1.5 μ g of GST or GST-IncV₁₆₇₋₃₆₃ attached to glutathione beads (determined empirically by comparison of Coomassie stained gel to BSA standard curve) or beads alone were suspended in 1x NEBuffer™ for Protein Kinases with 200 μ M ATP (Thermo) and 100 units of CK2 (NEB) at 30degC for 45 minutes. Beads were washed three times in sonication buffer. 1.25 μ g MBP-VAP_{MSP} suspended in 500 μ L sonication buffer was added to each tube with beads and binding was allowed to occur overnight at 4degC with rotation. 24 hours after binding, beads were washed three times in 1x TBS. After the final wash, all liquid was removed from the beads which were then suspended in 20 μ L 2x Laemmli buffer. The entire sample was separated by SDS-

PAGE, proteins transferred to a nitrocellulose membrane which was stained with Pon-
ceau S to detect the GST construct then probed with anti-MBP to detect MBP-VAP_{MSP}.

3.5.21 CK2 Inhibition.

CK2 was inactivated in HeLa cells using 4,5,6,7-tetrabromobenzotriazole (TBB)(Sigma). HeLa cells were seeded and transfected with CFP-VAPA DNA the following day. 24 hours post-transfection, cells were infected with *C. trachomatis* L2 *incV::bla* + pTet-IncV-3xFLAG. 18 hours post-infection, media containing 8 μ M TBB (final concentration) was added. 2 hours after TBB addition (and 20 hours post-infection), media containing 2ng/mL aTc (final concentration) was added to induce IncV-3xFLAG expression. Cells were fixed with 4% paraformaldehyde in 1x PBS at 24 hours post-infection for 20 minutes at room temperature then imaged and quantified as described in immunofluorescence and confocal microscopy and quantification of YFP-CK2 and CFP-VAP inclusion association.

3.6 Acknowledgments.

We thank Ted Hackstadt (NIH-Rocky Mountain Laboratories) and Mary Weber (University of Iowa) for the *incV::bla* strain; Fabien Alpy (Institut de Génétique et Biologie Moléculaire et Cellulaire) for the GFP-VAP constructs; Claude Cochet and Odile Filhol-Cochet (Institut Albert Bonniot Département Réponse et Dynamique Cellulaires) for the YFP-CK2 constructs.

Funding sources were NIAID F31 AI136283 to RS, Infectious Disease Training Grant T32AI007046 to RS and RE, NIAID R01AI101441 to ID, NIAID R21 AI141841 to ID. Wagner fellowship provided through the generosity of the Wagner family to RS and RE.

Chapter 4

Discussion, Conclusions, and Future Directions

Summary of Major Findings

IncV is a *Chlamydia* inclusion membrane protein that interacts with the host ER-resident protein VAP. IncV contains two eukaryotic FFAT motif mimics that mediate the interaction with the electropositive face of VAP. IncV recruits VAP and tethers the ER to the inclusion membrane.¹⁰⁹ The IncV-VAP interaction is regulated via the phosphorylation of IncV by Protein Kinase CK2.

4.1 Tethering the ER to the Inclusion Membrane

4.1.1 Tether definition

By definition, MCS must be held together at a certain distance, typically 10-30 nanometers, for functional proteins to perform their duties. Several groups have proposed that proteins must fulfill certain requirements to be considered a tether, and I will use the following definition from Eisenberg-Bord *et al.* for this discussion.^{157,162,163} First, the tether must be present exclusively in or enriched at the MCS. Second, the tether or tethering complex must simultaneously bind the opposing membranes. Third, a tether must apply a tethering force. In other words, a tether should increase the area of the MCS if the tether is overexpressed and decrease the area of the MCS if the tether is not redundant and is deleted.

4.1.2 IncV as a Tether

My studies have demonstrated that IncV fulfills the above listed requirements of being a tether. To show that IncV fulfills the first criterion, I have demonstrated that 3xFLAG-tagged IncV recruits and co-localizes with VAP (Figure 2.7). VAP was already

known to be a part of ER-Inclusion MCS via the IncD-CERT-VAP complex and is thus a marker for ER-Inclusion MCS.^{58,109,110} Results from Chapters 2 and 3 satisfy the second criterion. We demonstrated that IncV and VAP interacted directly in an *in vitro* binding assay (Figure 2.1 and 3.6).¹⁰⁹ An interaction was also demonstrated during infection when we observed that VAP co-immunoprecipitated with IncV (Figure 2.5). Moreover, mutating the FFAT motifs in IncV or the FFAT-binding domain in VAP abolished the IncV-VAP interaction and IncV-dependent VAP recruitment to the inclusion membrane (Figure 2.6). Since IncV localizes to the inclusion membrane and VAP localizes to the ER, their interaction bridges the ER and the inclusion membrane. The third criterion was demonstrated upon the overexpression of IncV, where both VAP and the ER membrane recruitment were increased dramatically (Figure 2.10). Despite the drastic phenotype observed upon IncV overexpression, an *incV* mutant was still competent in ER-Inclusion MCS formation, indicating IncV is not required for their formation (Figure 2.16). Interestingly, though the volume of ER-Inclusion MCS was unchanged with the *incV* mutant, the amount of VAP on the inclusion was modestly, but significantly, decreased, suggesting IncV is at least partially responsible for VAP recruitment to the inclusion (Figure 2.16). This also suggests that there are redundant mechanisms both for the recruitment of VAP to the inclusion membrane and for the formation of ER-Inclusion MCS. ER-Inclusion MCS tethering redundancy is discussed in detail in Section 4.2.5.

4.1.3 Types of MCS Tethers

Tethers come in many flavors, despite all having to fulfill the defining criteria described above. Tethers that are required for the formation of MCS and are sufficient to independently form MCS are referred to as principal tethers.¹⁶³ Conversely, an auxiliary tether is one that is not required to maintain an MCS but can support principal tethers and can increase the extent of a contact if overexpressed¹⁶³ Tethers can be static, in that they continuously tether membranes together, or they can be dynamic. Dynamic tethers are proteins that only act as a tether in certain conditions.¹⁶³ Tethers could be dedicated, such that the only function they perform is tethering.¹⁶³ Except for a few tethers in yeast, the majority of tethers identified to date are known to be multi-functional, meaning they act as a tether in addition to another function, such as lipid transfer.¹⁶³

4.1.4 What Type of Tether is IncV?

Because the *incV* mutant was not deficient in ER-Inclusion MCS formation, IncV is not a principal tether (Figure 2.11). IncV fits within the criteria to be an auxiliary tether because it is not required for ER-Inclusion MCS formation but is capable of increasing the amount of ER contacting the inclusion membrane (Figure 2.10). It is important to point out that being an auxiliary tether does not necessarily mean that the tethering function IncV is not important for the formation and/or maintenance of ER-Inclusion MCS. An interesting example that highlights the value of auxiliary tethers is the yeast protein Lam6 which resides in sites of contact between the ER and mitochondria.²³⁰ The principal tethering complex between the ER and mitochondria in yeast is called the endoplasmic reticulum mitochondria encounter structure (ERMES).²³¹ Similarly to

overexpressing IncV, overexpressing Lam6 in yeast generates more MCS between the mitochondria and the ER.²³⁰ Interestingly, in an ERMES mutant, Lam6 overexpression generated ER-mitochondria MCS equally as efficiently as the wild type yeast, despite the principal tether being absent.²³⁰ The authors of this study proposed that Lam6 is an auxiliary tether that is not required for MCS formation, but could be a modulator of MCS size or the activity at already formed ER-mitochondria MCS.¹⁶³ Considering this example, it is possible that IncV acts as an auxiliary tether in a similar manner. At this time, it is not possible to conclude whether IncV is static vs dynamic, or dedicated vs multifunctional and future experiments to address these questions are discussed in Section 4.4.

4.1.5 Tethering redundancy

4.1.5.1 IncV is a Redundant Tether

Redundancy in tethering proteins and protein complexes at given MCS has been established for several different pairs of organelles. One of the best characterized examples of redundant tethering mechanisms was discovered in yeast where there are at least six tethers between the ER and the plasma membrane (PM).¹⁷⁷ All six tethers had to be deleted to observe a reduction in ER-PM MCS, but even then, it was not a complete abolition, and about 10% of the contacts remained.¹⁷⁷ Because inclusions containing an *incV* mutant still formed ER-inclusion MCS of the same size as wild type bacteria, there must be other tethers and/or tethering pairs.

4.1.5.2 The IncD-CERT-VAP Complex as a Tether

One obvious candidate for ER-Inclusion membrane tethering is the IncD-CERT-VAP complex. Based on data from our laboratory, this complex fits the criteria of a tether. All three proteins are enriched in ER-Inclusion MCS, the complex bridges the ER and the inclusion, and overexpression of the IncD-CERT-VAP complex leads to the expansion of ER-Inclusion MCS area.^{58,110} An *incD* mutant could be useful in confirming its role as a tether and is discussed in Section 4.4.

4.1.5.3 STIM1 as a Tether

Another candidate for tethering the ER and the inclusion is stromal interaction molecule 1 (STIM1), which our lab identified as a component of ER-Inclusion MCS.¹⁵¹ Outside of the context of ER-Inclusion MCS, STIM1 in the ER membrane forms a dynamic tethering pair with Orai1 on the plasma membrane (PM) to make ER-PM MCS in response to depleted Ca²⁺ levels in the ER.¹⁷² Interestingly, though STIM1 localizes to ER-Inclusion MCS, Orai does not, which suggests that there may be other host or *Chlamydial* factors that bind to STIM1 that have not been previously recognized.¹⁵¹ STIM1 already associated with the inclusion membrane remains in place when ER Ca²⁺ stores are depleted instead of relocalizing to ER-PM MCS. Thus, it seems that STIM1 localized to ER-Inclusion MCS is not responsive to ER Ca²⁺ store depletion the same way as STIM1 responds outside ER-Inclusion MCS.¹⁵¹ This suggests that STIM1 plays a different or additional role than its known function. More studies would be needed to confirm the hypothesis that STIM1 and its interacting partner are tethers in ER-Inclusion MCS and are discussed in Section 4.4.

4.1.6 Regulation of the IncV-VAP Tethering Complex

There were several lines of evidence that led to the hypothesis that the IncV-VAP interaction and ER-Inclusion MCS formation are regulated. First, IncV expressed in *C. trachomatis* or ectopically in eukaryotic cells consistently exhibited a higher apparent molecular weight than is predicted by amino acid sequence (Section 3.1). Moreover, IncV expressed in *E. coli* exhibited a molecular weight that was lower than that of IncV expressed in *C. trachomatis*, which suggested that IncV was differentially modified during infection (Section 3.1). Additionally, overexpressing IncV early in the developmental cycle of *C. trachomatis* inhibits the growth of inclusions. Because overexpressing IncV generates more ER contact with the inclusion membrane, it is possible that having too much of the inclusion membrane covered with the ER is somehow inhibitory for the inclusion growth, which would be consistent with the smaller inclusions observed with early IncV overexpression.¹⁰⁹ Together, these observations suggest that a balance striking the right amount of ER contacts with the inclusion is important for the developmental cycle. Additionally, since *Chlamydia* interacts with many host factors, it is possible that the ER cannot fully encase the inclusion to allow other organelles, such as multivesicular bodies, to contact the inclusion membrane.

4.1.6.1 IncV as a Protein Kinase CK2 Substrate

Protein Kinase CK2, formerly known as Casein Kinase 2, is a constitutively active serine/threonine kinase expressed ubiquitously in eukaryotic cells.²¹¹ CK2 plays roles in many cell processes including, but not limited to, cell cycle regulation, apoptosis,

cytoskeleton dynamics, and so on.^{211,232} The tetrameric holoenzyme is comprised of a dimer of two regulatory subunits (β) and two catalytic subunits (α and/or α'). The β subunits recognize the consensus motifs **S/T**-x-x-D/E/pS/pY or **S/T**-x-D/E/pS/pY, where x is any amino acid (CK2 phosphorylated residue in bold). Perhaps unsurprisingly, most proteins contain one or more of these motifs as determined using a phosphorylation predictor algorithm such as PhosphoSitePlus.²³³ However, many predicted CK2 recognition sites are not phosphorylated *in vivo*. As such, multiple experimental approaches are necessary to prove a protein is a *bona fide* CK2 substrate. In Chapter 3, I demonstrated that, not only does CK2 directly phosphorylate IncV *in vitro*, but CK2 plays a role in the phosphorylation of IncV during infection.

4.1.6.2 Potential IncV phosphorylation sites

4.1.6.2.1 Potential phosphorylation in a C-Terminal Domain of IncV

To determine which residues in IncV are important for CK2-mediated regulation of the IncV-VAP interaction, we used several approaches. In Chapter 3, we showed that a small region downstream from the FFAT motifs in the cytosolic tail of IncV was required for IncV-dependent CK2 and VAP recruitment to the inclusion membrane. The region is highly enriched in serines (**S**³⁴²SESSDEESSSDSSQ³⁵⁶), seven of which could potentially be recognized by CK2 (underlined)(Figure 4.2). Additionally, four of those serines (bolded) could require a prior priming phosphorylation event to produce CK2 recognition motifs. Interestingly, we performed post-translational modification analysis of mass spectrometry data generated with samples of IncV that had been phosphorylated by

CK2 *in vitro* and identified one residue in the serine-rich region (S345). S345 is one of three residues in the serine-rich region that could be recognized by CK2 without any priming phosphorylation events, based on the canonical CK2 recognition motif, but expressing a S345A point mutant of IncV had no effect on VAP recruitment. However, if either of the two serines closest to the end of the serine-rich region (S354 and S355) were phosphorylated first by another kinase, it could initiate a CK2 phosphorylation cascade and potentially generate a hyperphosphorylated serine region, in which all nine serines in the serine-rich region are phosphorylated, in amino acids 342-356 (Figure 4.2).

Phosphorylation has a known role in inducing conformational changes in proteins, so it is possible that a hyperphosphorylated species of IncV could be conformationally different from a hypophosphorylated species.²³⁴ The conformation of IncV could modulate the IncV-VAP interaction such that hypophosphorylated IncV is closed with the FFAT motifs buried and hidden from VAP or hyperphosphorylated IncV is open and can bind to VAP, similar to the conformational change that occurs when CERT activity is regulated by phosphorylation of the CERT serine-repeat motif (SRM).¹⁶⁵ CERT contains several domains that allow it to transfer ceramide at ER-Golgi MCS. The Pleckstrin Homology (PH) domain binds to phosphatidylinositol 4-phosphate (PI4P) in Golgi membranes, the FFAT motif mediates the CERT-VAP interaction, and the StAR-related lipid-transfer domain (START) transfers ceramide from the ER to the Golgi membranes.¹⁶⁵ The CERT SRM is immediately downstream from the PH domain and phosphorylation of the CERT SRM by Casein Kinase 1 γ 2, a serine/threonine kinase unrelated to CK2, induces an

inhibitory interaction between the PH and START domains that down-regulates ceramide transfer by CERT.²³⁵ Interestingly, phosphorylation of the CERT SRM by CK1 γ 2 requires a prior priming phosphorylation event.²³⁵ Thus, the potential phosphorylation cascade described for IncV above would be reminiscent of the CERT SRM phosphorylation steps. In contrast to phosphorylation events down-regulating CERT activity, phosphorylation of IncV by CK2 promoted the IncV-VAP interaction (Figure 3.6). Though there could be similarities between conformation change mechanisms between IncV and CERT, the outcome is different in that IncV phosphorylation plays a role in the IncV-VAP interaction, whereas CERT SRM phosphorylation decreases the CERT-VAP interaction.^{165,235} Another clear difference is that CERT is a cytosolic protein while IncV is embedded in the inclusion membrane. The tail of IncV contains the FFAT motifs that mediate the IncV-VAP interaction, and instead of the PH domain of CERT, IncV is connected to the ER-opposing membrane through transmembrane domains. However, if the IncV serine-rich region were phosphorylated in a way that promoted binding of the C-terminus to a region of IncV close to the transmembrane domain, it could mimic the closed conformation of CERT.

A recent study of the phosphoproteome of *Chlamydia* and host proteins during infection identified three phosphorylated serines in the IncV cytosolic tail well upstream from the IncV FFAT motifs.²¹⁸ One of the residues (S184) identified in the Zadora *et al* study is a potential CK2 recognition site and was also identified in the post translational modification analysis of IncV phosphorylated by CK2 *in vitro* described above (Figure

4.2).²¹⁸ One possibility could be that phosphorylation of S184 works in cooperation with phosphorylation of the serine-rich region described in the previous paragraph and contributes to conformation changes. In addition to the phosphorylation of the CERT SRM, a residue seven amino acids upstream of the CERT FFAT motif (S315) can be phosphorylated to enhance binding to VAP.²⁰⁹ Thus, it is possible that IncV S184 is phosphorylated to enhance IncV binding to VAP, similar to how phosphorylation of S315 enhances the CERT-VAP interaction. Another possibility is that S184 could act as an initial docking site for CK2 which could then place CK2 in close proximity to other residues, such as the 342-356 serine-rich region in the C-terminal tail of IncV, to phosphorylate. It would be interesting to determine if phospho-S184 is a genuine CK2 phosphorylated residue during infection or if another kinase phosphorylates it. It would also be interesting to determine if phospho-S184 plays a role in the IncV-VAP interaction. Studies to assess the role(s) of potential phosphorylation sites in IncV are discussed in Section 4.4.

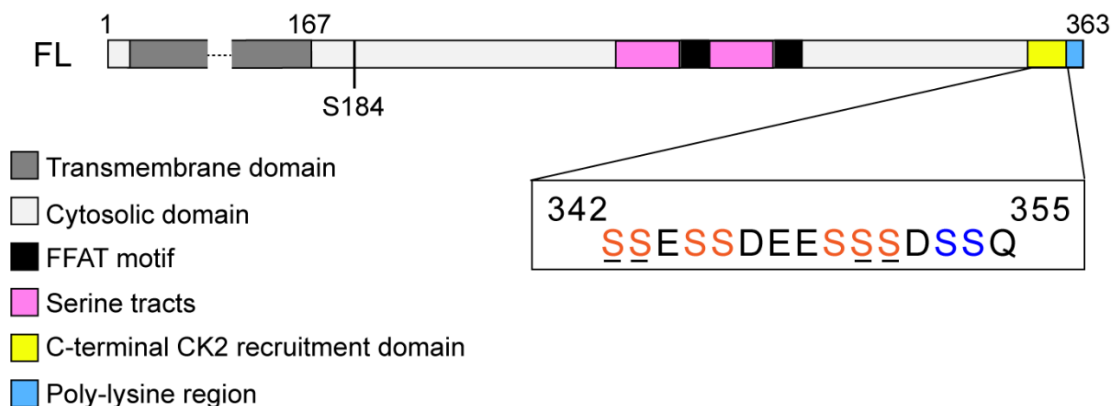


Figure 4.2. Schematic of IncV domains. IncV has a transmembrane domain (dark grey) and cytosolic tails (light grey). IncV contains two FFAT motifs (black) with flanking serine tracts (pink). The C-terminal domain required for CK2 recruitment demonstrated in Chapter 3 (yellow) contains seven potential CK2 phosphorylation sites (orange text) and two serines that could be primed by a separate kinase (blue text) to initiate a CK2 phosphorylation cascade (underlined residues). IncV also contains a poly-lysine region at its C-terminus (blue). S184 was identified in a phosphoproteome of *Chlamydia*-infected cells.²¹⁸

4.1.6.2.2 *Potential phosphorylation in the IncV serine tracts flanking the FFAT motifs*

In eukaryotic FFAT motifs, an enrichment of acidic residues surrounding the core of the motif, referred to as acidic tracts, are thought to provide a non-specific, initial interaction with the FFAT-binding region of VAP before the core then binds stably.¹⁷⁹ In addition to the C-terminal serine-rich region described above, IncV is enriched in serines flanking the FFAT motifs, that, if phosphorylated, could mimic the eukaryotic acidic tracts (Figure 4.3). To determine the role of the serine tracts in the IncV-VAP interaction, I mutated all the serines (18 in total) to alanines. Expression of the serine tract mutant disrupted the IncV-VAP interaction and IncV-dependent VAP recruitment to the inclusion membrane (not shown). Though long stretches of mutations could be detrimental to proper folding of IncV, the serine tract mutant was still inserted into the inclusion membrane, indicating that at least the translocation through the type III secretion system was not disrupted and the transmembrane domain remained intact. Further experiments to explore the acidic tract hypothesis are discussed in Section 4.4.

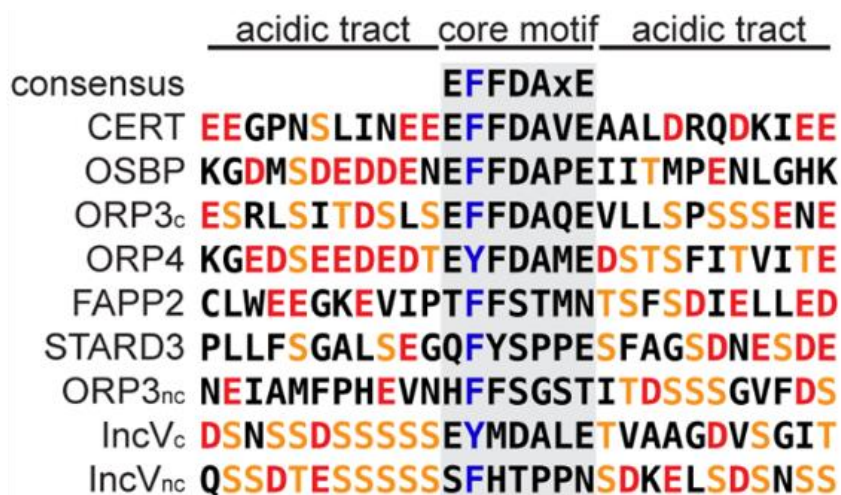


Figure 4.3. The IncV amino acid sequence flanking the FFAT motif core is enriched in **phosphorylatable residues**. An alignment of experimentally validated FFAT motifs, including the two FFAT motifs in IncV. The 7-amino acid core is highlighted with a grey box. Acidic tracts flank the core of the motif. Acidic residues, red text. Serine/Threonine, orange text. Essential position 2 amino acid, blue text.

4.1.6.2.3 Additional Kinases Playing a Role in IncV Phosphorylation

Given the large number of serines, it would not be surprising if multiple kinases acted on IncV. Additionally, the notion of phosphorylation priming described above makes it likely that kinases in addition to CK2 modify IncV. Accordingly, in addition to the IncV-CK2 interaction, the Inc-human interactome predicts IncV interactions with nine more kinases (Casein Kinase I α , Casein Kinase I ϵ , Phosphatidylinositol-5-Phosphate 4-Kinase Type 2 α , Phosphatidylinositol-5-Phosphate 4-Kinase Type 2 β , Phosphatidylinositol-5-Phosphate 4-Kinase Type 2 γ , Serine/threonine-protein kinase VRK2, Serine/threonine-protein kinase TAO2, Mitogen-activated protein kinase kinase kinase 4, and Focal adhesion kinase 1).⁶⁰ In support of multiple kinases phosphorylating IncV, the shift in apparent molecular weight when IncV was phosphorylated by CK2 *in vitro* was not as large as the shift in apparent molecular weight observed when IncV expressed in *C. trachomatis* was dephosphorylated using lambda phosphatase (Figure 3.1A and 3.6D). This suggests that CK2 could require other host factors or that multiple kinases play a role in phosphorylating IncV. However, inhibition of CK2 during infection leads to a seemingly complete decrease in the apparent molecular weight of IncV to the hypophosphorylated species (Figure 3.7C), mimicking the result observed upon lambda phosphatase treatment of IncV *in vitro* (Figure 3.1B). It is possible, however, that CK2 performs a large portion of phosphorylation of IncV, and other kinases perform minimal phosphorylation to prime some sites for CK2 to phosphorylate IncV. If this were the case, only some residues of IncV would be phosphorylated *in vitro* by CK2, with other

CK2 phosphorylation sites requiring additional host kinases to prime recognition motifs first. Then, during infection, inhibiting CK2 activity would prevent phosphorylation of residues that do and do not require priming. In addition to the Inc-human interactome kinases identified, the kinases that localize to the inclusion membrane microdomains, which are enriched in many Incs, host molecules (including active Src-Family kinases and Protein Kinase C), and cholesterol (Section 3.3.3)^{61,62,120,125} could potentially play a role in modifying IncV. Moreover, the phosphoproteome analysis performed by Zadora *et al.* identified three phosphorylated serines that fit the recognition for several host kinases including Protein Kinase A, Protein Kinase C, Glycogen synthase kinase-3, Cluster of Differentiation 5, Mitogen-activated protein kinase 3, Mitogen-activated protein kinase 1, Cyclin-dependent kinase 1).²¹⁸ Of the phosphoproteome kinases, only Protein Kinase C is known to localize to the inclusion in inclusion microdomains.²¹⁹ Future studies to examine the possibility of additional kinases phosphorylating IncV are discussed in Section 4.3.

4.2 Membrane Contact Sites in Host-Pathogen Interactions

MCS have been well studied in eukaryotic cells outside of the context of infection and we now know that, in addition to ER-Inclusion MCS in *Chlamydia*, several intracellular pathogens take advantage of this cellular process to benefit their replicative cycle. Obligate and facultative intracellular pathogens complete their replication cycles either in the host cytosol or within membrane bound vacuoles that resemble host organelles.²³⁶ The vacuolar membranes are derived from host membranes and/or contain

host membrane lipids which are modified to suit the needs of the pathogen.^{36,236} Interestingly, several pathogen-containing vacuoles have been shown to directly contact the ER and form pathogen-induced MCS.^{237–241} Since FFAT motif-containing proteins are often found at MCS with the ER, it is, perhaps, not surprising that pathogens have evolved mechanisms to exploit or mimic FFAT motif-containing proteins in their manipulation of the ER. In addition to IncV, there are other examples of proteins expressed by pathogens that contain FFAT motifs. Moreover, several examples demonstrate pathogen-encoded proteins that interact with FFAT-motif containing proteins and pathogen-mediated MCS formation that is FFAT-motif independent or unknown if FFAT motifs play a role. Figure 4.4 provides a schematic summary of the examples discussed in the following sections.

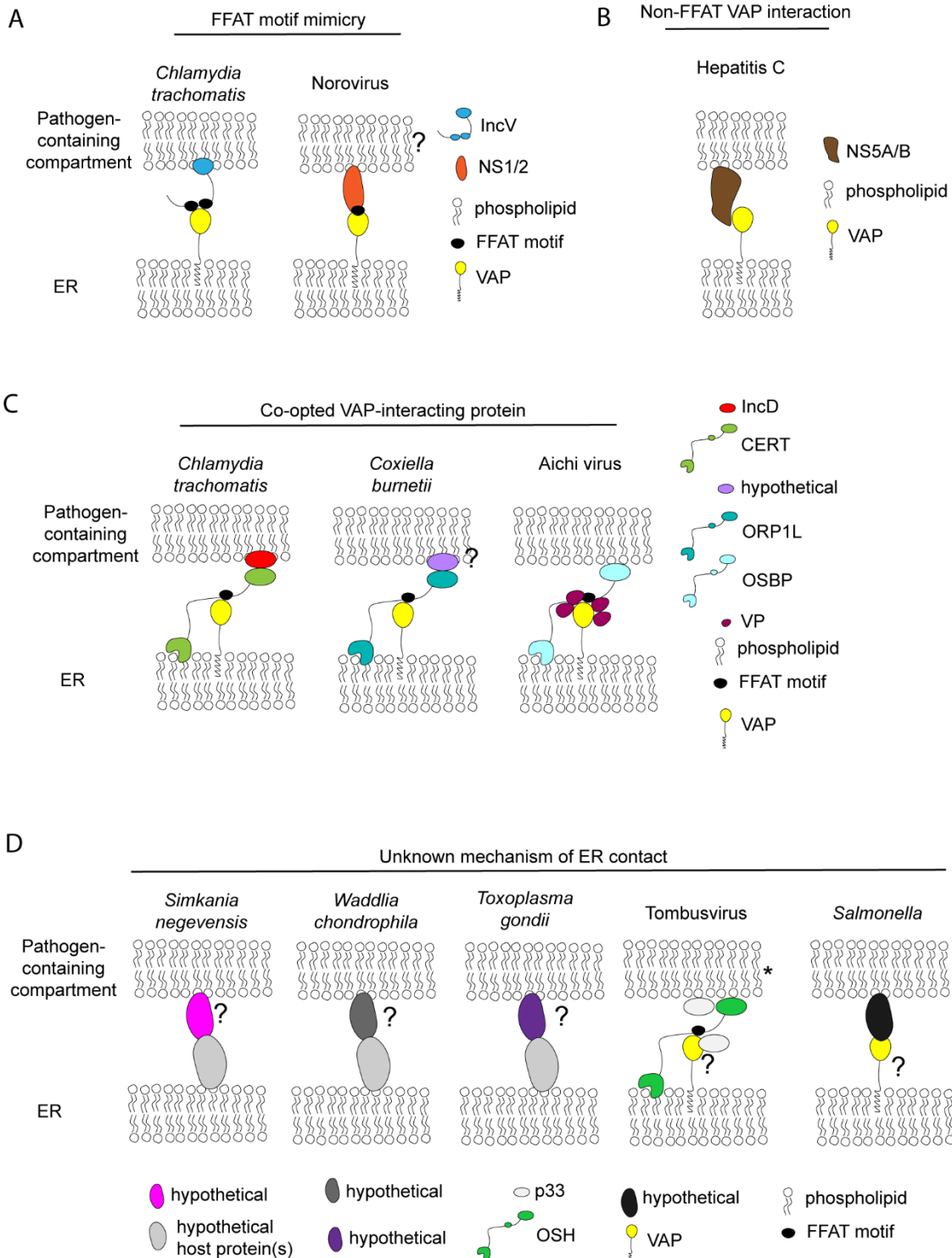


Figure 4.4. Summary of MCS during infection with intracellular pathogens. A) Models of pathogen-encoded proteins that directly mimic FFAT motifs. The *Chlamydia trachomatis* Inc protein IncV (blue) is inserted into the inclusion membrane and interacts with the host ER-resident VAP proteins (yellow) via two FFAT motifs (black). The norovirus nonstructural protein NS1/2 (orange) interact with VAP and the NS1/2-VAP interaction is proposed to play a role in the formation of MCS between the ER and the norovirus replication organelle. B) Model of pathogen-encoded proteins that interacts with VAP using a mechanism other than FFAT motifs. Hepatitis C virus nonstructural proteins NS5A and NS5B (brown) interact with VAP outside of its FFAT binding region. C) Models of pathogen-encoded proteins that interact with FFAT motif-containing host proteins. The *C. trachomatis* Inc protein IncD (red) is inserted into the inclusion membrane interacts with the host protein CERT (light green) which interacts with VAP on the ER. The *Coxiella burnetii*-containing vacuole membrane contacts the ER and an unknown *Coxiella* protein (purple) recruits the host protein ORP1L (teal) which interacts with VAP on the ER. The Aichi virus replication organelle contacts the ER via several Viral Proteins (VP, maroon) that interact with the host OSBP (cyan) and VAP. D) Models of MCS formed between the pathogen-containing compartment and the ER through unknown mechanisms. The *Simkania negevensis*-containing, *Waddlia chondrophila*-containing, and *Toxoplasma gondii*-containing vacuoles contact the ER through unknown protein interactions (pink, dark grey, dark purple, respectively). The Tombusvirus p33 (white) protein interacts with host OSH (lime green) and VAP through unknown mechanisms and

contacts between peroxisomes (*) and the ER are induced by the virus. The *Salmonella*-containing vacuole contacts the ER and the host VAP has been proposed to play a role through an interaction with an unknown *Salmonella* protein (black). Question marks (?) denote proposed components that have not been validated.

4.2.1 FFAT Motif-Containing Proteins Encoded by a Pathogen

In addition to the FFAT motifs in IncV, mimicry of FFAT motifs was also demonstrated in the plus strand RNA virus norovirus (Figure 4.4A). The nonstructural norovirus protein NS1/2 contains a FFAT motif that mediates an interaction with VAP.²⁰⁶ Knocking down VAP led to decreased viral replication, indicating that VAP is important for the virus lifecycle.²⁰⁶ Moreover, an intact FFAT motif in NS1/2 was required for both the NS1/2-VAP interaction and viral recovery.²⁰⁶ Though *C. trachomatis* inclusion size and infectious progeny production was negatively impacted by VAP knockdown,¹¹⁰ the IncV-VAP interaction was not required for infectious progeny production, suggesting the redundancy in VAP recruitment during *C. trachomatis* infection does not occur during Norovirus infection (Figure 2.15).¹⁰⁹ However, studies have fallen short of demonstrating the mechanistic role of VAP in norovirus replication. Several Norovirus proteins (NS1/2, NS3, and NS4) induce the formation of membrane-bound replication organelles that are derived from and reside near the ER.²⁴² Though electron micrographs have revealed the close proximity of replication organelles to the ER, it has not yet been demonstrated that ER-replication organelle MCS exist. McCune *et al.* hypothesized that the VAP-NS1/2 interaction could play a role in the formation of the replication organelle or could mediate MCS between the replication organelle and the ER.

4.2.2 Pathogen-Encoded Proteins That Interact With Eukaryotic FFAT Motif-Containing Proteins

In addition to directly mimicking FFAT motifs (IncV, described above), *C. trachomatis* expresses the Inc protein IncD which interacts with the FFAT motif-containing CERT (Figure 4.4C).^{58,110} In both infected and uninfected cells, CERT interacts with VAP, bridging the Golgi with the ER.¹⁶⁵ In infected cells, CERT also interacts with IncD and VAP to bridge the inclusion with the ER.

Like *C. trachomatis*, *Coxiella burnetii*, the causative agent of Q fever, is an obligate intracellular bacterium contained in pathogen-specified vacuole, referred to as the *Coxiella*-containing vacuole (CCV).²⁴³ The cholesterol transfer protein oxysterol binding protein related protein 1 longform (ORP1L) is recruited to the CCV and interacts with VAP via a FFAT motif in both infected and naïve cells (Figure 4.4C).²⁴⁴ It is possible that a *Coxiella*-encoded effector protein mediates the recruitment of ORP1L to the CCV (analogous to IncD recruiting CERT) because a type IV secretion system mutant of *Coxiella* that is unable to secrete effectors into the host cytosol does not recruit ORP1L to the CCV.²⁴⁴ Interestingly, ORP1L depletion leads to a decrease in CCV size which suggested that ORP1L could play a role in CCV membrane dynamics.²⁴⁴ It was proposed that ORP1L could play a role in transferring cholesterol and other sterols to the cholesterol-rich CCV membrane.²⁴⁴

The mechanism of pathogen-encoded proteins interacting with FFAT motif-containing proteins is also found in some viruses. The plus strand RNA virus aichi virus replicates its genome within a replication organelle, similar to noroviruses, which have been proposed to form MCS with the ER.²⁴⁵ OSBP is recruited to aichi virus replication sites

and interacts with several aichi virus proteins (Figure 4.4C).^{245,246} This host-viral protein complex facilitates the transfer of cholesterol to the aichi virus replication organelle and promotes the generation of the phospholipid phosphatidylinositol-4-phosphate at the replication organelle-ER MCS.^{245,246} The recruitment of VAP and OSBP are important for the aichi virus replication cycle as knocking down either VAP or OSBP inhibits viral replication.²⁴⁵

4.2.3 FFAT-Independent Pathogen-Mediated Membrane Contact Site Formation

To date, there is one example of a pathogen hijacking VAP independently of FFAT motif binding. VAP is required for hepatitis C virus replication.²⁴⁷ The hepatitis C virus replication organelle is enriched in nonstructural viral proteins NS5A and NS5B which interact with VAP by binding to the coiled-coil domain and the N-terminus of VAP, respectively (Figure 4.4B).^{247,248} The NS5A-VAP interaction, viral genome replication, and the localization of viral replication organelles are dependent on phosphorylation of NS5A serine 225.^{249,250}

4.2.4 Unknown mechanism of interaction between ER and Pathogen-Containing Compartment MCS

Simkania negevensis, a *Chlamydia*-like bacterium in the *Chlamydiales* order, replicates within a vacuole (*Simkania negevensis*-containing Vacuole (SnCV)) which contacts the ER (Figure 4.4D).²⁵¹ The composition of the SnCV membrane is unclear, but the extensive contacts formed between the ER and the SnCV suggest that host lipids could be incorporated into the SnCV membrane.²⁵¹ It is currently not known what mediates

SnCV-ER MCS formation. However, it was proposed that unidentified, *Chlamydia* Inc protein-like proteins play a role.²⁵¹

Another bacterium in the *Chlamydiales* order, *Waddlia chondrophila*, reside in a vacuole (*Waddlia*-containing vacuole (WCV)) that contacts mitochondria.²⁵² The ER surrounds the mitochondria and sometimes directly contacts the WCV membrane (Figure 4.4D).²⁵² How these WCV-ER contacts are formed and whether bacterial factors are involved is not known.

The eukaryotic parasite *Toxoplasma gondii* parasitophorous vacuole (TgPV) membrane contacts the host ER and these contacts are hypothesized to function in lipid transfer (Figure 4.4D).²⁵³ To date, however, the function of TgPV-ER MCS and how they are formed is unknown.

To replicate its genome in yeast, Tombusviruses, a genus of ssRNA(+) viruses whose natural hosts are plants, require the yeast oxysterol-binding homology (OSH) proteins.²⁵⁴ The tombusvirus replication protein p33 interacts with both VAP and OSH proteins (Figure 4.4D).²⁵⁴ Sterols are enriched near the tombusvirus replication organelle and overexpression of Scs2p, the yeast VAP homolog, increases viral replication.²⁵⁴ Though OSH proteins are known to interact with VAP via FFAT motifs, it is unclear how tombusvirus replication protein p33 interacts with VAP and OSH proteins.

Contact between a pathogen-containing vacuole and the ER is not limited to obligate intracellular pathogens. The facultative intracellular bacterium *Salmonella* resides in the *Salmonella*-containing vacuole (SCV) after it invades host cells and the SCV has

been shown to contact the ER (Figure 4.4D).²⁵⁵ Though the role has not been investigated, VAP was enriched in an SCV-Host proteome suggesting FFAT motif(s) may facilitate SCV-ER MCS formation.²⁵⁵

Many intracellular pathogens clearly co-opt eukaryotic proteins and generate MCS with the ER. The precise functions of most MCS discussed here have not been described. However, the field of MCS, in general, is constantly advancing and I hypothesize that the study of MCS in host-pathogen interactions will contribute to our general understanding of MCS.

4.3 Future Directions

Since ER-Inclusion MCS are an important component of the *Chlamydia* intracellular lifestyle, it will be important to further characterize their formation, maintenance, and function during the multiple stages of the developmental cycle.

4.3.1 Dynamics of IncV Phosphorylation

My data presented in Chapter 3 demonstrate that the IncV-VAP is regulated via the phosphorylation of IncV by CK2. Since the data in Chapter 3 were all assessed at 24 hours post-infection, we do not have a sense of the temporal dynamics of both IncV phosphorylation and the IncV-VAP interaction. IncV was previously shown to be expressed throughout the entire developmental cycle.⁸⁷ Additionally, VAP was shown to associate with the inclusion as early as 2 hours post-infection.^{149,151} It is possible that the IncV-VAP interaction remains constant once established to form a stable tethering complex. It is also conceivable that differential phosphorylation of IncV modulates the IncV-

VAP interaction such that other complexes could displace IncV-VAP and perform different functions depending on the needs of the bacteria at the time. To determine the phosphorylation state of IncV throughout the developmental cycle, a simple experiment would be to infect cells with the *incV* mutant strain complemented with the tet-inducible IncV plasmid and induce IncV expression at different times during infection. Then protein samples could be analyzed via western blot to determine if the apparent molecular weight changes throughout the developmental cycle. Since CK2 phosphorylation experiments done in Chapter 3 were performed at 24 hours post-infection, it would be important to determine whether IncV phosphorylation is dependent on CK2 at other times during *Chlamydia* replication. For example, if IncV is phosphorylated early in the developmental cycle in a CK2-independent manner, a protein band doublet corresponding to hypo and hyperphosphorylated species of IncV would still be observed in Western blot.

4.3.2 *IncV Serine Tracts, More Mimicry of Eukaryotic FFAT Motifs?*

An unresolved aspect of the FFAT motif-mediated interaction between IncV and VAP is whether the serine tracts immediately upstream of each FFAT motif core in IncV are involved in binding to VAP. Eukaryotic FFAT motifs are enriched in acidic residues that are thought to non-specifically bind to the electronegative face of VAP before the core of the FFAT motif binds stably.¹⁹⁹ Since IncV contains serine tracts instead of acidic tracts, we hypothesized that these serine tracts would be phosphorylated to mimic the eukaryotic acidic tracts. Individually mutating each of the 18 serines in the serine tracts is not a practically feasible approach because of the possibility that certain combinations

of multiple mutations would be necessary. Ideally, post-translational modification analysis of mass spectrometry of IncV isolated from infected cells would provide candidate residues to mutate. It could also reveal additional phosphorylated residues that could generate new hypotheses. Additionally, to determine if CK2 plays a role in the potential phosphorylation of the IncV serine tracts, data from mass spectrometry analysis of samples from infected cells that had been treated with the CK2 inhibitor CX-4945 could be compared to data from untreated, infected cells. This could provide insight into CK2-phosphorylated residues in IncV that are not appreciated using an *in vitro* approach.

4.3.3 Role of Other Potential Phosphorylated Residues in the IncV-VAP interaction

Since there are many potential phosphorylation sites that could play a role in the IncV-VAP interaction, there are numerous hypotheses to test. The first hypothesis to test would be the notion of priming. As discussed in Section 4.2.6.2.1, there are two serines within the domain of IncV required for CK2 recruitment (amino acids 342-356) that, if phosphorylated, generate additional CK2 recognition sites. A simple experiment to test this hypothesis would be to mutate each of the two potential priming serines and perform an *in vitro* kinase assay as performed in Section 3.5. A complementary approach would be to assess whether phosphomimetic mutations further increased the apparent molecular weight after CK2 phosphorylation, it would indicate that CK2 requires a priming phosphorylation. To test the hypothesis that the serine-rich region of IncV from amino acids 342-456 plays a role in the IncV-VAP interaction, IncV with single alanine point mutations or a combination of alanine mutations of the serines in that

region could be utilized in the *in vitro* kinase assay coupled with the *in vitro* IncV-VAP binding assay as performed in Section 3.6. Similarly, the importance of IncV S184 identified as a phosphorylated residue in the phosphoproteome study could be assessed by making either an alanine or phosphomimetic mutation and determining if either mutation affects IncV-VAP binding *in vitro*.²¹⁸

4.3.4 Other Kinases Potentially Phosphorylating IncV

In addition to CK2, there are several other candidate kinases that could phosphorylate IncV, as discussed in Section 4.2.6.2.3. One way to test a potential association between these candidate kinases and IncV would be to infect HeLa cells with wild-type *C. trachomatis* and stain for each kinase individually to determine if there is any enrichment of a given kinase around the inclusion. Since there are some kinases that are already known to be enriched in patches on the inclusion membrane, i.e. inclusion microdomain kinases, it would be straightforward to test whether they are associated with IncV. The kinases identified in the Inc-Human interactome could also be tested to confirm their association with IncV.⁶⁰ Cells expressing fluorescent versions of each kinase could be infected with the strain of *C. trachomatis* that can overexpress IncV and determine if there is an increase in kinase recruitment upon IncV overexpression. Then, combinations of identified kinases and CK2 could be utilized in an *in vitro* assay to determine if multiple kinases work in cooperation to fully phosphorylate IncV *in vitro*.

4.3.5 Other Possible Roles for IncV

Many tethering pairs at eukaryotic MCS include proteins that perform functions in addition to acting as a tether. For example, many lipid transfer proteins have a dual role in tethering and transferring specific lipids between membrane. The CERT-VAP complex acts as a tether at ER-Golgi MCS but its major function is to transfer ceramide from the ER to the Golgi. Though IncV has no known sequence homology with eukaryotic domains other than the FFAT motifs, it is possible that there are domains that structurally mimic functional domains. There is also a unique enrichment of lysines at the C-terminus of IncV that is reminiscent of the polybasic tail of STIM1 that targets it to the plasma membrane. Though a mutant version of IncV missing the c-terminal lysines still recruits VAP to the inclusion membrane as efficiently as wild type IncV (not shown), it is still possible that the lysines could play a role in interactions with the plasma membrane. During the later stages of the developmental cycle, the inclusion takes up a large volume of the host cell cytosol and its membrane is close to the plasma membrane. It is possible that the poly-lysine domain of IncV plays a structural role in contacting the plasma membrane to prepare for host cell exit via extrusion. It was recently shown that STIM1 is required for extrusion,⁶¹ so it would be interesting if the poly-lysine regions of STIM1 and IncV play any role in extrusion. One way to test this hypothesis would be to measure extrusion from cells infected with the incV mutant complemented with the version of IncV lacking the poly-lysine tail or wild type IncV. Extrusion is measured by enumerating intact inclusions that are not next to host cell nuclei from infected cell supernatant using a hemocytometer.^{32,33,40,61} To test the role of the polylysine region of

STIM1 in extrusion, cells depleted of STIM1 and expressing an siRNA-resistant STIM1 lacking its poly-lysine region or wild type STIM1 could be infected with wild type *C. trachomatis* to measure differences in extrusion.

4.3.6 Interplay between IncV and other ER-Inclusion MCS components

It is well established at this point that VAP is part of two different complexes at ER-Inclusion MCS. The IncD-CERT-VAP complex was proposed to facilitate acquisition of host lipids by the bacteria and the IncV-VAP complex as a tether of ER-Inclusion MCS.^{58,109,110} It is reasonable to hypothesize that because they are both in complex with VAP, IncV and IncD interact. Inc-Inc interactions have been demonstrated before using several different systems including overexpression in eukaryotic cells, yeast two-hybrid, bacteria two-hybrid, a simple, single cell culture infection model, and a *C. trachomatis* co-infection cell culture model in which two strains expressing two different tagged Inc proteins were used.^{59,68,113,117,125} A bacterial two-hybrid setup predicted that both IncD and IncV self-interact but did not interact with each other. However, it is important to note that many components were missing from this system including the inclusion membrane and host factors. The IncD-IncD interaction was confirmed using our labs co-infection model system and this experimental setup could also be used to determine an IncD-IncV interaction. However, even if IncD and IncV do not directly interact, they could still be part of a larger complex including CERT, VAP, and other possible unidentified factors. One possible scenario is that the IncD-CERT-VAP complex brings the inclusion membrane and the ER together and the IncV-VAP auxiliary tethering pair could

subsequently form to stabilize the contact site. This could possibly be tested by assessing VAP and IncV co-localization in CERT-knockout cells to determine if CERT is necessary for the IncV-VAP interaction to occur. Another approach might be to generate an IncD mutant. *IncD* is the first gene in a four-gene operon and mutating it could cause polar effects.¹⁴² However, there is at least one promising approach, FLAEM, described in Section 1.2.2, which combines allelic replacement and subsequent removal of the fluorescence and selection markers that could mitigate polar effects.⁷⁵ In support of the hypothesis that IncV and IncD are part of a larger complex, the Inc-Human interactome predicts that the uncharacterized Inc protein CT556 also interacts with VAPA and that IncV is predicted to interact with multiple host proteins that have more than one predicted interacting Inc partner.⁶⁰ To identify potential novel components of such a complex, IncV and/or IncD could be overexpressed by *C. trachomatis* and inserted into the inclusion membrane, then immunoprecipitated so that protein samples could be analyzed via mass spectrometry. Comparing the list of interacting proteins from each condition would reveal any commonalities and provide candidate proteins to test using co-immunoprecipitation and immunofluorescence microscopy approaches.

4.3.7 ER-Inclusion MCS and Inclusion Microdomains: One and the Same?

Inclusion microdomains provide an interesting source of new potential members of ER-Inclusion MCS component because STIM1 also localizes to inclusion microdomains.⁶¹ Inclusion microdomains are defined by small sections of the inclusion membrane enriched in 9 Inc proteins (MrcA, CT222, IPAM, CT224, CT228, IncB, IncC, CT288,

and CT850), and a large group of host molecules including active Src-family kinases (SFKs), Protein Kinase C, myosin light-chain kinase (MLCK), myosin phosphatase target subunit 1 (MYPT1), inositol 1,4,5-trisphosphate receptor, type 3 (ITPR3), STIM1, and cholesterol.^{61,62,120,125} The Inc proteins MrcA and CT228 and the host proteins ITPR3 and STIM1 were shown to play roles in the extrusion mechanism of *Chlamydia* exit from the host cell.^{61,120} Inc proteins CT223 and CT850 have been implicated in associations between the inclusion and the host cytoskeleton.^{120,134} It was also shown that CERT co-localizes with SFKs on the inclusion membrane.⁶¹ Because both CERT and STIM1 localize to inclusion microdomains, it was proposed that ER-Inclusion MCS and microdomains are the same structure.⁶¹ If ER-Inclusion MCS and inclusion microdomains are indeed the same structure, there are many more candidate proteins that could be involved in regulating MCS formation given the enrichment of host kinases. It would also be interesting to determine if CK2 plays a role in the association of the inclusion with cytoskeletal elements or the extrusion process. Since the cytoskeleton is highly involved in the *Chlamydia* developmental cycle, there are many possibilities to test for CK2 involvement. Similar to assessing VAP recruitment in the context of CK2 inhibition in Section 3.7, actin and microtubule cage formation could be assessed in conditions where CK2 was inhibited.

4.3.8 Subclasses of ER-Inclusion MCS

There is a growing appreciation that there can be specialized subclasses of MCS between a given pair of organelles. For example, in yeast, there are at least two ER-

plasma membrane MCS that are functionally and compositionally distinct.²⁵⁶ It is possible that there are multiple classes of ER-inclusion MCS that perform different functions throughout the developmental cycle. If ER-Inclusion MCS and inclusion microdomains are not the same structure, it could indicate that, despite some compositional overlap (STIM1 and CERT), they perform distinct functions. To test these possibilities, cells depleted of one or more of the host factors known to localize to the inclusion membrane (STIM1, CERT, VAP, Src-Family Kinases, Protein Kinase C) could be infected and analyzed to determine the effect on outcomes such as localization of the other factors involved, inclusion size, infectious progeny production, and extrusion rate. If depletion of ER-Inclusion MCS components had no effect on the localization of inclusion microdomain components, it would support the hypothesis that there are multiple subclasses of ER-Inclusion MCS.

4.3.9 Dynamics of ER-Inclusion MCS formation

Our lab has previously provided evidence that ER-Inclusion MCS are formed throughout the developmental cycle and could remain stable in certain conditions.¹⁵¹ The addition of Thapsigargin induced the formation of STIM1 puncta at ER-plasma membrane MCS, but the STIM1 already associated with the inclusion membrane remained associated.¹⁵¹ Though these findings suggested that ER-Inclusion MCS already formed could be resistant to stimuli outside of the contact site, it is not currently known whether ER-Inclusion MCS that are formed early during infection remain stably tethered throughout the remainder of the developmental cycle. Further understanding this could

potentially provide insight into the metabolic needs of the bacteria at different stages of the developmental cycle. For example, if MCS are a source of lipids for inclusion membrane expansion, their formation and expansion might be required during RB replication. To test this hypothesis, it would be necessary to create conditions in which ER-Inclusion MCS are disrupted and measure the effect on inclusion size and infectious progeny production. It is also possible that MCS play a role in keeping the inclusion localized to a perinuclear region by concentrating certain structural molecules and facilitating interactions with host cytoskeletal factors. As described in Chapter 1, several host and bacterial factors are involved in remodeling the host cell cytoskeleton. Live imaging of ER-Inclusion MCS formation and tracking their location on the inclusion could provide insight into whether their formation and maintenance is a dynamic process. Coupled with fluorescent cytoskeleton subunits, live imaging could reveal a relationship between the dynamics of ER-Inclusion MCS formation and the localization of the inclusion within the host cell.

4.4 Final Conclusions

Overall, my thesis presents data demonstrating the role of IncV as a tether of ER-Inclusion MCS. *C. trachomatis* displays IncV on the surface of the inclusion where it interacts with VAP via the molecular mimicry of two eukaryotic FFAT motifs which tethers the ER to the inclusion membrane. The IncV-VAP interaction is regulated by CK2. My studies add two new molecules (IncV and CK2) to the ER-Inclusion MCS model and further characterized the function of a known ER-Inclusion MCS molecule (VAP) (Figure

4.5). Though there is still much to learn about ER-Inclusion MCS, my studies have provided insight into the tethering of the ER to the inclusion membrane. The fact that there must be redundant mechanisms for ER-Inclusion MCS formation suggests that these contacts are essential for *Chlamydia* replication. It will be important to further characterize ER-Inclusion MCS to fully elucidate their function. Not only will this knowledge be useful for understanding the *Chlamydia* intracellular niche, but it will provide insight into MCS biology, in general. Because there are few examples of regulation of the formation and maintenance of MCS by kinases, my studies could shed light on the regulation of other MCS, which are being increasingly recognized as essential components of cells and important in human disease.^{208,209,257} Because MCS are important in cell homeostasis and in host-pathogen interactions, a deeper understanding of their formation, maintenance, and function could lead to the development of new therapeutic targets for *Chlamydia* infection and beyond.

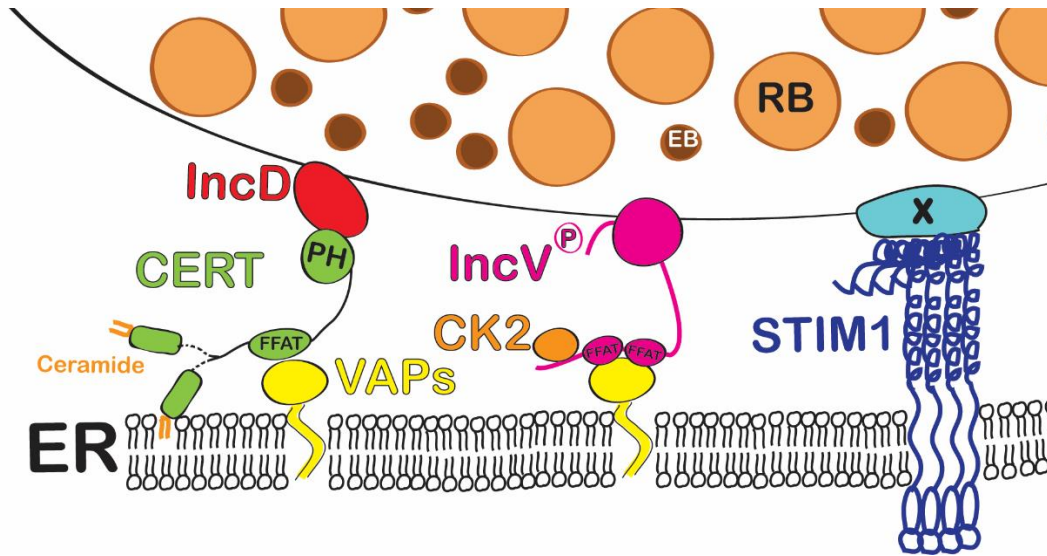


Figure 4.5. Current model of ER-Inclusion MCS. The IncD (red)-CERT (green)-VAP (yellow) complex had been proposed to facilitate lipid acquisition by the bacteria. STIM1 (blue) localizes to ER-Inclusion MCS but has an unknown function or interacting partner (protein X (light blue) that we hypothesize to be an Inc) there. To this model, we now add the ER-Inclusion MCS tether IncV (pink) that interacts with VAP. We also add Protein Kinase CK2 (orange), which regulates the IncV-VAP interaction via the phosphorylation of IncV.

Chapter 5
References

Chapter 5: References

1. WHO. Sexually transmitted infections Evidence brief. *World Health Organization* (2019).
2. WHO. Report on global sexually transmitted infection surveillance. *World Health Organization* (2018).
3. CDC. Sexually transmitted disease surveillance 2018. *Centers Dis. Control Prev.* (2019). doi:DOI: 10.15620/cdc.79370
4. Farley, T. A., Cohen, D. A. & Elkins, W. Asymptomatic sexually transmitted diseases: The case for screening. *Prev. Med. (Baltim)*. **36**, 502–509 (2003).
5. Owusu-Edusei, K. *et al.* The estimated direct medical cost of selected sexually transmitted infections in the United States, 2008. *Sex. Transm. Dis.* **40**, 197–201 (2013).
6. Huffam, S. *et al.* *Chlamydia* Infection Between Men and Women: A Cross-Sectional Study of Heterosexual Partnerships. *Open Forum Infect. Dis.* **4**, 1–6 (2017).
7. Cornelisse, V. J. *et al.* Concordance of *Chlamydia* infections of the rectum and urethra in same-sex male partnerships: A cross-sectional analysis. *BMC Infect. Dis.* **17**, 1–6 (2017).
8. Karlsson, A., Österlund, A. & Forssén, A. Pharyngeal *Chlamydia trachomatis* is not

- uncommon any more. *Scand. J. Infect. Dis.* **43**, 344–348 (2011).
9. Wilson Chialepeh, N. & Sathiyasusuman, A. Associated risk factors of stis and multiple sexual relationships among youths in Malawi. *PLoS One* **10**, (2015).
 10. Kongnyuy, E. J., Wiysonge, C. S., Mbu, R. E., Nana, P. & Kouam, L. Wealth and sexual behaviour among men in Cameroon. *BMC Int. Health Hum. Rights* **6**, (2006).
 11. Mah, T. L. & Halperin, D. T. Concurrent sexual partnerships and the HIV epidemics in Africa: Evidence to move forward. *AIDS Behav.* **14**, 11–16 (2010).
 12. Niccolai, L. M., Livingston, K. A., Laufer, A. S. & Pettigrew, M. M. Behavioural sources of repeat *Chlamydia trachomatis* infections: Importance of different sex partners. *Sex. Transm. Infect.* **87**, 248–253 (2011).
 13. Joseph, S. J. *et al.* *Chlamydiaceae* genomics reveals interspecies admixture and the recent evolution of *Chlamydia abortus* infecting lower mammalian species and humans. *Genome Biol. Evol.* **7**, 3070–3084 (2015).
 14. Burillo, A. & Bouza, E. *Chlamydia pneumoniae*. *Infect. Dis. Clin. North Am.* **24**, 61–71 (2010).
 15. Pichon, N., Guindre, L., Laroucau, K., Cantaloube, M. & Nallatamby, A. *Chlamydia abortus*. **26**, 2–3 (2020).
 16. Gaede, W. *et al.* *Chlamydia psittaci* infections in humans during an outbreak

- of psittacosis from poultry in Germany. *Zoonoses Public Health* **55**, 184–188 (2008).
17. Mishori, R., McClaskey, E. L. & Winklerprins, V. J. *Chlamydia Trachomatis* infections: Screening, diagnosis, and management. *Am. Fam. Physician* **86**, 1127–1132 (2012).
 18. Nunes, A. & Gomes, J. P. Evolution, phylogeny, and molecular epidemiology of *Chlamydia*. *Infect. Genet. Evol.* **23**, 49–64 (2014).
 19. Wright, H. R., Turner, A. & Taylor, H. R. Trachoma. *Lancet* **371**, 1945–54 (2007).
 20. Geisler, W. M., Suchland, R. J., Whittington, W. L. H. & Stamm, W. E. The relationship of serovar to clinical manifestations of urogenital *Chlamydia trachomatis* infection. *Sex. Transm. Dis.* **30**, 160–165 (2003).
 21. Stoner, B. P. & Cohen, S. E. Lymphogranuloma Venereum 2015: Clinical Presentation, Diagnosis, and Treatment. *Clin. Infect. Dis.* **61**, S865–S873 (2015).
 22. Lesiak-Markowicz, I., Schötta, A. M., Stockinger, H., Stanek, G. & Markowicz, M. *Chlamydia trachomatis* serovars in urogenital and ocular samples collected 2014–2017 from Austrian patients. *Sci. Rep.* **9**, 1–4 (2019).
 23. Mallika, P. S. *et al.* Neonatal conjunctivitis - A review. *Malaysian Family Physician* **3**, 77–81 (2008).
 24. Hu, V. H. *et al.* Epidemiology and control of trachoma: Systematic review. *Tropical*

- Medicine and International Health* **15**, 673–691 (2010).
25. Haggerty, C. L. *et al.* Risk of Sequelae after *Chlamydia trachomatis* Genital Infection in Women . *J. Infect. Dis.* **201**, 134–155 (2010).
 26. McConaghy, J. R. & Panchal, B. Epididymitis: An overview. *Am. Fam. Physician* **94**, 723–726 (2016).
 27. McLean, C. A., Stoner, B. P. & Workowski, K. A. Treatment of Lymphogranuloma Venereum. *Clin. Infect. Dis.* **44**, S147–S152 (2007).
 28. Rihl, M., Köhler, L., Klos, A. & Zeidler, H. Persistent infection of *Chlamydia* in reactive arthritis. *Ann. Rheum. Dis.* **65**, 281–284 (2006).
 29. Taylor, B. D. & Haggerty, C. L. Management of *Chlamydia trachomatis* genital tract infection: Screening and treatment challenges. *Infect. Drug Resist.* **4**, 19–29 (2011).
 30. Frieden, T. R. *et al.* *Sexually Transmitted Diseases Treatment Guidelines, 2015* *Morbidity and Mortality Weekly Report CONTENTS (Continued) Centers for Disease Control and Prevention MMWR Editorial and Production Staff (Serials) MMWR Editorial Board.* (2015).
 31. Nogueira, A. T., Braun, K. M. & Carabeo, R. A. Characterization of the Growth of *Chlamydia trachomatis* in *In vitro*-Generated Stratified Epithelium. *Front. Cell. Infect. Microbiol.* **7**, 1–16 (2017).

32. Zuck, M., Ellis, T., Venida, A. & Hybiske, K. Extrusions are phagocytosed and promote *Chlamydia* survival within macrophages. *Cell. Microbiol.* **19**, 1–12 (2017).
33. Sherrid, A. M. & Hybiske, K. *Chlamydia trachomatis* cellular exit alters interactions with host dendritic cells. *Infect. Immun.* **85**, 1–13 (2017).
34. Gitsels, A., Sanders, N. & Vanrompay, D. *Chlamydial* Infection From Outside to Inside. *Front. Microbiol.* **10**, 1–27 (2019).
35. AbdelRahman, Y. M. & Belland, R. J. The *Chlamydial* developmental cycle. *FEMS Microbiol. Rev.* **29**, 949–959 (2005).
36. Moore, E. R. & Ouellette, S. P. Reconceptualizing the *Chlamydial* inclusion as a pathogen-specified parasitic organelle: an expanded role for Inc proteins. *Front. Cell. Infect. Microbiol.* **4**, 1–10 (2014).
37. Clausen, J. D., Christiansen, G., Holst, H. U. & Birkelund, S. *Chlamydia trachomatis* utilizes the host cell microtubule network during early events of infection. *Mol. Microbiol.* **25**, 441–449 (1997).
38. Grieshaber, S. S., Grieshaber, N. A. & Hackstadt, T. *Chlamydia trachomatis* uses host cell dynein to traffic to the microtubule-organizing center in a p50 dynamitin-independent process. *J. Cell Sci.* **116**, 3793–3802 (2003).
39. Hackstadt, T., Scidmore-Carlson, M. A., Shaw, E. I. & Fischer, E. R. The *Chlamydia trachomatis* InCA protein is required for homotypic vesicle fusion. *Cell. Microbiol.*

- 1**, 119–130 (1999).
40. Hybiske, K. & Stephens, R. S. Mechanisms of host cell exit by the intracellular bacterium *Chlamydia*. *Proc. Natl. Acad. Sci. U. S. A.* **104**, 11430–11435 (2007).
41. Bastidas, R. J. *et al.* *Chlamydial* Intracellular Survival Strategies. *Cold Spring Harb. Perspect. Biol.* 1–20 (2013). doi:10.1101/cshperspect.a010256
42. Dolat, L. & Valdivia, R. H. A renewed tool kit to explore *Chlamydia* pathogenesis: From molecular genetics to new infection models. *F1000Research* **8**, (2019).
43. Valdivia, R. H. & Bastidas, R. J. The Expanding Molecular Genetics Tool Kit in *Chlamydia*. *J. Bacteriol.* **200**, 1–3 (2018).
44. Hooppaw, A. J. & Fisher, D. J. A Coming of Age Story: *Chlamydia* in the Post-Genetic Era. *Infect. Immun.* **84**, 612–621 (2016).
45. Stephens, R. S. *et al.* Genome sequence of an obligate intracellular pathogen of humans: *Chlamydia trachomatis*. *Science (80-.)*. **282**, 754–759 (1998).
46. Gong, S., Yang, Z., Lei, L., Shen, L. & Zhong, G. Characterization of *Chlamydia trachomatis* plasmid-encoded open reading frames. *J. Bacteriol.* **195**, 3819–3826 (2013).
47. Zhong, G. *Chlamydial* Plasmid-Dependent Pathogenicity. *Trends in Microbiology* **25**, 141–152 (2017).
48. Pickett, M. A., Everson, J. S., Pead, P. J. & Clarke, I. N. The plasmids of *Chlamydia*

- trachomatis and *Chlamydia pneumoniae* (N16): Accurate determination of copy number and the paradoxical effect of plasmid-curing agents. *Microbiology* **151**, 893–903 (2005).
49. Song, L. *et al.* *Chlamydia* trachomatis plasmid-encoded *pgp4* is a transcriptional regulator of virulence-associated genes. *Infect. Immun.* **81**, 636–644 (2013).
50. O’Connell, C. M., Ingalls, R. R., Andrews, C. W., Scurlock, A. M. & Darville, T. Plasmid-Deficient *Chlamydia muridarum* Fail to Induce Immune Pathology and Protect against Oviduct Disease. *J. Immunol.* **179**, 4027–4034 (2007).
51. McClure, E. E. *et al.* Engineering of obligate intracellular bacteria: Progress, challenges and paradigms. *Nat. Rev. Microbiol.* **15**, 544–558 (2017).
52. Hatch, T. P. MINIREVIEW Disulfide Cross-Linked Envelope Proteins: the Functional Equivalent of Peptidoglycan in *Chlamydiae*? *JOURNAL OF BACTERIOLOGY* **178**, (1996).
53. Wang, Y. *et al.* Development of a transformation system for *Chlamydia* trachomatis: Restoration of glycogen biosynthesis by acquisition of a plasmid shuttle vector. *PLoS Pathog.* **7**, (2011).
54. Agaisse, H. & Derré, I. A *C. trachomatis* Cloning Vector and the Generation of *C. trachomatis* Strains Expressing Fluorescent Proteins under the Control of a *C. trachomatis* Promoter. *PLoS One* **8**, (2013).

55. Wickstrum, J., Sammons, L. R., Restivo, K. N. & Hefty, P. S. Conditional Gene Expression in *Chlamydia trachomatis* Using the Tet System. *PLoS One* **8**, e76743 (2013).
56. Johnson, C. M. & Fisher, D. J. Site-specific, insertional inactivation of *inca* in *Chlamydia trachomatis* using a group II intron. *PLoS One* **8**, (2013).
57. Bauler, L. D. & Hackstadt, T. Expression and Targeting of secreted proteins from *Chlamydia trachomatis*. *J. Bacteriol.* **196**, 1325–1334 (2014).
58. Agaisse, H. & Derré, I. Expression of the effector protein IncD in *Chlamydia trachomatis* mediates recruitment of the lipid transfer protein CERT and the endoplasmic reticulum-resident protein VAPB to the inclusion membrane. *Infect. Immun.* **82**, 2037–2047 (2014).
59. Han, Y. & Derré, I. A Co-infection Model System and the Use of Chimeric Proteins to Study *Chlamydia* Inclusion Proteins Interaction. *Front. Cell. Infect. Microbiol.* **7**, 1–9 (2017).
60. Mirrashidi, K. M. *et al.* Global mapping of the *inc*-human interactome reveals that retromer restricts *Chlamydia* infection. *Cell Host Microbe* **18**, 109–121 (2015).
61. Nguyen, P. H., Lutter, E. I. & Hackstadt, T. *Chlamydia trachomatis* inclusion membrane protein MrcA interacts with the inositol 1,4,5-trisphosphate receptor type 3 (ITPR3) to regulate extrusion formation. *PLOS Pathog.* **14**, e1006911 (2018).

62. Weber, M. M., Bauler, L. D., Lam, J. & Hackstadt, T. Expression and localization of predicted inclusion membrane proteins in *Chlamydia trachomatis*. *Infect. Immun.* **83**, 4710–4718 (2015).
63. Kokes, M. *et al.* Integrating chemical mutagenesis and whole-genome sequencing as a platform for forward and reverse genetic analysis of *Chlamydia*. *Cell Host Microbe* **17**, 716–725 (2015).
64. Nguyen, B. D. & Valdivia, R. H. Forward genetic approaches in *Chlamydia trachomatis*. *J. Vis. Exp.* e50636 (2013). doi:10.3791/50636
65. Kari, L. *et al.* Generation of targeted *Chlamydia trachomatis* null mutants. *Proc. Natl. Acad. Sci. U. S. A.* **108**, 7189–7193 (2011).
66. Shaw, J. H. *et al.* Genetic Inactivation of *Chlamydia trachomatis* Inclusion Membrane Protein CT228 Alters MYPT1 Recruitment, Extrusion Production, and Longevity of Infection. *Front. Cell. Infect. Microbiol.* **8**, 415 (2018).
67. Weber, M. M. *et al.* Absence of Specific *Chlamydia trachomatis* Inclusion Membrane Proteins Triggers Premature Inclusion Membrane Lysis and Host Cell Death. *Cell Rep.* **19**, 1406–1417 (2017).
68. Sixt, B. S. *et al.* The *Chlamydia trachomatis* Inclusion Membrane Protein CpoS Counteracts STING-Mediated Cellular Surveillance and Suicide Programs. *Cell Host Microbe* **21**, 113–121 (2017).

69. Wesolowski, J. *et al.* *Chlamydia* hijacks ARF GTPases to coordinate microtubule posttranslational modifications and golgi complex positioning. *MBio* **8**, 1–14 (2017).
70. Weber, M. M. *et al.* A functional core of IncA is required for *Chlamydia trachomatis* inclusion fusion. *J. Bacteriol.* **198**, 1347–1355 (2016).
71. Carpenter, V., Chen, Y.-S., Dolat, L. & Valdivia, R. H. The Effector TepP Mediates Recruitment and Activation of Phosphoinositide 3-Kinase on Early *Chlamydia trachomatis* Vacuoles. *mSphere* **2**, 1–15 (2017).
72. Lowden, N. M., Yeruva, L., Johnson, C. M., Bowlin, A. K. & Fisher, D. J. Use of aminoglycoside 3' adenylyltransferase as a selection marker for *Chlamydia trachomatis* intron-mutagenesis and *in vivo* intron stability. *BMC Res. Notes* **8**, 570 (2015).
73. Karberg, M. *et al.* Group II introns as controllable gene targeting vectors for genetic manipulation of bacteria. *Nat. Biotechnol.* **19**, 1162–1167 (2001).
74. Mueller, K. E., Wolf, K. & Fields, K. A. Gene deletion by fluorescence-reported allelic exchange mutagenesis in *Chlamydia trachomatis*. *MBio* **7**, 1–9 (2016).
75. Keb, G., Hayman, R. & Fields, K. A. Floxed-Cassette Allelic Exchange Mutagenesis Enables Markerless Gene Deletion in *Chlamydia trachomatis* and Can Reverse Cassette-Induced Polar Effects. *J. Bacteriol.* **200**, 1–12 (2018).

76. Wagner, S. *et al.* Bacterial type III secretion systems: a complex device for the delivery of bacterial effector proteins into eukaryotic host cells. *FEMS Microbiol. Lett.* **365**, (2018).
77. Hsia, R. C., Pannekoek, Y., Ingerowski, E. & Bavoil, P. M. Type III secretion genes identify a putative virulence locus of *Chlamydia*. *Mol. Microbiol.* **25**, 351–359 (1997).
78. Kalman, S. *et al.* Comparative genomes of *Chlamydia pneumoniae* and *C. trachomatis*. *Nat. Genet.* **21**, 385–389 (1999).
79. Read, T. D. *et al.* Genome sequences of *Chlamydia trachomatis* MoPn and *Chlamydia pneumoniae* AR39. *Nucleic Acids Res.* **28**, 1397–1406 (2000).
80. Read, T. D. *et al.* Genome sequence of *Chlamydophila caviae* (*Chlamydia psittaci* GPIC): examining the role of niche-specific genes in the evolution of the *Chlamydiaceae*. doi:10.1093/nar/gkg321
81. Thomson, N. R. *et al.* The *Chlamydophila abortus* genome sequence reveals an array of variable proteins that contribute to interspecies variation. *Genome Res.* **15**, 629–640 (2005).
82. Azuma, Y. *et al.* Genome sequence of the cat pathogen, *Chlamydophila felis*. *DNA Res.* **13**, 15–23 (2006).
83. Clifton, D. R. *et al.* A *Chlamydial* type III translocated protein is tyrosine-

phosphorylated at the site of entry and associated with recruitment of actin.

Proc. Natl. Acad. Sci. U. S. A. **101**, 10166–71 (2004).

84. Chen, Y. S. *et al.* The *Chlamydia trachomatis* Type III Secretion Chaperone Slc1 Engages Multiple Early Effectors, Including TepP, a Tyrosine-phosphorylated Protein Required for the Recruitment of Crkl-II to Nascent Inclusions and Innate Immune Signaling. *PLoS Pathog.* **10**, (2014).
85. McKuen, M. J., Mueller, K. E., Bae, Y. S. & Fields, K. A. FRAEM reveals a role for *C. trachomatis* TmeA in invasion that is independent of host AHNAK. *Infect. Immun.* IAI.00640-17 (2017). doi:10.1128/IAI.00640-17
86. Mueller, K. E., Plano, G. V. & Fields, K. A. New frontiers in type III secretion biology: The *Chlamydia* perspective. *Infect. Immun.* **82**, 2–9 (2014).
87. Shaw, E. I. *et al.* Three temporal classes of gene expression during the *Chlamydia trachomatis* developmental cycle. *Mol. Microbiol.* **37**, 913–925 (2000).
88. Elwell, C., Mirrashidi, K. & Engel, J. *Chlamydia* cell biology and pathogenesis. *Nat. Rev. Microbiol.* **14**, 385–400 (2016).
89. (No Title). Available at: <https://chlambase.org/>. (Accessed: 3rd July 2020)
90. Gehre, L. *et al.* Sequestration of host metabolism by an intracellular pathogen. *Elife* **5**, (2016).
91. Fields, K. A. & Hackstadt, T. Evidence for the secretion of *Chlamydia trachomatis*

- CopN by a type III secretion mechanism. *Mol. Microbiol.* **38**, 1048–1060 (2000).
92. Pais, S. V. *et al.* CteG is a *Chlamydia trachomatis* effector protein that associates with the Golgi complex of infected host cells. *Sci. Rep.* **9**, (2019).
 93. Da Cunha, M., Pais, S. V., Bugalhão, J. N. & Mota, L. J. The *Chlamydia trachomatis* type III secretion substrates CT142, CT143, and CT144 are secreted into the lumen of the inclusion. *PLoS One* **12**, (2017).
 94. Jewett, T. J., Dooley, C. A., Mead, D. J. & Hackstadt, T. *Chlamydia trachomatis* tarp is phosphorylated by src family tyrosine kinases. *Biochem. Biophys. Res. Commun.* **371**, 339–344 (2008).
 95. Jewett, T. J., Miller, N. J., Dooley, C. A. & Hackstadt, T. The conserved tarp actin binding domain is important for *Chlamydial* invasion. *PLoS Pathog.* **6**, 1–11 (2010).
 96. Mehlitz, A. *et al.* Tarp regulates early *Chlamydia*-induced host cell survival through interactions with the human adaptor protein SHC1. *J. Cell Biol.* **190**, 143–157 (2010).
 97. Lane, B. J., Mutchler, C., Al Khodor, S., Grieshaber, S. S. & Carabeo, R. A. *Chlamydial* entry involves TARP binding of guanine nucleotide exchange factors. *PLoS Pathog.* **4**, (2008).
 98. Mueller, K. E. & Fields, K. A. Application of β -lactamase reporter fusions as an

- indicator of effector protein secretion during infections with the obligate intracellular pathogen *Chlamydia trachomatis*. *PLoS One* **10**, (2015).
99. Bullock, H. D., Hower, S. & Fields, K. A. Domain analyses reveal that *Chlamydia trachomatis* CT694 protein belongs to the membrane-localized family of type III effector proteins. *J. Biol. Chem.* **287**, 28078–28086 (2012).
 100. Saka, H. A. *et al.* *Chlamydia trachomatis* infection leads to defined alterations to the lipid droplet proteome in epithelial cells. *PLoS One* **10**, (2015).
 101. Fling, S. P. *et al.* CD8+ T cells recognize an inclusion associated protein from the pathogen *Chlamydia trachomatis*. *Proc. Natl. Acad. Sci. U. S. A.* **98**, 1160–1165 (2001).
 102. Vromman, F., Perrinet, S., Gehre, L. & Subtil, A. The DUF582 proteins of *Chlamydia trachomatis* bind to components of the ESCRT machinery, which is dispensable for bacterial growth *in vitro*. *Front. Cell. Infect. Microbiol.* **6**, (2016).
 103. Gong, S., Lei, L., Chang, X., Belland, R. & Zhong, G. *Chlamydia trachomatis* secretion of hypothetical protein CT622 into host cell cytoplasm via a secretion pathway that can be inhibited by the type III secretion system inhibitor compound 1. *Microbiology* **157**, 1134–1144 (2011).
 104. Cossé, M. M. *et al.* The loss of expression of a single type 3 effector (CT622) strongly reduces *Chlamydia trachomatis* infectivity and growth. *Front. Cell. Infect. Microbiol.* **8**, (2018).

105. Hower, S., Wolf, K. & Fields, K. A. Evidence that CT694 is a novel *Chlamydia trachomatis* T3S substrate capable of functioning during invasion or early cycle development. *Mol. Microbiol.* **72**, 1423–1437 (2009).
106. Muschiol, S. *et al.* Identification of a family of effectors secreted by the type III secretion system that are conserved in pathogenic *Chlamydiae*. *Infect. Immun.* **79**, 571–580 (2011).
107. Pennini, M. E., Perrinet, S., Dautry-Varsat, A. & Subtil, A. Histone Methylation by NUE, a Novel Nuclear Effector of the Intracellular Pathogen *Chlamydia trachomatis*. *PLoS Pathog.* **6**, e1000995 (2010).
108. Lu, C. *et al.* *Chlamydia trachomatis* GlgA Is Secreted into Host Cell Cytoplasm. *PLoS One* **8**, (2013).
109. Stanhope, R., Flora, E., Bayne, C. & Derré, I. IncV, a FFAT motif-containing *Chlamydia* protein, tethers the endoplasmic reticulum to the pathogen-containing vacuole. *Proc. Natl. Acad. Sci.* **114**, 201709060 (2017).
110. Derré, I., Swiss, R. & Agaisse, H. The lipid transfer protein CERT interacts with the *Chlamydia* inclusion protein IncD and participates to ER-*Chlamydia* inclusion membrane contact sites. *PLoS Pathog.* **7**, (2011).
111. Elwell, C. A. *et al.* *Chlamydia* interfere with an interaction between the mannose-6-phosphate receptor and sorting nexins to counteract host restriction. *Elife* **6**, (2017).

112. Scidmore, M. A. & Hackstadt, T. Mammalian 14-3-3 β associates with the *Chlamydia trachomatis* inclusion membrane via its interaction with IncG. *Mol. Microbiol.* **39**, 1638–1650 (2001).
113. Hackstadt, T., Scidmore-Carlson, M. A., Shaw, E. I. & Fischer, E. R. The *Chlamydia trachomatis* Inca protein is required for homotypic vesicle fusion. *Cell. Microbiol.* **1**, 119–130 (1999).
114. Ronzone, E. & Paumet, F. Two Coiled-Coil Domains of *Chlamydia trachomatis* Inca Affect Membrane Fusion Events during Infection. *PLoS One* **8**, e69769 (2013).
115. Delevoeye, C. *et al.* SNARE protein mimicry by an intracellular bacterium. *PLoS Pathog.* **4**, (2008).
116. Bannantine, J. P., Griffiths, R. S., Viratyosin, W., Brown, W. J. & Rockey, D. D. A secondary structure motif predictive of protein localization to the *Chlamydial* inclusion membrane. *Cell. Microbiol.* **2**, 35–47 (2000).
117. Gaudiard, E., Ouellette, S. P., Rueden, K. J. & Ladant, D. Characterization of interactions between inclusion membrane proteins from *Chlamydia trachomatis*. *Front. Cell. Infect. Microbiol.* **5**, 1–11 (2015).
118. Dumoux, M., Menny, A., Delacour, D. & Hayward, R. D. A *Chlamydia* effector recruits CEP170 to reprogram host microtubule organization. *J. Cell Sci.* **128**, 3420–3434 (2015).

119. Alzhanov, D. T., Weeks, S. K., Burnett, J. R. & Rockey, D. D. Cytokinesis is blocked in mammalian cells transfected with *Chlamydia trachomatis* gene CT223. *BMC Microbiol.* **9**, (2009).
120. Lutter, E. I., Barger, A. C., Nair, V. & Hackstadt, T. *Chlamydia trachomatis* Inclusion Membrane Protein CT228 Recruits Elements of the Myosin Phosphatase Pathway to Regulate Release Mechanisms. *Cell Rep.* **3**, 1921–1931 (2013).
121. Rzomp, K. A., Moorhead, A. R. & Scidmore, M. A. The GTPase Rab4 interacts with *Chlamydia trachomatis* inclusion membrane protein CT229. *Infect. Immun.* **74**, 5362–5373 (2006).
122. Faris, R. *et al.* *Chlamydia trachomatis* CT229 Subverts Rab GTPase-Dependent CCV Trafficking Pathways to Promote *Chlamydial* Infection. *Cell Rep.* **26**, 3380-3390.e5 (2019).
123. Almeida, F., Luís, M. P., Pereira, I. S., Pais, S. V. & Mota, L. J. The Human Centrosomal Protein CCDC146 Binds *Chlamydia trachomatis* Inclusion Membrane Protein CT288 and Is Recruited to the Periphery of the *Chlamydia*-Containing Vacuole. *Front. Cell. Infect. Microbiol.* **8**, 254 (2018).
124. Delevoye, C. *et al.* SNARE protein mimicry by an intracellular bacterium. *PLoS Pathog.* **4**, (2008).
125. Mital, J., Miller, N. J., Fischer, E. R. & Hackstadt, T. Specific *Chlamydial* inclusion membrane proteins associate with active Src family kinases in microdomains that

- interact with the host microtubule network. *Cell. Microbiol.* **12**, 1235–1249 (2010).
126. Toh, H., Miura, K., Shirai, M. & Hattori, M. In silico inference of inclusion membrane protein family in obligate intracellular parasites *Chlamydiae*. *DNA Res.* **10**, 9–17 (2003).
127. Dehoux, P., Flores, R., Dauga, C., Zhong, G. & Subtil, A. Multi-genome identification and characterization of *Chlamydiae*-specific type III secretion substrates: the Inc proteins. *BMC Genomics* **12**, 109 (2011).
128. Lutter, E. I., Martens, C. & Hackstadt, T. Evolution and conservation of predicted inclusion membrane proteins in *Chlamydiae*. *Comp. Funct. Genomics* **2012**, (2012).
129. Bugalhão, J. N. & Mota, L. J. The multiple functions of the numerous *Chlamydia trachomatis* secreted proteins: The tip of the iceberg. *Microb. Cell* **6**, 414–449 (2019).
130. Elwell, C. A. & Engel, J. N. Lipid acquisition by intracellular *Chlamydiae*. *Cell. Microbiol.* **14**, 1010–1018 (2012).
131. Clifton, D. R. *et al.* Tyrosine phosphorylation of the *Chlamydial* effector protein Tarp is species specific and not required for recruitment of actin. *Infect. Immun.* **73**, 3860–3868 (2005).

132. Kumar, Y. & Valdivia, R. H. Actin and Intermediate Filaments Stabilize the *Chlamydia trachomatis* Vacuole by Forming Dynamic Structural Scaffolds. *Cell Host Microbe* **4**, 159–169 (2008).
133. Kumar, Y. & Valdivia, R. H. Actin and Intermediate Filaments Stabilize the *Chlamydia trachomatis* Vacuole by Forming Dynamic Structural Scaffolds. *Cell Host Microbe* **4**, 159–169 (2008).
134. Mital, J., Lutter, E. I., Barger, A. C., Dooley, C. A. & Hackstadt, T. *Chlamydia trachomatis* inclusion membrane protein CT850 interacts with the dynein light chain DYNLT1 (Tctex1). *Biochem. Biophys. Res. Commun.* **462**, 165–170 (2015).
135. Al-Zeer, M. A. *et al.* *Chlamydia trachomatis* remodels stable microtubules to coordinate Golgi stack recruitment to the *Chlamydial* inclusion surface. *Mol. Microbiol.* **94**, 1285–1297 (2014).
136. Al-Younes, H. M. *et al.* Autophagy-independent function of MAP-LC3 during intracellular propagation of *Chlamydia trachomatis*. *Autophagy* **7**, 814–828 (2011).
137. Fields, K. A. & Hackstadt, T. The *Chlamydial* Inclusion: Escape from the Endocytic Pathway. *Annu. Rev. Cell Dev. Biol.* **18**, 221–245 (2002).
138. Damiani, M. T., Gambarte Tudela, J. & Capmany, A. Targeting eukaryotic Rab proteins: A smart strategy for *Chlamydial* survival and replication. *Cell. Microbiol.* **16**, 1329–1338 (2014).

139. Tudela, J. G. *et al.* The late endocytic Rab39a GTPase regulates the interaction between multivesicular bodies and *Chlamydial* inclusions. *J. Cell Sci.* **128**, 3068–3081 (2015).
140. Leiva, N., Capmany, A. & Damiani, M. T. Rab11-Family of Interacting Protein 2 associates with *Chlamydial* inclusions through its Rab-binding domain and promotes bacterial multiplication. *Cell. Microbiol.* **15**, 114–129 (2013).
141. Aeberhard, L. *et al.* The Proteome of the Isolated *Chlamydia trachomatis* Containing Vacuole Reveals a Complex Trafficking Platform Enriched for Retromer Components. *PLoS Pathog.* **11**, 1–25 (2015).
142. Scidmore-Carlson, M. A., Shaw, E. I., Dooley, C. A., Fischer, E. R. & Hackstadt, T. Identification and characterization of a *Chlamydia trachomatis* early operon encoding four novel inclusion membrane proteins. *Mol. Microbiol.* **33**, 753–765 (1999).
143. Beatty, W. L. Trafficking from CD63-positive late endocytic multivesicular bodies is essential for intracellular development of *Chlamydia trachomatis*. *J. Cell Sci.* **119**, 350–359 (2006).
144. Heuer, D. *et al.* *Chlamydia* causes fragmentation of the Golgi compartment to ensure reproduction. *Nature* **457**, 731–735 (2009).
145. Gurumurthy, R. K. *et al.* Dynamin-mediated lipid acquisition is essential for *Chlamydia trachomatis* development. *Mol. Microbiol.* **94**, 186–201 (2014).

146. Hackstadt, T., Rockey, D. D., Heinzen, R. A. & Scidmore, M. A. *Chlamydia trachomatis* interrupts an exocytic pathway to acquire endogenously synthesized sphingomyelin in transit from the Golgi apparatus to the plasma membrane. *Embo J* **15**, 964–977 (1996).
147. Van Ooij, C. *et al.* Host cell-derived sphingolipids are required for the intracellular growth of *Chlamydia trachomatis*. *Cell. Microbiol.* **2**, 627–637 (2000).
148. Giles, D. K. & Wyrick, P. B. Trafficking of *Chlamydial* antigens to the endoplasmic reticulum of infected epithelial cells. *Microbes Infect.* **10**, 1494–1503 (2008).
149. Elwell, C. A. *et al.* *Chlamydia trachomatis* co-opts gbf1 and cert to acquire host sphingomyelin for distinct roles during intracellular development. *PLoS Pathog.* **7**, (2011).
150. Dumoux, M., Clare, D. K., Saibil, H. R. & Hayward, R. D. *Chlamydiae* assemble a pathogen synapse to hijack the host endoplasmic reticulum. *Traffic* **13**, 1612–1627 (2012).
151. Agaisse, H. & Derré, I. STIM1 is a novel component of ER-*Chlamydia trachomatis* inclusion membrane contact sites. *PLoS One* **10**, 1–18 (2015).
152. Kaplan, M. R. & Simoni, R. D. Intracellular transport of phosphatidylcholine to the plasma membrane. *J. Cell Biol.* **101**, 441–445 (1985).
153. Vance, J. E., Aasman, E. J. & Szarka, R. Brefeldin a does not inhibit the movement

- of phosphatidylethanolamine from its sites of synthesis to the cell surface. *J. Biol. Chem.* **266**, 8241–8247 (1991).
154. Levine, T. & Loewen, C. Inter-organelle membrane contact sites: through a glass, darkly. *Curr. Opin. Cell Biol.* **18**, 371–378 (2006).
155. Lev, S. Non-vesicular lipid transport by lipid-transfer proteins and beyond. *Nature Reviews Molecular Cell Biology* **11**, 739–750 (2010).
156. Lev, S. Nonvesicular Lipid Transfer from the Endoplasmic Reticulum. *Cold Spring Harb. Perspect. Biol.* 1–16 (2012). doi:10.1101/cshperspect.a013300
157. Helle, S. C. J. *et al.* Organization and function of membrane contact sites. *Biochim. Biophys. Acta - Mol. Cell Res.* **1833**, 2526–2541 (2013).
158. Prinz, W. A. Bridging the gap: Membrane contact sites in signaling, metabolism, and organelle dynamics. *J. Cell Biol.* **205**, 759–769 (2014).
159. Quon, E. & Beh, C. T. Membrane contact sites: Complex zones for membrane association and lipid Exchange. *Lipid Insights* **2015**, 55–63 (2015).
160. Phillips, M. J. & Voeltz, G. K. Structure and function of ER membrane contact sites with other organelles. *Nat. Rev. Mol. Cell Biol.* **17**, 69–82 (2016).
161. Hoffmann, P. C. & Kukulski, W. Perspective on architecture and assembly of membrane contact sites. *Biol. Cell* 400–408 (2017). doi:10.1111/boc.201700031
162. Scorrano, L. *et al.* Coming together to define membrane contact sites. *Nat.*

- Commun.* **10**, 1–11 (2019).
163. Eisenberg-Bord, M., Shai, N., Schuldiner, M. & Bohnert, M. A Tether Is a Tether Is a Tether: Tethering at Membrane Contact Sites. *Dev. Cell* **39**, 395–409 (2016).
 164. Takeshima, H., Komazaki, S., Nishi, M., Iino, M. & Kangawa, K. Junctophilins: A novel family of junctional membrane complex proteins. *Mol. Cell* **6**, 11–22 (2000).
 165. Kumagai, K. & Hanada, K. Structure, functions and regulation of CERT, a lipid-transfer protein for the delivery of ceramide at the ER–Golgi membrane contact sites. *FEBS Letters* **593**, 2366–2377 (2019).
 166. Raiborg, C., Wenzel, E. M., Pedersen, N. M. & Stenmark, H. Phosphoinositides in membrane contact sites. *Biochemical Society Transactions* **44**, 425–430 (2016).
 167. Hönscher, C. *et al.* Cellular metabolism regulates contact sites between vacuoles and mitochondria. *Dev. Cell* **30**, 86–94 (2014).
 168. Montero, M. *et al.* Monitoring dynamic changes in free Ca²⁺ concentration in the endoplasmic reticulum of intact cells. *EMBO J.* **14**, 5467–5475 (1995).
 169. Burdakov, D., Petersen, O. H. & Verkhratsky, A. Intraluminal calcium as a primary regulator of endoplasmic reticulum function. *Cell Calcium* **38**, 303–310 (2005).
 170. Mekahli, D., Bultynck, G., Parys, J. B., de Smedt, H. & Missiaen, L. Endoplasmic-reticulum calcium depletion and disease. *Cold Spring Harbor Perspectives in Biology* **3**, 1–30 (2011).

171. Burgoyne, T., Patel, S. & Eden, E. R. Calcium signaling at ER membrane contact sites. *Biochimica et Biophysica Acta - Molecular Cell Research* **1853**, 2012–2017 (2014).
172. Lunz, V., Romanin, C. & Frischauf, I. STIM1 activation of Orai1. *Cell Calcium* **77**, 29–38 (2019).
173. Park, C. Y. *et al.* STIM1 Clusters and Activates CRAC Channels via Direct Binding of a Cytosolic Domain to Orai1. *Cell* **136**, 876–890 (2009).
174. Fagone, P. & Jackowski, S. Membrane phospholipid synthesis and endoplasmic reticulum function. *Journal of Lipid Research* **50**, S311 (2009).
175. Raychaudhuri, S. & Prinz, W. A. Nonvesicular phospholipid transfer between peroxisomes and the endoplasmic reticulum. *Proc. Natl. Acad. Sci. U. S. A.* **105**, 15785–15790 (2008).
176. Hanada, K. Lipid transfer proteins rectify inter-organelle flux and accurately deliver lipids at membrane contact sites. *J. Lipid Res.* **59**, 1341–1366 (2018).
177. Manford, A. G., Stefan, C. J., Yuan, H. L., MacGurn, J. A. & Emr, S. D. ER-to-Plasma Membrane Tethering Proteins Regulate Cell Signaling and ER Morphology. *Dev. Cell* **23**, 1129–1140 (2012).
178. Murphy, S. E. & Levine, T. P. VAP, a Versatile Access Point for the Endoplasmic Reticulum: Review and analysis of FFAT-like motifs in the VAPome. *Biochim.*

Biophys. Acta - Mol. Cell Biol. Lipids **1861**, 952–961 (2016).

179. Kaiser, S. E. *et al.* Structural basis of FFAT motif-mediated ER targeting. *Structure* **13**, 1035–1045 (2005).
180. Loewen, C. J. R., Roy, A. & Levine, T. P. A conserved ER targeting motif in three families of lipid binding proteins and in Opi1p binds VAP. *EMBO J.* **22**, 2025–2035 (2003).
181. Loewen, C. J. R. & Levine, T. P. A highly conserved binding site in vesicle-associated membrane protein-associated protein (VAP) for the FFAT motif of lipid-binding proteins. *J. Biol. Chem.* **280**, 14097–14104 (2005).
182. Mikitova, V. & Levine, T. P. Analysis of the key elements of FFAT-like motifs identifies new proteins that potentially bind VAP on the ER, including two AKAPs and FAPP2. *PLoS One* **7**, (2012).
183. Novick, P. & Schekman, R. Secretion and cell-surface growth are blocked in a temperature-sensitive mutant of *Saccharomyces cerevisiae*. *Proc. Natl. Acad. Sci. U. S. A.* **76**, 1858–1862 (1979).
184. Balch, W. E., Dunphy, W. G., Braell, W. A. & Rothman, J. E. Reconstitution of the transport of protein between successive compartments of the golgi measured by the coupled incorporation of N-acetylglucosamine. *Cell* **39**, 405–416 (1984).
185. Kaiser, C. A. & Schekman, R. Distinct sets of SEC genes govern transport vesicle

- formation and fusion early in the secretory pathway. *Cell* **61**, 723–733 (1990).
186. Perin, M. S., Fried, V. A., Mignery, G. A., Jahn, R. & Südhof, T. C. Phospholipid binding by a synaptic vesicle protein homologous to the regulatory region of protein kinase C. *Nature* **345**, 260–263 (1990).
187. Hata, Y., Slaughter, C. A. & Südhof, T. C. Synaptic vesicle fusion complex contains unc-18 homologue bound to syntaxin. *Nature* **366**, 347–351 (1993).
188. Söllner, T. *et al.* SNAP receptors implicated in vesicle targeting and fusion. *Nature* **362**, 318–324 (1993).
189. Alpy, F. *et al.* STARD3 or STARD3NL and VAP form a novel molecular tether between late endosomes and the ER. *J. Cell Sci.* **126**, 5500–5512 (2013).
190. Wilhelm, L. P. *et al.* STARD 3 mediates endoplasmic reticulum-to-endosome cholesterol transport at membrane contact sites. *EMBO J.* **36**, 1412–1433 (2017).
191. Manford, A. G., Stefan, C. J., Yuan, H. L., MacGurn, J. A. & Emr, S. D. ER-to-Plasma Membrane Tethering Proteins Regulate Cell Signaling and ER Morphology. *Dev. Cell* **23**, 1129–1140 (2012).
192. Lev, S., Halevy, D. Ben, Peretti, D. & Dahan, N. The VAP protein family: from cellular functions to motor neuron disease. *Trends Cell Biol.* **18**, 282–290 (2008).
193. Kawano, M., Kumagai, K., Nishijima, M. & Hanada, K. Efficient trafficking of ceramide from the endoplasmic reticulum to the golgi apparatus requires a

- VAMP-associated protein-interacting FFAT motif of CERT. *J. Biol. Chem.* **281**, 30279–30288 (2006).
194. Peretti, D., Dahan, N., Shimoni, E., Hirschberg, K. & Lev, S. Coordinated Lipid Transfer between the Endoplasmic Reticulum and the Golgi Complex Requires the VAP Proteins and Is Essential for Golgi-mediated Transport. *Mol. Biol. Cell* **19**, 3871–3884 (2008).
195. Rocha, N. *et al.* Cholesterol sensor ORP1L contacts the ER protein VAP to control Rab7-RILP-p150Glued and late endosome positioning. *J. Cell Biol.* **185**, 1209–1225 (2009).
196. De vos, K. J. *et al.* VAPB interacts with the mitochondrial protein PTPIP51 to regulate calcium homeostasis. *Hum. Mol. Genet.* **21**, 1299–1311 (2012).
197. Mesmin, B. *et al.* XA four-step cycle driven by PI(4)P hydrolysis directs sterol/PI(4)P exchange by the ER-Golgi Tether OSBP. *Cell* **155**, 830 (2013).
198. Hua, R. *et al.* VAPs and ACBD5 tether peroxisomes to the ER for peroxisome maintenance and lipid homeostasis. *J. Cell Biol.* **216**, 367–377 (2017).
199. Furuita, K., Jee, J., Fukada, H., Mishima, M. & Kojima, C. Electrostatic interaction between oxysterol-binding protein and VAMP-associated protein a revealed by NMR and mutagenesis studies. *J. Biol. Chem.* **285**, 12961–12970 (2010).
200. Hanada, K. *et al.* Molecular machinery for non-vesicular trafficking of ceramide.

Nature **426**, 803–809 (2003).

201. Weber-Boyvat, M. *et al.* OSBP-related protein 3 (ORP3) coupling with VAMP-associated protein A regulates R-Ras activity. *Exp. Cell Res.* **331**, 278–291 (2015).
202. Asrat, S., Dugan, A. S. & Isberg, R. R. The Frustrated Host Response to *Legionella pneumophila* Is Bypassed by MyD88-Dependent Translation of Pro-inflammatory Cytokines. *PLoS Pathog.* **10**, (2014).
203. Hackstadt, T., Scidmore, M. A. & Rockey, D. D. Lipid metabolism in *Chlamydia trachomatis*-infected cells: directed trafficking of Golgi-derived sphingolipids to the *Chlamydial* inclusion. *Proc. Natl. Acad. Sci. U.S.A.* **92**, 4877–4881 (1995).
204. Saita, S., Shirane, M., Natume, T., Iemura, S. I. & Nakayama, K. I. Promotion of neurite extension by protrudin requires its interaction with vesicle-associated membrane protein-associated protein. *J. Biol. Chem.* **284**, 13766–13777 (2009).
205. Yang, C. *et al.* *Chlamydia trachomatis* ChxR is a transcriptional regulator of virulence factors that function in *in vivo* host pathogen interactions. *Pathog. Dis.* **75**, 1–8 (2017).
206. Mccune, B. T. *et al.* Noroviruses Co-opt the Function of Host Proteins VAPA and VAPB for Replication via a Phenylalanine–Phenylalanine- Acidic-Tract-Motif Mimic in Nonstructural Viral Protein NS1/2. *MBio* **8**, 1–17 (2017).
207. Derré, I., Pypaert, M., Dautry-Varsat, A. & Agaisse, H. RNAi screen in *Drosophila*

- cells reveals the involvement of the tom complex in *Chlamydia* infection. *PLoS Pathog.* **3**, 1446–1458 (2007).
208. Kumagai, K., Kawano, M., Shinkai-Ouchi, F., Nishijima, M. & Hanada, K. Interorganelle trafficking of ceramide is regulated by phosphorylation- dependent cooperativity between the PH and START domains of CERT. *J. Biol. Chem.* **282**, 17758–17766 (2007).
209. Kumagai, K., Kawano-Kawada, M. & Hanada, K. Phosphoregulation of the ceramide transport protein CERT at serine 315 in the interaction with VAMP-associated protein (VAP) for inter-organelle trafficking of ceramide in mammalian cells. *J. Biol. Chem.* **289**, 10748–10760 (2014).
210. Kumagai, K., Elwell, C. A., Ando, S., Engel, J. N. & Hanada, K. Both the N- and C-terminal regions of the *Chlamydial* inclusion protein D (IncD) are required for interaction with the pleckstrin homology domain of the ceramide transport protein CERT. *Biochem. Biophys. Res. Commun.* **505**, 1070–1076 (2018).
211. Litchfield, D. W. Protein kinase CK2: structure, regulation and role in cellular decisions of life and death. *Biochem. J.* **369**, 1–15 (2003).
212. Allen, J. J. *et al.* A semisynthetic epitope for kinase substrates. *Nat. Methods* **4**, 511–516 (2007).
213. Ferguson, A. D. *et al.* Structural basis of CX-4945 binding to human protein kinase CK2. *FEBS Lett.* **585**, 104–110 (2011).

214. Anderes, K. *et al.* Abstract #4660: Discovery and characterization of CX-4945 a selective orally bioavailable small molecule inhibitor of protein kinase CK2: Phase 1 initiated. *Cancer Res.* **69**, (2009).
215. De Oliveira, P. S. L. *et al.* Revisiting protein kinase-substrate interactions: Toward therapeutic development. *Science Signaling* **9**, re3–re3 (2016).
216. Bedard, L. G. *et al.* Quantitative analysis of dynamic protein interactions during transcription reveals a role for casein kinase II in Polymerase-associated Factor (PAF) complex phosphorylation and regulation of histone H2B monoubiquitylation. *J. Biol. Chem.* **291**, 13410–13420 (2016).
217. Rockey, D. D. *et al.* *Chlamydia psittaci* InCA is phosphorylated by the host cell and is exposed on the cytoplasmic face of the developing inclusion. *Mol Microbiol* **24**, 217–228 (1997).
218. Zadora, P. K. *et al.* Integrated Phosphoproteome and Transcriptome Analysis Reveals *Chlamydia*-Induced Epithelial-to-Mesenchymal Transition in Host Cells. *Cell Rep.* **26**, 1286-1302.e8 (2019).
219. Sah, P., Nelson, N. H., Shaw, J. H. & Lutter, E. I. *Chlamydia trachomatis* recruits protein kinase C during infection. *Pathog. Dis.* **77**, (2019).
220. Mital, J. & Hackstadt, T. Role for the Src family kinase Fyn in sphingolipid acquisition by *Chlamydiae*. *Infect. Immun.* **79**, 4559–4568 (2011).

221. Chong, R. *et al.* Regulatory Mimicry in *Listeria monocytogenes* Actin-Based Motility. *Cell Host Microbe* **6**, 268–278 (2009).
222. Alvarez, D. E. & Agaisse, H. Casein kinase 2 regulates vaccinia virus actin tail formation. *Virology* **423**, 143–151 (2012).
223. Nogalski, M. T., Podduturi, J. P., DeMeritt, I. B., Milford, L. E. & Yurochko, A. D. The Human Cytomegalovirus Virion Possesses an Activated Casein Kinase II That Allows for the Rapid Phosphorylation of the Inhibitor of NF- κ B, I κ B. *J. Virol.* **81**, 5305–5314 (2007).
224. Modrof, J., Lympereopoulos, K. & Roy, P. Phosphorylation of Bluetongue Virus Nonstructural Protein 2 Is Essential for Formation of Viral Inclusion Bodies. *J. Virol.* **79**, 10023–10031 (2005).
225. Piirsoo, A. *et al.* Activity of CK2 α protein kinase is required for efficient replication of some HPV types. *PLoS Pathog.* **15**, 1–25 (2019).
226. Yeh, T. S., Lo, S. J., Chen, P. J. & Lee, Y. H. Casein kinase II and protein kinase C modulate hepatitis delta virus RNA replication but not empty viral particle assembly. *J. Virol.* **70**, 6190–6198 (1996).
227. Reiss, S. *et al.* Recruitment and activation of a lipid kinase by hepatitis C virus NS5A is essential for integrity of the membranous replication compartment. *Cell Host Microbe* **9**, 32–45 (2011).

228. Filhol, O. *et al.* Live-cell fluorescence imaging reveals the dynamics of protein kinase CK2 individual subunits. *Mol. Cell. Biol.* **23**, 975–87 (2003).
229. Cortina, M. E., Ende, R. J., Clayton Bishop, R., Bayne, C. & Derré, I. *Chlamydia trachomatis* and *Chlamydia muridarum* spectinomycin resistant vectors and a transcriptional fluorescent reporter to monitor conversion from replicative to infectious bacteria. *PLoS One* **14**, (2019).
230. Elbaz-Alon, Y. *et al.* Lam6 Regulates the Extent of Contacts between Organelles. *Cell Rep.* **12**, 7–14 (2015).
231. Kornmann, B. *et al.* An ER-mitochondria tethering complex revealed by a synthetic biology screen. *Science (80-.)*. **325**, 477–481 (2009).
232. de Villavicencio-Díaz, T. N., Rabalski, A. J. & Litchfield, D. W. Protein kinase CK2: Intricate relationships within regulatory cellular networks. *Pharmaceuticals* **10**, (2017).
233. Hornbeck, P. V. *et al.* PhosphoSitePlus: A comprehensive resource for investigating the structure and function of experimentally determined post-translational modifications in man and mouse. *Nucleic Acids Res.* **40**, 261–270 (2012).
234. Nishi, H., Shaytan, A. & Panchenko, A. R. Physicochemical mechanisms of protein regulation by phosphorylation. *Frontiers in Genetics* **5**, 270 (2014).

235. Tomishige, N., Kumagai, K., Kusuda, J., Nishijima, M. & Hanada, K. Casein kinase I γ 2 down-regulates trafficking of ceramide in the synthesis of sphingomyelin. *Mol. Biol. Cell* **20**, 348–357 (2009).
236. Martinez, E., Siadous, F. A. & Bonazzi, M. Tiny architects: biogenesis of intracellular replicative niches by bacterial pathogens. *FEMS Microbiol. Rev.* **013**, 425–447 (2018).
237. Romero-Brey, I. & Bartenschlager, R. Endoplasmic reticulum: The favorite intracellular niche for viral replication and assembly. *Viruses* **8**, 1–26 (2016).
238. Inoue, T. & Tsai, B. How viruses use the endoplasmic reticulum for entry, replication, and assembly. *Cold Spring Harb. Perspect. Biol.* **5**, 1–17 (2013).
239. Roy, C. R., Salcedo, S. P. & Gorvel, J. P. E. Pathogen-endoplasmic-reticulum interactions: In through the out door. *Nat. Rev. Immunol.* **6**, 136–147 (2006).
240. Roy, C. R. Exploitation of the endoplasmic reticulum by bacterial pathogens. *Trends Microbiol.* **10**, 418–424 (2002).
241. Derre, I. *Chlamydiae* interaction with the endoplasmic reticulum: Contact, function and consequences. *Cell. Microbiol.* **17**, 959–966 (2015).
242. Doerflinger, S. Y. *et al.* Membrane alterations induced by nonstructural proteins of human norovirus. *PLoS Pathogens* **13**, (2017).
243. Kohler, L. J. & Roy, C. R. Biogenesis of the lysosome-derived vacuole containing

- Coxiella burnetii*. *Microbes Infect.* **17**, 766–771 (2015).
244. Justis, A. V. *et al.* Interactions between the *Coxiella burnetii* parasitophorous vacuole and the endoplasmic reticulum involve the host protein ORP1L. *Cell. Microbiol.* **19**, (2017).
245. Ishikawa-Sasaki, K., Nagashima, S., Taniguchi, K. & Sasaki, J. A model of OSBP-mediated cholesterol supply to Aichi virus RNA replication sites involving protein-protein interactions among viral proteins, ACBD3, OSBP, VAP-A/B, and SAC1. *J. Virol.* **92**, JVI.01952-17 (2018).
246. Sasaki, J., Ishikawa, K., Arita, M. & Taniguchi, K. ACBD3-mediated recruitment of PI4KB to picornavirus RNA replication sites. *EMBO J.* **31**, 754–766 (2012).
247. Hamamoto, I. *et al.* Human VAP-B Is Involved in Hepatitis C Virus Replication through Interaction with NS5A and NS5B. *J. Virol.* **79**, 13473–13482 (2005).
248. Tu, H. *et al.* Hepatitis C virus RNA polymerase and NS5A complex with a SNARE-like protein. *Virology* **263**, 30–41 (1999).
249. Goonawardane, N., Gebhardt, A., Bartlett, C., Pichlmair, A. & Harrisa, M. Phosphorylation of Serine 225 in Hepatitis C Virus NS5A Regulates Protein-Protein Interactions. *J. Virol.* **91**, (2017).
250. Ross-Thriepland, D., Mankouri, J. & Harris, M. Phosphorylation of Serine 225 in Hepatitis C Virus NS5A Regulates Protein-Protein Interactions. *J. Virol.* **89**, 3123–

- 3135 (2015).
251. Mehlitz, A. *et al.* The *Chlamydial* organism *Simkania negevensis* forms ER vacuole contact sites and inhibits ER-stress. *Cell. Microbiol.* **16**, 1224–1243 (2014).
 252. Croxatto, A. & Greub, G. Early intracellular trafficking of *Waddlia chondrophila* in human macrophages. *Microbiology* **156**, 340–355 (2010).
 253. Melo, E. J. T. T., de Souza, W. & Souza, W. De. Relationship between the host cell endoplasmic reticulum and the parasitophorous vacuole containing *Toxoplasma gondii*. *Cell Struct. Funct.* **22**, 317–323 (1997).
 254. Barajas, D. *et al.* Co-opted Oxysterol-Binding ORP and VAP Proteins Channel Sterols to RNA Virus Replication Sites via Membrane Contact Sites. *PLoS Pathog.* **10**, 34–45 (2014).
 255. Santos, J. C. *et al.* The COPII complex and lysosomal VAMP7 determine intracellular *Salmonella* localization and growth. *Cell. Microbiol.* **17**, 1699–1720 (2015).
 256. Besprozvannaya, M. *et al.* GRAM domain proteins specialize functionally distinct ER-PM contact sites in human cells. *Elife* **7**, (2018).
 257. Hönscher, C. *et al.* Cellular metabolism regulates contact sites between vacuoles and mitochondria. *Dev. Cell* **30**, 86–94 (2014).

Appendices

**Appendix 1 - Primers and templates used for generating constructs in chapter 2
(dataset 1 from Stanhope et al. 2017)**

Primer pairs (name and sequence) and corresponding templates used in this study

Cloning of pYFP-VAP WT or KFM/DFD

- VAPA

Primers: VAPAN1H3 AAGAAGCTTATGGCGTCCGCTCAGGGGCCATGGCG
VAPAN1Age ACCACCGGTGGCAAGATGAATTTCCCTAGAAAG

Templates:

VAPA_{WT} : pGFP-VAPA_{WT}
VAPA_{KFM/DFD}: pGFP-VAPA_{KFM/DFD}

- VAPB

Primers: VAPBN1Eco GAAGAATTCATGGCGAAGGTGGAGCAGGTCC
VAPBN1Age ACCACCGGTGGCAAGGCAATCTTCCCAATAATTAC

Templates:

VAPB_{WT} : pGFP-VAPB_{WT}
VAPB_{KFM/DFD}: pGFP-VAPB_{KFM/DFD}

Cloning of pCMV- IE-N2-IncV-3xFLAG WT, F263A, Y287A and FY-AA

Primers: 0260ATG Xho 5 CTCCTCGAGATGACTCCAGTAACACCAGTC
0260NoTAA Bam 3 GGAGGATCCCTTTACGAGAGGGTTTCTCTTTTG

Templates:

IncV_{WT}: p2TK2SW2 mCh(Gro) TetR TetA^P **IncV_{WT}3xFLAG** IncDTerm
IncV_{F263A}: p2TK2SW2 mCh(Gro) TetR TetA^P **IncV_{F263A}3xFLAG** IncDTerm
IncV_{Y287A}: p2TK2SW2 mCh(Gro) TetR TetA^P **IncV_{Y287A}3xFLAG** IncDTerm
IncV_{F263AY287A}: p2TK2SW2 mCh(Gro) TetR TetA^P **IncV_{F263AY287}3xFLAG** IncDTerm

Cloning of pCMV- IE-N2-IncV₁₆₇₋₃₆₃-3xFLAG WT and FY-AA

Primers: 0260 ATG167 Xho 5 CTCCTCGAGATGCAAGTTGAGTTAGCTGCCTG
0260NoTAA Bam 3 GGAGGATCCCTTTACGAGAGGGTTTCTCTTTTG

Templates:

IncV_{WT}: p2TK2SW2 mCh(Gro) TetR TetA^P **IncV_{WT}3xFLAG** IncDTerm
IncV_{F263AY287A}: p2TK2SW2 mCh(Gro) TetR TetA^P **IncV_{F263AY287}3xFLAG** IncDTerm

Cloning of pCMV- IE-N2-PM-IncV₁₆₇₋₃₆₃-3xFLAG WT and FY-AA

Constructed by overlapping PCR

PCR A:

Primers: PM Xho 5 CTCCTCGAGatgctgtgctgtatgagaag
PM0260ATG167 3 GCAGCTAACTCAACTTGCATgatcttttggctctcatc

Template: pDsRed-Monomer-Mem

PCR B:

Primers: PM0260ATG167 5 gatgaggacccaaaagatcATGCAAGTTGAGTTAGCTGC
0260NoTAA Bam 3 GGAGGATCCCTTTACGAGAGGGTTTCTTCTTTTG

Templates:

PM-IncV_{WT}: p2TK2SW2 mCh(Gro) TetR TetA^P IncV_{WT}3xFLAG IncDTerm

PM-IncV_{FY-AA}: p2TK2SW2 mCh(Gro) TetR TetA^P IncV_{FY-AA}3xFLAG IncDTerm

Cloning of pGST-VAPA_{MSP} WT or KFM/DFD

Primers: VAPAATG Bam 5 GGAGGATCCATGGCGTCCGCCTCAGGGGC
VAPAMSP EcoRI 3 GAAGAATTCctaCATTTCAAATACGCATCTC

Templates:

VAPA_{WT}: pYFP-VAPA_{WT}

VAPA_{KFM/DFD}: pYFP-VAPA_{KFM/DFD}

Cloning of p2TK2-SW2 mCh(Gro) Tet-IncV-3xFLAG WT, F263A, Y287A and FY-AA

Constructed by overlapping PCR

- TetR-TetA^P-IncV_{WT}3xFLAG-IncDTerm

PCR A:

Primers: TetR STOP 5 Kpn GGTGGTACCTTAAGACCCACTTTCACATTTAAG
Tet0260 3 GGGACTGGTGTACTGGAGTCATtccacttttctctatcactg

Template: p2TK2SW2 mCh(Gro) TetR TetA^P IncD3xFLAG IncDTerm

PCR B:

Primers: Tet0260 5 cagtgatagagaaaagttaaATGACTCCAGTAACACCAGTCCC
0260FLAG 3 CATGGTCTTTGTAGTCcatTTTACGAGAGGGTTTCTTCTTTTG

Template: CtL2 genomic DNA

PCR C:

Primers: 0260FLAG 5 CAAAAGAAGAAACCCTCTCGTAAAatgGACTACAAAGACCATG
IncDTerm 3 Not GCGGGCGGCCGctcttaggagctttttgcaatgc

Template: p2TK2SW2 mCh(Gro) TetR TetA^P IncD3xFLAG IncDTerm

- TetR-TetA^P-IncV_{F263A}3xFLAG-IncDTerm

PCR A:

Primers: TetR STOP 5 Kpn GGTGGTACCTTAAGACCCACTTTCACATTTAAG
0260F263A 3 CGCTATTTGGTGGAGTGTGGGCGCTAGAAGAAGAGGAGG

Template: p2TK2-SW2 mCh(Gro) TetR-TetA^P-CTL02603xFLAG-IncDTerm

PCR B:

Primers: 0260F263A 5 CCTCCTTCTTCTAGCGCCCACTCCACCAAATAGCG
IncDTerm 3 Not GCGGGCGGCCGCgtcttaggagcttttgcgatgc

Template: p2TK2-SW2 mCh(Gro) TetR-TetA^P-CTL02603xFLAG-IncDTerm

- TetR-TetA^P-IncV_{V287A}3xFLAG-IncDTerm

PCR A:

Primers TetR STOP 5 Kpn GGTGGTACCTTAAGACCCACTTTCACATTTAAG
0260Y287A 3 CGGTTTCAAGAGCATCCATAGCTTCAGAAGAAGAGCTGC

Template: p2TK2-SW2 mCh(Gro) TetR-TetA^P-CTL02603xFLAG-IncDTerm

PCR B:

Primers 0260Y287A 5 GCAGCTTCTTCTGAAGCTATGGATGCTCTTGAAACCG
IncDTerm 3 Not GCGGGCGGCCGCgtcttaggagcttttgcgatgc

Template: p2TK2-SW2 mCh(Gro) TetR-TetA^P-CTL02603xFLAG-IncDTerm

- TetR-TetA^P-IncV_{F263AY287A}3xFLAG-IncDTerm

PCR A:

Primers: TetR STOP 5 Kpn GGTGGTACCTTAAGACCCACTTTCACATTTAAG
0260nt806-828 3 CGAGTCGGACAGTTCTTTATCGC

Template: p2TK2-SW2 mCh(Gro) TetR-TetA^P-CTL0260_{F263A}3xFLAG-IncDTerm and

PCR B:

Primers: 0260nt806-828 5 GCGATAAAGAAGTCCGACTCG
IncDTerm 3 Not GCGGGCGGCCGCgtcttaggagcttttgcgatgc

Template: p2TK2-SW2 mCh(Gro) TetR-TetA^P-CTL0260_{V287A}3xFLAG-IncDTerm

Appendix 2 – Primers and templates used for generating constructs in chapter 3**Cloning of pCFP-VAPA**

Primers:	VAPAN1H3	AAGAAGCTTATGGCGTCCGCCTCAGGGGCCATGGCG
	VAPAN1Age	ACCACCGGTGGCAAGATGAATTTCCCTAGAAAAG

Template:	pGFP-VAPA _{WT}
-----------	-------------------------

Cloning of MBP-VAPA_{MSP}

Primers:	VAPAATG Not 5	GCGGGCGGCCGCATGGCGTCCGCCTCAGGGGC
	VAPAMSP Bam 3	GGAGGATCCCTACATTTCAAATACGCATCTC

Template:	pGFP-VAPA _{WT}
-----------	-------------------------

Cloning of GST-IncV₁₆₇₋₃₆₃

Primers:	0260ATG167 Bam 5	GGAGGATCCATGCAAGTTGAGTTAGCTGCCTG
	0260STOP Xho 3	CTCCTCGAGTTATTTACGAGAGGGTTTCTTCTTTTG

Template:	pCMV-IE-N2-IncV- 3xFLAG WT
-----------	-------------------------------

Cloning of pTet-IncV-3xFLAG₁₋₃₀₅

PCR A

Primers:	TetR STOP 5 Kpn	GGTGGTACCTTAAGACCCACTTTCACATTTAAG
	0260 1-305 3	CATGGTCTTTGTAGTCcatGACATCTCCTGCAGCTACGG

Template:	p2TK2SW2 mCh(Gro) TetR TetAP CTL0260 3xFLAG IncDTerm
-----------	--

PCR B

Primers:	0260 1-305 5	CCGTAGCTGCAGGAGATGTCatgGACTACAAAGACCATG
	IncDTerm 3 Not	GCGGGCGGCCGCgtcttaggagctttttgcaatgc

Template: p2TK2SW2 mCh(Gro)
TetR TetAP CTL0260
3xFLAG IncDTerm

PCR C

Primers: TetR STOP 5 Kpn GGTGGTACCTTAAGACCCACTTTCACATTTAAG
IncDTerm 3 Not GCGGGCGGCCGCgtcttaggagcttttgcaatgc

Template: PCR A + PCR B

Cloning of pTet-IncV-3xFLAG₁₋₃₄₁

PCR A

Primers: TetR STOP 5 Kpn GGTGGTACCTTAAGACCCACTTTCACATTTAAG
0260 1-341 3 CATGGTCTTTGTAGTCcatGTCTTGCTTTGCTCTTGCTC

Template: p2TK2SW2 mCh(Gro)
TetR TetAP CTL0260
3xFLAG IncDTerm

PCR B

Primers: 0260 1-341 5 GACCAAGAGCAAAGACAAGACatgGACTACAAAGACCATG
IncDTerm 3 Not GCGGGCGGCCGCgtcttaggagcttttgcaatgc

Template: p2TK2SW2 mCh(Gro)
TetR TetAP CTL0260
3xFLAG IncDTerm

PCR C

Primers: TetR STOP 5 Kpn GGTGGTACCTTAAGACCCACTTTCACATTTAAG
IncDTerm 3 Not GCGGGCGGCCGCgtcttaggagcttttgcaatgc

Template: PCR A + PCR B

Cloning of pTet-IncV-3xFLAG₁₋₃₅₆

PCR A

Primers: TetR STOP 5 Kpn GGTGGTACCTTAAGACCCACTTTTCACATTTAAG
 0260 1-356 3 CATGGTCTTTGTAGTCcatTTGAGATGAATCGGAAGAGG

Template: p2TK2SW2 mCh(Gro)
 TetR TetAP CTL0260
 3xFLAG IncDTerm

PCR B

Primers: 0260 1-356 5 CCTCTTCCGATTCATCTCAAatgGACTACAAAGACCATG
 IncDTerm 3 Not GCGGGCGGCCGCgtcttaggagcttttgcaatgc

Template: p2TK2SW2 mCh(Gro)
 TetR TetAP CTL0260
 3xFLAG IncDTerm

PCR C

Primers: TetR STOP 5 Kpn GGTGGTACCTTAAGACCCACTTTTCACATTTAAG
 IncDTerm 3 Not GCGGGCGGCCGCgtcttaggagcttttgcaatgc

Template: PCR A + PCR B